

Chapter one

Introduction

1-1 Introduction

The sun, an inexhaustible source of energy on the ground, is one of many renewable energy sources. Obviously the direct exploitation of solar energy is the best choice because it is renewable energy, and pollution free can be sufficient for humans possibly forever if possible exploited efficiently [1].

Si-based solar cells have been utilized in many occasions as a renewable energy source; however, it has been impossible to replace other conventional nonrenewable energy sources with the solar cells because its manufacturing cost is much higher than that of other nonrenewable energy sources. However the organic based solar cells, can possibly offer special opportunities as renewable energy source because they can be fabricated over large area using low cost printing technologies. The progress in the field of the polymer based solar cells has been promising with the recently reported power-conversion efficiency of ~6%. Although it is still ineffective to be the technology utilized in commercial products, there could be plenty of room for the improvement in the power-conversion efficiency of the polymer based solar cells. In this research, we will present the synthesis methodology to produce high mobility polymers that can possibly be utilized in polymer-based solar cells with improved power-conversion efficiency.[2,3,4,5].

It is important to understand how organic or polymer based solar cells work to improve its power-conversion efficiency. A simple organic solar cell has the planer structures, and the structure is very similar to that of the Si-based solar cells with the p-n junction sandwiched with the transparent conductor such as ITO and metal electrodes. The working principle is also similar to each other. The photo excited

species are generated in the p- or n-type semiconductor materials, and they are separated as holes and electrons at the p-n junction. To take out energy from a solar cell, the separated holes and electrons have to be collected at the electrodes. Thus, the materials need to satisfy the following criteria to be a good solar cell material: 1) high absorption of light; 2) efficient charge separation; 3) sufficient charge transport [6,7,8,9,10].

Solar energy can be exploited in many important purposes in our life.

1-2 Application of solar cell

Solar cells had been in the operation of many devices thirty years ago or more. The most important use was in space satellites. It has now become possible to use them to run various mechanisms such as fans, pumps, refrigerators, calculators and other electronic appliances [3].

Power generated is used in

- Water pumping
- Lighting
- Refrigeration and air conditioning

1-2 Principle of solar cell

Silicon solar cells are based on the physical principles described by Planck's law. This law states that the energy of a single photon is equal to $h\nu$, where h is Planck's constant and ν is the frequency of the light. The energy is thus proportional to the frequency and inversely proportional to the wavelength [11].

When light, with a frequency corresponding to an energy larger than the band gap, hits a semiconductor like silicon some of the electrons are excited into higher energy levels. Only if the energy of the photons are larger than the band gap, the electron can be excited. If the energy is much larger than the band gap the electron

can be ejected from the material. This is known as the photoelectric effect. In these excited states the electrons are more free to move, and can thus lead a current if a potential difference is imposed across the cell. This potential difference arises from a built in asymmetry in the cell.

SSCs are built from several different layers, two of them being n-type silicon (negative - excess of electrons) and p-type silicon (positive - excess of holes). Naturally found silicon has 14 electrons, 4 of them being valence electrons. In the solid state silicon forms covalent bonds with four neighboring silicon atoms, and this forms the crystal lattice. To create n-type and p-type silicon, impurities are introduced into the crystal lattice. This controlled and on purpose contamination of silicon is known as doping. N-type silicon can be created by doping with phosphorus.

Phosphorus is incorporated into the crystal lattice where it occupies a lattice point which would otherwise be occupied by a silicon atom. Because phosphorus contains five valence electrons, and only four of them are used for bonding, there is one excess electron per unit cell. Similarly, to create p-type silicon, atoms with three valence electrons, for example boron, are incorporated into the lattice producing an excess amount of holes.

When p-type and n-type silicon are brought together a p-n junction is formed at the interface. Because of the excess of electrons on one side, and the excess of holes on the other side electrons and holes recombine at the junction creating an insulating junction which is termed the depletion zone. When electrons flow from the n-type side towards the junction, excess positive charge is left behind. Similarly, excess negative charge is left behind when holes flow to the junction. This excess charge is not free to move because it is part of the chemical bonds between atoms. As a result an electric field directed from the n-type side to the p-type side is established.

This is illustrated in Figure 1.1. [12,13,14].

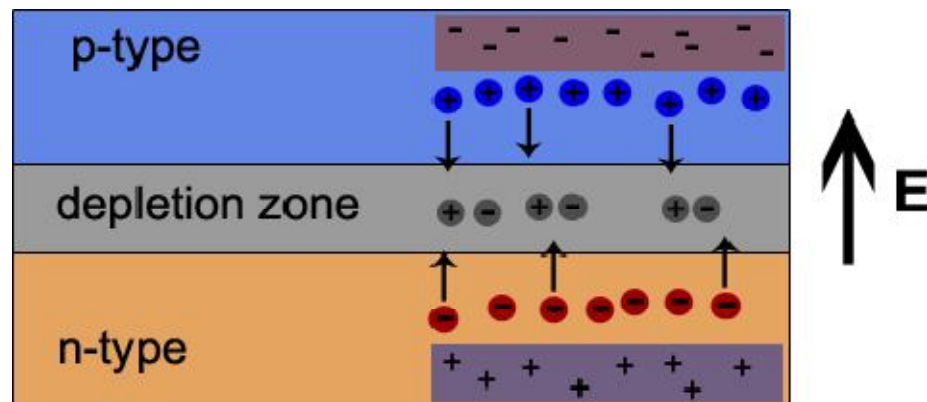


Fig: 1-1: Illustration of the depletion layer. When the p-type and n-type layer are brought together, electrons from the n-type side recombine with holes from the p-type side at the depletion layer. The depletion layer is therefore an insulating layer because there are no free charge carriers.

A basic SSC unit produces a photo-voltage of between 0.5 and 1.0 volt and a photocurrent of some tens of milliamps per cm^2 when illuminated by the sun. This voltage is too small for most applications and therefore multiple cells are connected in series into modules [4].

Although the manufacturing costs of SSCs have dropped dramatically since the first cells were produced in the 1950's, the costs are still too high for large scale energy production. Furthermore, the production is not an easy task, the SSCs are not very flexible and silicon is in great demand due to the ever growing computer industry. This is not subject to change, therefore different paths must be examined.

1-3 Type of solar cells (Three generations)

1-3-1 First Generations

First-generation cells are based on expensive silicon and make up 85% of the current commercial market due efficiency to 26%.. [15,16] .

1-3-1-1 Single Crystalline Silicon

- Single crystal wafers made by Czochralski process, as in silicon electronics
- Comprise 31% of market
- Efficiency as high as 24.7%
- Expensive—batch process involving high temperatures, long times, and mechanical slicing Wafers are not the ideal geometry
- Benefits from improvements developed for electronics industry

1-3-1-2 polycrystalline silicon

1-3-2 Second Generations

Second-generation cells are based on thin films of materials such as amorphous silicon, Nanocrystalline silicon, cadmium telluride, or copper indium selenide. The materials are less expensive, but research is needed to raise the cells' efficiency to the levels shown if the cost of delivered power is to be reduced[17,18].

1-3-2-1 Flat-Plate Thin-Films

- Potential for cost advantages over crystalline silicon
 - Lower material use
 - Fewer processing steps
 - Simpler manufacturing technology

1-3-2-2 Three Major Systems

- Amorphous Silicon

- Cadmium Telluride
- Copper Indium Diselenide (CIS)

1-4-3 Third Generations

Third-generation cells are the research goal: a dramatic increase in efficiency that maintains the cost advantage of second-generation materials. Their design may make use of carrier multiplication, hot electron extraction, multiple junctions, sunlight concentration, or new materials. The horizontal axis represents the cost of the solar module only; it must be approximately doubled to include the costs of packaging and mounting.

- High-efficiency Multi-junction Concentrator Solar Cells based on III-V's and III-V ternary analogs
 - Dye-sensitized cells
 - Organic (excitonic) cells
 - Polymeric Cells
 - Nanostructured cells including Multi-carrier per photon cells [5].

1-4 Silicon solar cell

The silicon solar cell is the traditional solar cell and has found applications in various areas such as calculators, garden lamps, and roof mounted large area cells etc. The SSC has so far been the best candidate for conversion of sunlight and therefore the development and research of solar cells has been dominated by this.

The SSCs trace their history back to the 1950s where the first SSC was reported by Chapin, Fuller and Pearson. It had a power conversion efficiency of 6%. The price per watt was very high, being as much as \$ 200 per watt. This meant that SSCs were not seriously considered as an everyday power source for many decades, only in very remote places and if the costs were made unimportant by the benefits of

SSCs, e.g. satellites. The SSCs has benefited from the fast development in the integrated circuit industry. This means that it is now possible to produce SSCs with efficiencies as high as 25%. In addition, this will lead to inexpensive, efficient and reliable SSCs than what was previously estimated. The prices for a solar cell generated power today lies between \$ 10 and $12W^{-1}$, based on today's prices on the internet [19,20].

1-5 Polymer solar cell

Polymer solar cells (PSC) is one of the possible replacements. These solar cells add some very interesting properties to the solar cell as well as reducing the price considerably [7]. have demonstrated that the production of large area PSC ($1m^2$) can be done at a cost 100 times lower than that of Nano crystalline silicon solar cells in terms of material cost. Another area where the PSC has advantages over silicon cells is in flexibility. Whereas silicon crystal is rigid a polymer layer is very flexible yielding the possibility of a very flexible thin film solar cell. This is a property that can enable a variety of new applications [21,22,23].

However there are still challenges to overcome. Firstly the service life of a PSC is very short, only a few hours for a simple metal/polymer/metal solar cell. Secondly the efficiency of the PSC is not high compared to the SSCs. PSCs has power conversion efficiencies around 3% using different optimization methods [24,25,26]. In This research we used thin film method to fabrication polymer solar cell.

1-6 Research problem:-

The silicon solar cells are expensive and have lower efficiency. Other Solar cells like polymer and nano cells are still facing many problems like low efficiency; chemical instability and lack of well define theoretical background. The important of theoretical back ground comes from the fact that the parameters that affect

the efficiency gives a guide on the suitable experimental treatment that increase the cell performance.

1-7 Aim of the work:-

The aim of the work is to find a theoretical framework that can explain the effect of atomic type and structure of the doping atoms beside the crystal structure and the nanno micro structure of the substrate and host crystal an the efficiency of the cell and their performance.

1-8 Presentation of the Thesis :-

This Thesis Consists of five Chapters. Chapters one and tow are the introduction and silicon Solar cells respectively. Chapters three and four are concerned with polymer cells and Literature review .The contribution is in Chapters five

Chapter Two

Silicon Solar Cell

(2-1) Introduction

silicon Solar cells were widely for a longtime to generate electricityfor a long time . This Chapter is Concord widely Structure and performacne

2.2 Silicon Solar Cell:

The sunlight is absorbed by a solar cell in a solar panel. The absorbed light causes electrons in the material to increase in energy. At the same time making they free to move around in the material. However, the electrons remain at this higher energy for only a short time before returning to their original lower energy position. Therefore, to collect the carriers before they lose the energy gained from the light, a PN junction is typically used. PN junction consists of two different regions of a semiconductor material (usually silicon), with one side called the p type region and the other the n-type region. During the incident of light energy, in p-type material, electrons can gain energy and move into the n-type region. Then they can no longer go back to their original low energy position and remain at a higher energy. The process of moving a light- generated carrier from p-type region to n-type region is called collection. These collections of carriers (electrons) can be either extracted from the device to give a current, or it can remain in the device and gives rise to a voltage. The electrons that leave the solar cell as current give up their energy to whatever is connected to the solar cell, and then re-enter the solar cell. Once back in the solar cell, the process begins again [10]:The mechanism of electricity production- Different stage:[27,28,29,30].

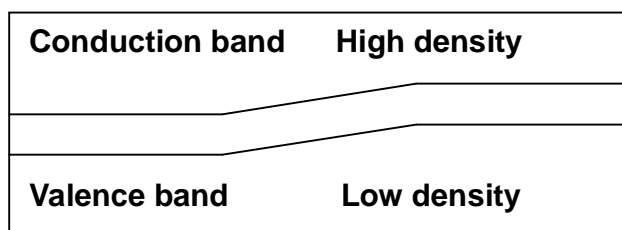


Fig (2.1) p-n junction

The above diagram shows the formation of p-n junction in a solar cell. The valence band is a low-density band and conduction band is high-density band.

▪ Stage-1

When light falls on the semiconductor surface, the electron from valence band promoted to conduction band

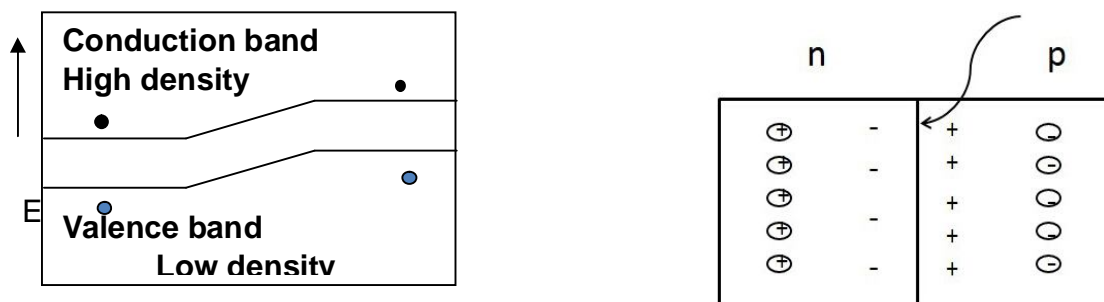


Fig (2.2) charge generation by light

Therefore, the hole (vacancy position left by the electron in the valence band) is generated. Hence, there is a formation of electron-hole pair on the sides of p-n junction. Where positive ions exist at n type negative ions exist at p type.

▪ Stage-2

In the stage 2, the electron and holes are diffuse across the p-n junction. Where positive ions at (n) type attracts electrons, while negative ions at (p) type attracts holes.

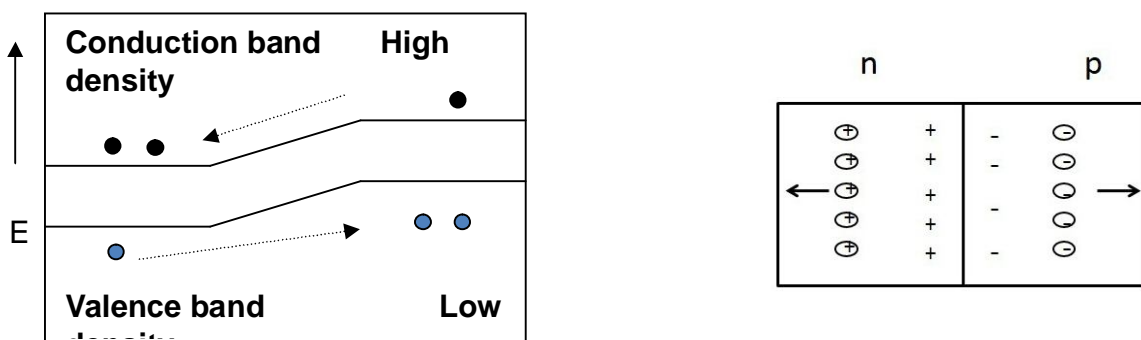


Fig (2.3): charge separation at p-n junction by ions

▪ Stage-3

In the stage 3, due to accumulation of high concentrated electron build due to contraction gradient to the left side of the p-n junction. The same hold far holes, where they diffuse to the left from high concert region to low concentration region.

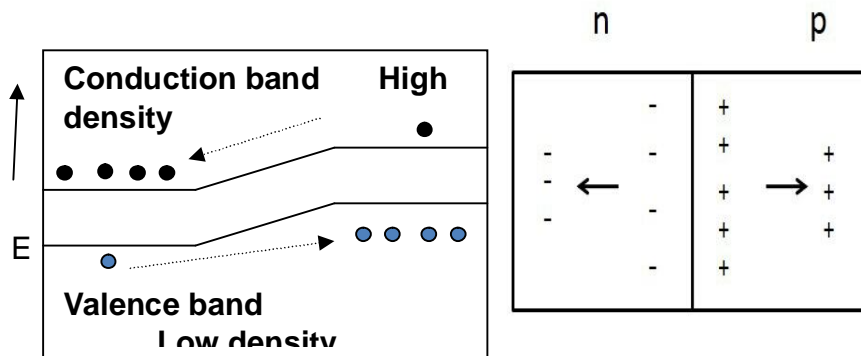


Fig (2.4): Diffusion of charge

▪ Stage-4

When the PN junction is connected with external circuit, the current flows

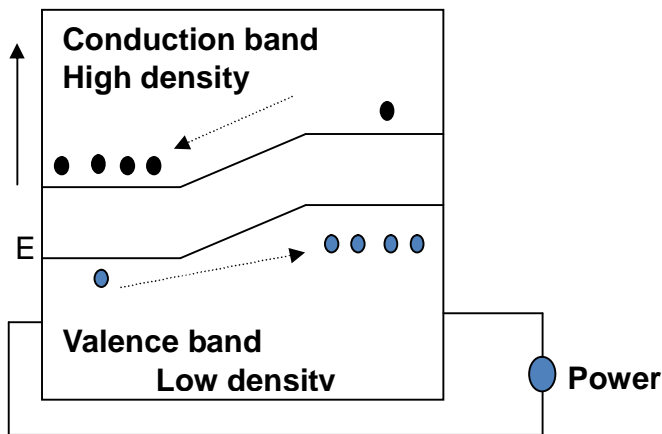


Fig (2.5): PN junction is connected with external circuit

$$I = I_0(e^{\beta v} - 1) - I_p \quad (2.1)$$

Where I_0 is the saturation current, v is the voltage and I_p is the photon current. The cells are characterized by many parameters, one of these parameter, is the short-current it is

defined as the current that flows when the cells terminals are connected with resistant less wire. In this case $v = 0$ and $I = I_{sc}$ and equation (2.2.1) gives:

$$I_{sc} = I_0(e^0 - 1) - I_p = -I_p \quad (2.2)$$

$$I_{sc} = -I_p \quad (2.3)$$

The other parameter is the so called open circuit voltage V_{oc} it is defined as the volt, when no current flows. For open-circuit voltage:

$$At I = 0 \quad v = v_{oc} \quad (2.4)$$

$$I = I_0(e^{\beta v} - 1) - I_p$$

$$0 = I_0(e^{\beta v_{oc}} - 1) - I_p$$

$$e^{\beta v_{oc}} = \frac{I_0 + I_p}{I_0} = \left(1 + \frac{I_p}{I_0}\right) \quad (2.5)$$

$$FF = \frac{V_m I_m}{V_{oc} I_{sc}} \quad (2.6)$$

Where FF is the fill factor.

The power P is given by:

$$P = IV = V_{IO} (e^{\beta v} - 1) - VI_p \quad (2.7)$$

To find $V_{max} = V_m$ at which P_{max}

$$\frac{dP}{dV} = 0 \quad 1 + \frac{v_{dI}}{dv} = 0 \quad (2.8)$$

$$I = I_o(e^{\beta v} - 1) - I_p$$

$$\frac{dI}{dV} = I_o \beta e^{\beta v} \quad (2.9)$$

$$I + V_m(I_o \beta e^{\beta v_m}) = 0$$

$$I_o (e^{\beta v_m}) - I_o - I_p + I_o \beta V_m e^{\beta v_m} = 0$$

$$(1 + \beta V_m) e^{\beta v_m} = \frac{I_o + I_p}{I_o} = 1 + \frac{I_p}{I_o}$$

$$\beta v_m = \ln \left\{ 1 + \frac{I_p}{I_o} \middle| 1 + I_o \beta V_m \right\} \ln \left(1 + \frac{I_p}{I_o} \right) - \ln(1 + \beta V_m)$$

$$V_m + \frac{1}{\beta} \ln(1 + \beta V_m) = \frac{1}{\beta} \ln \left(1 + \frac{I_p}{I_o} \right) = V_{oc}$$

$$V_m + \frac{AKT}{q} \ln \left(1 + \frac{qV_m}{AKT} \right) = V_{oc} \quad (2.10)$$

To find $I_{max} = I_m$ at which

$$P = \max \quad P = VI$$

$$\frac{dP}{dI} = 0 \quad V + \frac{IdV}{dI} = 0 \quad (2.11)$$

But from (2.2.9):

$$\frac{dV}{dI} = \frac{dI}{dV} \frac{1}{\beta I_0} e^{-\beta V_m} \quad (2.12)$$

Thus inserting (2.2.12) in (2.2.11) and substituting ($I = I_m$, $V = V_m$) yields

$$V_m + I_m \frac{1}{\beta I_0} e^{-\beta V_m} = 0$$

$$\frac{I_m}{\beta I_0} e^{-\beta V_m} = -V_m$$

$$I_m = -\beta I_0 V_m e^{-\beta V_m} = -\frac{q V_m I_0}{AKT} e^{q V_m / AKT}$$

$$I_{\max} = I_m = -\frac{q V_m I_0}{AKT} e^{q V_m / AKT} \quad (2.13)$$

Many different designs of this general p-i-n type silicon solar cell have been developed. Single crystalline and multi-crystalline cells nowadays reach 15-20% measured solar energy conversion efficiencies. In essence silicon is not the optimal material for solar cells, its band gap of 1.1 eV (Crystalline Si) is at the lower limit for optimal solar light harvesting. The requirements for an ideal solar cell are:

1. Band gap between 1.1 and 1.7 eV
2. Direct band structure
3. Non-toxic readily available materials
4. Easy reproducible deposition technique, suitable for large area
5. Good photovoltaic conversion efficiency

6. Long term stability.

Silicon also suffers from its disadvantage of being an indirect semiconductor; as a result it is only a weakly absorbing material. For a silicon film to absorb 90% of the light, at least a 100 μm thick film is needed. Using direct semiconductors, like GaAs, a 1 μm thin film is sufficient. Because the photo carriers have to reach the p-n junction for separation, the silicon has to be of very high purity and crystalline perfection. For this reason the production of crystalline silicon is far from easy and cheap, and much attention is paid to the development of multi-crystalline and amorphous silicon solar cells, promising high efficiencies at lower costs. Nonetheless single crystalline silicon solar cells still have a market share of 43%, versus 48% for multi-crystalline silicon and only 8% for amorphous silicon, leaving 1% for non-silicon based solar devices [11].

Chapter Three

Polymer Solar Cell

3.1 Introduction

It is expected that the global energy demand will double within the next 50 years. Fossil fuels, however, are running out and are held responsible for the increased concentration of carbon dioxide in the earth's atmosphere. Hence, developing environmentally friendly, renewable energy is one of the challenges to society in the 21st century. One of the renewable energy technologies is photovoltaic (PV), the technology that directly converts daylight into electricity. PV is one of the fastest growing of all the renewable energy technologies, in fact, it is one of the fastest growing industries at present.1Solar cell

manufacturing based on the technology of crystalline, silicon devices is growing by approximately 40% per year and this growth rate is increasing. This has been realized mainly by special market implementation programs and other government grants to encourage a substantial use of the current PV technologies based on silicon. Unfortunately, financial support by governments is under constant pressure [12].

3.2 Organic Solar Cell:

An organic solar cell or plastic solar cell is a type of polymer solar cell that uses organic electronics, a branch of electronics that deals with conductive organic polymers or small organic molecules for light absorption and charge transport to produce electricity from sunlight by the photovoltaic effect [30,31].

The plastic used in organic solar cells has low production costs in high volumes. Combined with the flexibility of organic molecules, organic solar cells are potentially cost-effective for photovoltaic applications. Molecular engineering (e.g. changing the length and functional group of polymers) can change the energy gap, which allows chemical change in these materials. The optical absorption coefficient of organic molecules is high, so a large amount of light can be absorbed with a small amount of materials. The main disadvantages associated with organic photovoltaic cells are low efficiency, low stability and low strength compared to inorganic photovoltaic cells [13].

3.2.1 Basic Processes in an Organic Solar Cell:

Various architectures for organic solar cells have been investigated in recent years. In general, for a successful organic photovoltaic cell four important processes have to be optimized to obtain a high conversion efficiency of solar energy into electrical energy[32,33,34].

1. Absorption of light

2. Charge transfer and separation of the opposite charges
3. Charge transport
4. Charge collection

For an efficient collection of photons, the absorption spectrum of the photoactive organic layer should match the solar emission spectrum and the layer should be sufficiently thick to absorb all incident light. A better overlap with the solar emission spectrum is obtained by lowering the band gap of the organic material, but this will ultimately have some bearing on the open-circuit voltage. Increasing the layer thickness is advantageous for light absorption, but burdens the charge transport [13].

3.3 Types of Organic Solar Cells:

They are some types such as:

1. Dye sensitized solar cells: Electrochemical cells.
2. Polymer solar cells: Made by solution, low temperature processing.

3.3.1 Dye Sensitized Solar Cells:

In 1991 Brian O'Regan and Michael Grätzel introduced the dye sensitized solar cell (DSSC). This type of solar cell is considered as a cost effective alternative for silicon solar cells. The heart of the DSSC is a high surface area TiO₂ nanoparticulate electrode, covered with a monolayer of dye molecules. Upon photo excitation of the dye an electron is injected into the conduction band of the TiO₂. A redox couple (I⁻/I₃⁻) in an electrolyte.

Solution covering the whole TiO₂ electrode regenerates the dye, and is itself in return regenerated at the counter electrode. The layout of the DSSC is shown in figure (2.6). Often, transition metal complexes are used as dyes, e.g. RuL₂-(NCS)₂ (known as N3)

dyes), where L is a π -conjugated ligand with TiO_2 anchoring groups. The best DSSCs reach efficiencies higher than 10% measured under AM1.5 solar irradiation. The main drawback of the traditional DSSC, hampering wide use, is the application of a liquid electrolyte. This liquid electrolyte is often related to its poor thermo-stability, and responsible for the corrosion of the Pt covered counter electrode. For this reason alternatives for an electrolyte are being developed, aiming at solid-state version of the DSSC. Current state of the art quasi-solid-state dye, Figure 2.6 Schematic scheme of the traditional dye-sensitized solar cell.[35,36,37].

Sensitized solar cells based on the iodide/triiodide couple, reach stable and $> 6\%$ efficient solar cells. Commercial application of this type of solar cells in consumer products is currently explored by Hitachi Maxell for application in a film-like lightweight solar battery. One recent result, also by the Grätzel group, is a solvent-free dye-sensitized solar cell based on an ionic liquid electrolyte and using $\text{SeCN}^- / (\text{SeCN})_3^-$ as the redox couple, replacing the iodide/triiodide redox couple. This solar cell reaches measured AM1.5 efficiencies of 8%. Another elegant example of recent progress is the quasi solid-state tandem DSSC developed by Dürr and coworkers. The device layout and working Principles are shown in figure 3.1. Two separate dye-sensitized cells are connected in parallel and placed on top of each other. The cell first exposed to illumination contains a Red dye, the other a so-called black dye. This assures an effective absorption of the solar emission, leading to a high power conversion efficiency of 10.5%, measured under AM1.5 conditions [14].

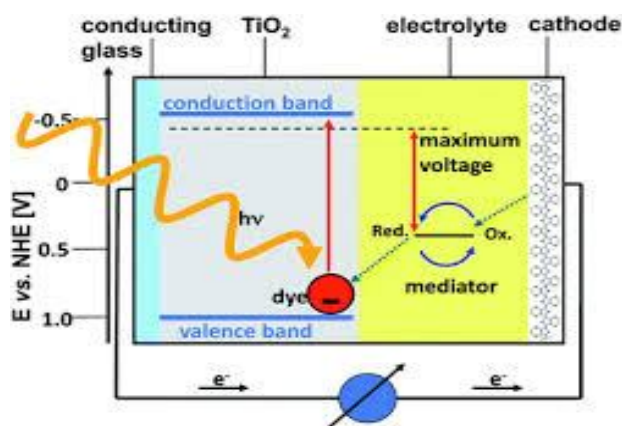


Fig (3.1) Schematic scheme of the traditional dye-Sensitized solar cell

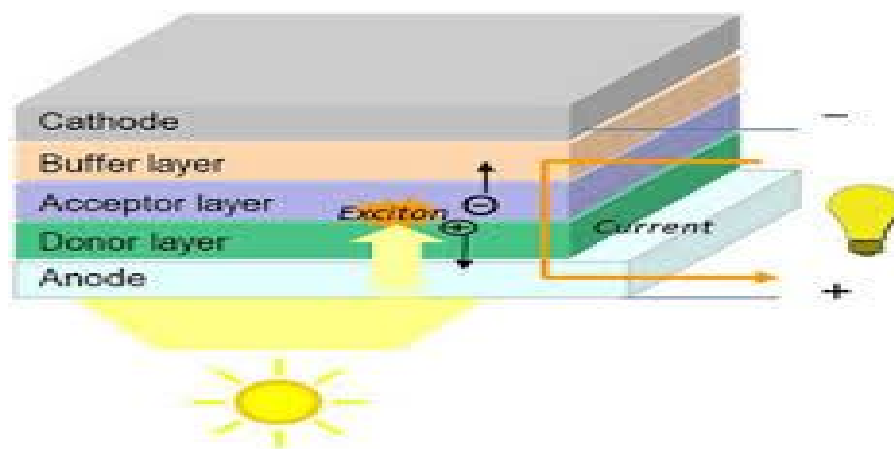
3.3.2 Polymer Solar Cells:

A polymer solar cell is a type of flexible solar cell made with polymers, large molecules with repeating structural units, that produce electricity from sunlight by the photovoltaic effect. Polymer solar cells include organic solar cells (also called "plastic solar cells"). They are one type of thin film solar cell, others include the currently more stable amorphous silicon solar cell [3]. Polymer solar cell technology is relatively new and is currently being very actively researched by universities, national laboratories, and companies around the world.[38,39,40].

Compared to silicon-based devices, polymer solar cells are lightweight (which is important for small autonomous sensors), potentially disposable and inexpensive to fabricate (sometimes using printed electronics), flexible, and customizable on the molecular level, and they have lower potential for negative environmental impact. An example device is shown in Fig. 3.1. The disadvantages of polymer solar cells are also serious: they offer about 1/3 of the efficiency of hard materials, and they are relatively unstable toward photochemical degradation. For these reasons, despite continuing

advances in semiconducting polymers, the vast majority of solar cells rely on inorganic materials.

Polymer solar cells currently suffer from a lack of enough efficiency for large scale applications and stability problems but their promise of extremely cheap production and eventually high efficiency values has led them to be one of the most popular fields in solar cell research. It is worth mentioning that state-of-the-art devices produced in academic labs – with the record currently held by Yang Yang’s group in UCLA – have reached certified efficiencies above 8% while devices produced which have remained unpublished – probably to maintain secrecy for industrial applications – are known to have already gone above 10% [15].



Figure(3.2) Polymer solar cells

3.4 Polymer Solar Cells Work:

Like all solar cells, the polymer solar cell converts light into electricity, by converting a flux of photons (light) into a flux of charged particles (a current). This conversion process is made possible by the combination of several types of materials, all having

distinct electrical and optical characteristics as described in the text presenting the polymer solar cell layer stack, but most importantly is the inclusion of semiconductors. Explain how polymer solar cell is able to generate electricity, and will do so in three sections signifying the three main steps of the conversion process which can be summarized in brief.

1. A photon incident on a semiconductor, having an energy that exceeds the semiconductor band gap, excites an electron to an unoccupied state above band gap, creating an electron-hole (e-h) pair.
2. The electron-hole pair is subsequently separated over a built-in gradient in the electrochemical potential of the solar cell.
3. Finally, the electron and hole is collected at opposite electrodes and led to recombine after being put to work in an external circuit [13].

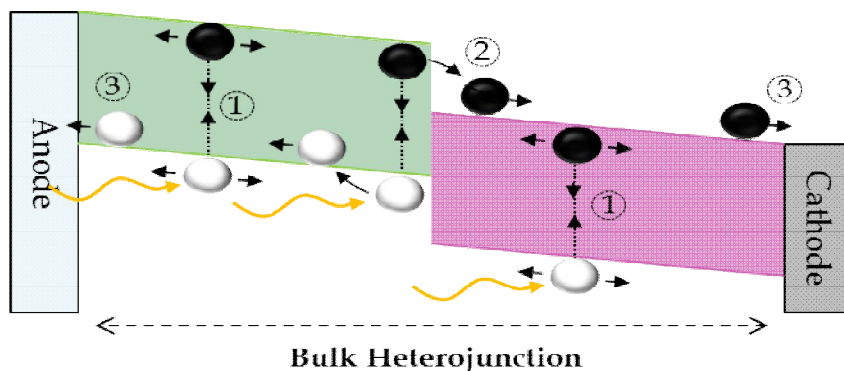


Figure (3.3). The working principleThe working principle of the solar cell. Light enters the cell through the transparent anode, and is absorbed in the bulk heterojunction layer through generation of excitons (1). The excitons diffuse in the bulk heterojunction until they either recombine or reach a donor-acceptor interface, where they separate into electrons (black) and holes (white) (2). The electrons and holes will then move to the respective anode and cathode, through the donor and acceptor material phase (3) [16].

3.5 Consist of Polymer Solar Cell:

Making a polymer solar cell is often done using polymers dissolved in organic solvents, which are transferred by printing or coating methods to a substrate. The materials are added in layers in a certain order to build a solar cell stack. The materials needed in the solar cell stack are; a central active (light absorbing) layer, which translate the impinging photons into separate electrons and holes, a selective charge transport layer on each side of the active layer, allowing only passage of either electrons (ETL) or holes (HTL), and finally two electrodes for extracting the charges from the solar cell, with at least one of the electrodes having a requirement of transparency such that the light can pass through and reach the active layer [17].

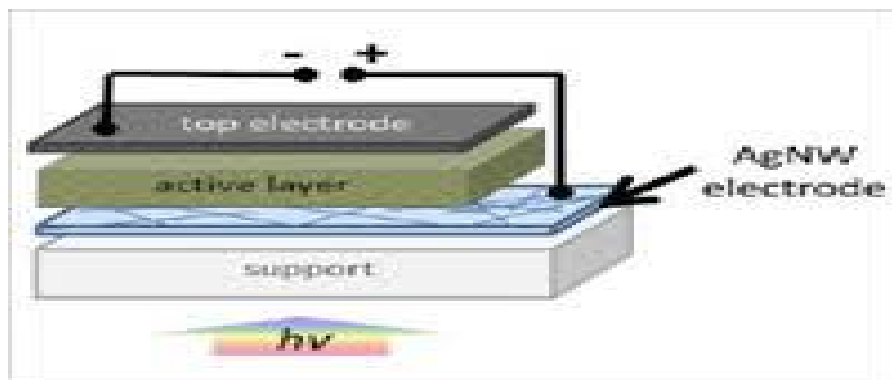


Figure (3.4) Consist of Polymer Solar Cell

3.5.1 Geometries:

Polymer solar cells are often divided into two groups based on the solar cell stack geometry. A normal and an inverted geometry. The definition of the two geometries lies within the direction of the charge flow. In a normal geometry solar cell the substrate and the transparent electrode on it is the positive electrode, with the light passing through the substrate and this electrode before being absorbed in the active layer. The top electrode is

then the negative electrode. In the inverted geometry the two electrodes and the charge selective layers are switched around, such that the transparent electrode at the substrate is the negative electrode, with a ETL layer between it and the active layer, while the top electrode is the positive electrode with a HTL layer between it and the active layer [18].

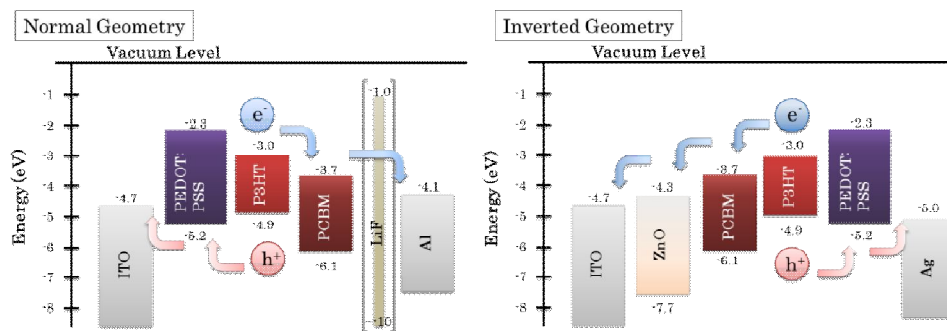


Figure (3.5) Energy levels for normal and inverted geometry solar cells

3.5.2 Active layer:

The active layer consists of two components in the polymer solar cells. A donor which absorbs the light and an acceptor which extracts the electron from the excitonic bound electron hole, resulting in an electron travelling in the acceptor phase of the active layer and a hole travelling in the donor phase. For this to occur successfully the low lifetime of an excitation in the donor materials necessitates a donor-acceptor boundary at which the excitation can be broken within approximately 10 nm. Furthermore, since the holes and electrons have to travel out of the active layer towards the electrodes, the domains of donor and acceptor needs to be connected in an interconnected network allowing both efficient dissociation of the excitations and efficient transport of the charge carriers to the respective electrodes. In this research used polymer with natural dye as active layer [18].

3.5.2.1 Polymer (MEH-PPV):

Poly [2-methyl-5-(2-ethyl-hexyloxy)-1, 4-phenylene vinylene](MEH-PPV) is widely used in the fabrication of polymer light emitting diodes and as donor material in the fabrication of bulk-heterojunction photovoltaic cells because of its excellent processibility and favorable electronic and spectroscopic properties. It is very important to understand the relationship between the morphology and the processing conditions, and their influence on the electronic and photonic properties of polymer thin films [19].

3.5.2.2 Dyes:

In these polymer solar cells used seven different types of dyes:

- Ecerchrom:

Preferred IUPAC name: Sodium 1-[1-Hydroxynaphthylazo]-6-nitro-2-naphthol-4-sulfonate
Systematic name: Sodium 4-[2-(1-hydroxynaphthalen-2-yl)hydrazin-1-ylidene]-7-nitro-3-oxo-3,4-dihydronaphthalene-1-sulfonate
Other names: Sodium 4-[2-(1-hydroxynaphthalen-2-yl)hydrazin-1-ylidene]-7-nitronaphthalene-1-sulfonate;

Solochrome Black T; ET-00 Eriochrome Black T is a complexometric indicator that is part of the complexometric titrations, e.g. in the water hardness determination process. It is an azo dye. Eriochrome is a trademark of Ciba-Geigy. In its protonated form, Eriochrome Black T is blue. It turns red when it forms a complex with calcium, magnesium, or other metal ions [19].

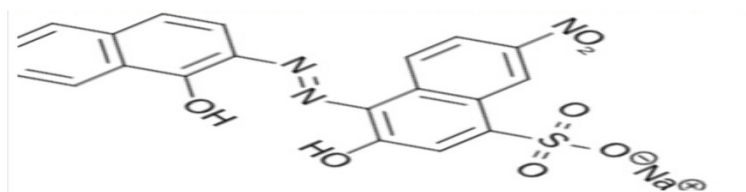


Figure (3.6) Ecerchrom structure

- Rhodamine B
- Coumarin 500
- Blue 8GX
- DDTTC
- Hena
- Roselle

3.5.3 Transport layers:

The transport layers are based on materials which have the capability of being able to primarily transfer either electrons or holes due to a suitable positioning of the energy levels [18].

3.5.4 Electrodes:

The main issue with choosing the electrodes is to find electrodes with a suitable energy level and with one of the electrodes being transparent to allow sufficient light to enter the solar cell. The most commonly used electrode material has been indium tin oxide (ITO), due to a high optical transmission combined with a low resistance; on glass a transmission of >85% at <10 Ohm/sq. is often seen. Another electrode used in solar cell is Fluorine-doped tin oxide (FTO) coated glass is electrically conductive and ideal for use in a wide range of devices, including applications such as opto-electronics, touch screen displays, thin film photovoltaics, energy-saving windows, RFI/EMI shielding and other electro-optical and insulating applications. Fluorine doped tin oxide has been recognized as a very promising material because it is relatively stable under atmospheric conditions, chemically inert, mechanically hard, high-temperature resistant, has a high tolerance to physical abrasion and is less expensive than indium tin oxide(ITO) [18].

3.5.5 Substrates:

When making polymer solar cells the substrates used for supporting the layered solar cell stack, can be divided into two distinct groups: glass and plastics. The two most commonly used types being floated glass substrates with ITO transparent electrodes used [18].

Chapter Four

Literature Review

(4-1)introduction

- Recently many types of solar cells were fabricated. Their materials and made operation are different (41,42,43,44,45)Some of them are based dyes and nano materials(46,47,48)While others are based on polymers (49,50,51) Her some attempts are presented.

(4-2) Polymer solar cells are one of the promising alternative energies which can be easily manufactured with low cost. In this work polymer cells with different thicknesses and three different type of organic dyes (Rhodamine 6G, Coumarin 500 and Dibenzocyanin 45) are used in fabrication. The effect of the concentration of different organic dye on various electrical and optical properties of the samples produced has been studied. It was found that when the conjugate polymer layer deposition on the slides at low speeds by spin coating technique (increasing the thickness of the conjugate polymer layer), results gave a recognized higher efficiency in the tested cell. The use of the organic dye (DDTTCI) led to improve in efficiency and absorption coefficient of light in the samples used. In addition, the optical absorption spectra were recorded for those samples with a UV-VIS spectrophotometer (model: UV mini-1240) within the wavelength range of 200–800 nm, at room temperature. The samples show variations in absorption coefficient directly depending on the type of organic dye used as well as the concentration of conjugate polymer. The short-circuit current, open circuit voltage and the fill factor of each sample have been calculated. The efficiency was found in the range of(10.28-1.744)% for designed samples . Materials &Methods

The material utilized in this work:

1- Titanium Dioxide glass (ITO) and conjugate polymer Poly [2-methoxy-5-(2-ethylhexyloxy)-1,4phenylenevinylene] (MEH-PPV) beside different organic dyes (Rhodamine 6G- Coumarin 500 – Dibenzocyanin 45).

2- The coating will done using the Spin Coating Machine.

3-The concentration of different organic dyes (Rhodamine 6G- Coumarin 500 – Dibenzocyanin 45) was changed and the corresponding output current voltage, power and efficiency were recorded.

4- The empirical relations are compared with previous studies and theoretical relations.

ITO (Indium Tin Oxide) is a transparent conductive material. It is a mixture of indium oxide (In_2O_3) and tin oxide (SnO_2). ITO is used as one of the electrodes in the solar cell.(6)

MEH-PPV Poly[2-methoxy-5-(2-ethyl-hexyloxy)-1,4-phenylenevinylene] (MEH-PPV) seen in Figure 1 is the active material of the solar cell. It is a modification of PPV, modified by the MEH-group, which makes it more soluble in some liquids. It is appearance in dark brown or red granules (6).

(4-3)Solar cells were fabricated from (Muscovite/ TiO_2 / Dye/Al), the effect of temperature, concentration and light intensity on the electrical properties of (Muscovite/ TiO_2 /Dye/Al) was studied. The relationship between current and voltage was found to be logarithm, which is in agreement with the ordinary relation for solar cells. When dye concentration was increased the conductivity, fill factor and efficiency were also increased. This result is found to be in conformity with the theoretical relations. The small energy gaps for their samples show that they are semiconductors. The maximum efficiency obtained is 33.2%.

Solder (Sn/Pb) Tin/lead solders, also called soft solders, are commercially available with tin concentrations between 5% and 70% by weight. The greater the tin concentration, the greater the solder's tensile and shear strengths. Alloys commonly used for electrical soldering are 60/40 Tin/lead (Sn/Pb) which melts at 370 °F or 188 °C and 63/37 Sn/Pb used principally in electrical/electronic work.

MATERIALS

Titanium dioxide (TiO_2) is a multifaceted compound. Titanium dioxide is a fascinating low-cost material exhibiting unique properties of stability and photo activity. It is useful for practical applications in areas such as the preparation of

hybrid organic/TiO₂ materials or as thermo labile devices substrates. Titanium oxide is also used as a semiconductor.

Dye-sensitized semiconductor systems were recently introduced as alternatives to conventional semiconductor materials in solar cells. Additional applications are in photo catalysis, sensors etc. A thin film of a nanostructure wide band gap semiconductor (only absorbing UV- light), typically TiO₂, SnO₂, or ZnO, sensitized to visible light by an organic dye molecule or other sensitizer is the key component of the system. Light absorption by the sensitizer initiates electron transfer from the semiconductor to the sensitizer, where free electrons can be harvested as current (solar cell), used for redox actions (catalysis), or constitutes an electrical impulse (sensor). Rhodamine B is a family of related chemical compounds, fluorine dyes. It is used as a dye and as a dye laser gain medium. Molecular Formula . 283123Mica Group is a complexity of alumina silicate that consists of potassium, magnesium, iron (Fe). Mostly, mica is found in Granite Rhyolite, Phyllite or Mica Schist (Muscovite or white mica, formula KAl₂(AlSi₃O₁₀)(OH)₂)

.(4-4) The energy gaps for CuO and ZnO are obtained by using optical absorption and transmittance. The optical absorption for CuO and ZnO, shows a peak corresponding to the energy gaps in the ranges (1.3 – 2 eV) and (2.2 – 3.6 eV) respectively. These values are compatible with the observed values 0.2 eV and 3.3 eV for CuO, which acts as a p-type semiconductor, and for ZnO, which acts as an n-type semiconductor. These values measure acceptor and donor levels for CuO and ZnO. However the transmittance spectrum for CuO and ZnO shows band gaps about $E_g \sim 3.7$ eV, and 3.6 eV. These values measure the energy gap between conduction and valence band for both, respectively. The solar cell fabricated from

FTO/ ZnO/ CuO/ Al shows decrease in efficiency as the cross section area increase.

MATERIALS and Methods

Zinc oxide (ZnO) is considered as an excellent materials in this work because of it's a wide band gap (~3 – 3.5 eV), high free carrier concentrations for electron conduction (10^{18} cm^{-3}), and very similar electron affinity (4.35 eV)[6]. These properties suggest minimal voltage loose during charge transport across the interface. The oxide has been shown to form a chemically stable p-n hetero junction[7] such that the photo generated electrons (minority carriers) from the absorber can be collected effectively and transported to their respective contacts with minimal current losses. Also the low toxicity and relatively easy processing of ZnO makes it an attractive with other materials. As n-type metal oxide semiconductors zinc oxide (ZnO) has attracted intensive research attention owing to its diverse interesting properties such as electro-optical, piezoelectronic, and magnetic properties. With a direct band gap and relatively large exciting binding energy of (60 m eV) [8].

Cupric oxide (CuO) is another metal oxide material that has been substantially explored for various fields of applications. As a p-type semiconductor having a narrow band gap of (1.35 eV), CuO has great potential as a field emitter, catalyst and as a gas sensing medium. The physiochemical properties of CuO such as the photoconductivity and the photochemistry can be tailored for fabricating optical switches and solar cells [9]. As a solar material, cuprous oxide Cu_2O has the advantages of low cost, great availability, non-toxic nature for use in thin film solar cells, a theoretical solar efficiency of about 9-11% an abundance of copper and the simple and inexpensive process for semiconductor layer formation. In addition to everything else, cuprous oxide has band gap of 2.0 eV which is within the

acceptable range for solar energy conversion, because all semiconductors with band gap between 1 eV and 2 eV are favorable material for photovoltaic cells [10].

UV –VIS 1240 Spectrophotometer device was used to measure the absorption and the transmission of the solutions and solvents before use in cavity. It is covering a wavelength from 190-1100 nm with auto lamp switch from visible to ultraviolet range. UV-VIS spectrophotometer from SHIMADZU contains a cell of thickness 0.1 mm as a sample holder.

(4-5) Two types of highly ordered TiO₂ nanotubes were grown by anodic oxidation on titanium foil and titanium films deposited by rf-sputtering onto transparent conducting glass. The anodized foil sample exposes nanotube arrays with pore diameter of about 130 nm and an average nanotube length of about 6 nm, while the nanotube arrays grown on the deposited titanium film reveal nanotube arrays with pore diameter of about 60 nm and an average nanotube length of about 400 nm. The photo-electrochemical parameters for both samples were characterized and compared to each other. Observations showed that the back-side illuminated dye-sensitized solar cell (DSSC) exhibit higher value of short-circuit current density compared with the front-side illuminated cell, which was ascribed to the increased light harvesting provided by the thick layer of the TiO₂ nanotube arrays. On the other hand, the limitation of growing longer nanotube arrays on the front-side illuminated DSSC was found to hinder progress in harvesting light due to the decreased dye adsorption by the very thin layer of nanotube arrays. Therefore significant photoconversion efficiencies may be obtained by the front-side illuminated DSSC with an increase of the nanotube-array length to several micrometers.

Materials and Methods Highly-ordered TiO₂ nanotube arrays were grown by

first one was TiO₂ nanotube arrays grown on titanium foil, where the foil was anodized in a viscous electrolyte of ethylene glycol containing ammonium fluoride (NH₄F) with a concentration of 1.75 wt% at constant voltage of 60V for 60 minutes. The second type of nanotube arrays was grown by anodization of titanium films (1 nm thick) deposited by rf-sputtering onto transparent conducting glass (TCO). The anodization was performed at a constant voltage of 20 V for 15 minutes in an ethylene glycol electrolyte containing 1.5 wt% NH₄F. Both types of nanotube arrays were annealed after anodization at 550°C for 2 hours with heating and cooling rates of 20°C/ min to improve their crystallinity. After cooling, the resulting electrodes were immersed for 24 h in a solution of the sensitizer: cis-di(thiocyanato)bis(2,2'-bipyridyl-4,4'-dicarboxylate)ruthenium(II) (N-719, Solaronix Inc.) dissolved in absolute ethanol. The dye-adsorbed mesoporous electrode faced to a platinum sputtered conducting glass as a counter electrode. A drop of the redox electrolyte containing 0.3M LiI and 0.03M I₂ in propylene carbonate, was introduced between the clamped electrodes by the capillary force to finalize the assembly of the DSSC. The photocurrent (I) and photovoltage (V) of the cell were measured with an active area of 0.08 cm² using simulated sunlight at AM-1.5 (standard spectrum at the Earth's surface) produced by Oriel 91192 solar simulator. The anodized samples were assembled into front-side and back-side illuminated DSSCs according to their illumination side. Figure 1 illustrates the assembly of the front-side and back-side illumination DSSCs. In the back-side illumination DSSC, the cell is illuminated through a transparent counter electrode coated with 2 nm thin layer of platinum (Pt), while in the front-side illuminated DSSC, the cell is directly illuminated through the transparent back side of its working electrode

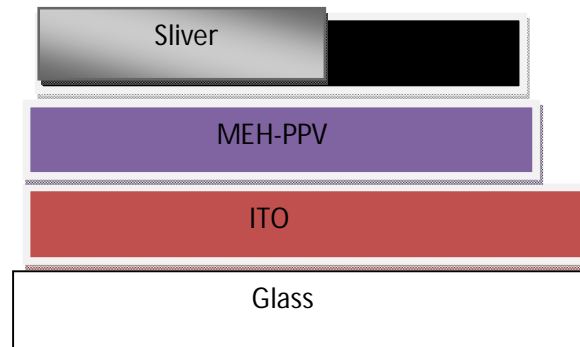


Fig -4-1: schematic structure of polymer solar cell formed with a single organic layer of MEH-PPV

4-6 The Materials of an Organic Solar Cell

4-6-1 polymer

Polymer is a Greek phrase which means many parts. Large molecules made of repeating units of smaller molecules. Small molecules are called "monomers" monomers link together like a chain resulting in new and exciting properties.

Conjugated polymers are organic macromolecules with alternating single and double bonds. Conjugated polymers are organic semiconductors, the semi-conducting behavior being associated with the pi-molecular orbitals delocalized along the polymer chain. Due to the sp² hybridization of the electron system, conjugated polymers are mostly planar, extended macromolecules.

They combine the optical and electrical properties with the mechanical advantages for preparation of optoelectronic devices.

There is one unpaired p_z-electron per C-atom, which forms pi-pi* conduction and valence bands in the macromolecule due to the fact, that they describe a one-dimensional crystal[20].

The Noble Prize in Chemistry 2000 was awarded jointly to Alan J. Heeger, Alan G. MacDiarmid and Hideki Shirakawa "for the discovery and development of conductive polymers". This discovery led, subsequently, to the discovery of electroluminescence in a poly(p-phenylenevinylene) (PPV) [12]. In 1990 the first light-emitting products based on electroluminescence in conjugated polymers have already been launched at the consumer market by Philips (The Netherlands) in 2002, whereas light-emitting products based on conjugated molecules have been introduced by the joint venture of Kodak and Sanyo (Japan). Going from discovery to product within a little bit more than one decade truly holds a huge promise for the future of plastic electronics. Other emerging applications are coatings for electrostatic dissipation and electromagnetic-interference shielding [21].

Conjugated polymers and molecules have the immense advantage of facile, chemical tailoring to alter their properties, such as the band gap. Conjugated polymers combine the electronic properties known from the traditional semiconductors and conductors with the ease of processing and mechanical flexibility of plastics.

In this research we used poly (2-methoxy-5-(2'-ethyl-hexyloxy)-1,4 phenylene) (MEH-PPV) due to the corresponding internal quantum efficiency. The absorbed photons to electrons, is estimated to be nearly 100% in the short circuit case. The main limiting factor towards higher efficiencies is the spectral mismatch of the active layer absorption, with a maximum around 500 nm, to the terrestrial solar spectrum with a maximal photon flux between 600 and 800 nm [14]. Therefore, the use of low band gap $\{E_g \sim 2.0 \text{ eV}\}$ polymers is a viable route to increase the amount of absorbed photons and consequently the power efficiency of solar cells [22].

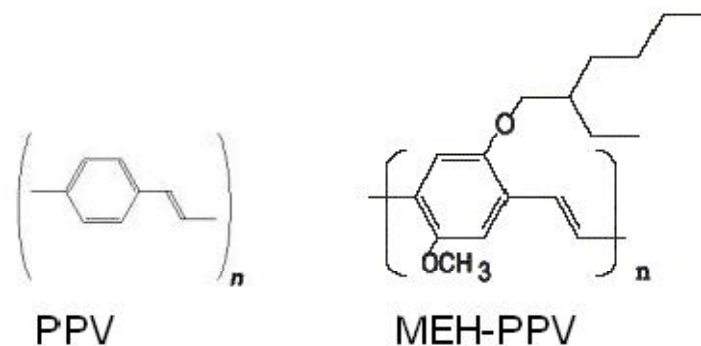


Fig 4-2: The two figures is the monomer of MEH-PPV (right) and the monomer of PPV (left)

Characterized polymers that can be turned into solids or semi-conductive for electricity as we mentioned earlier, and to make solar cells must first add a certain percentage of oxidizing substances or shorthand to become Article polymeric. Similar properties semiconductors inorganic and lead impurities to situations within the scope of the gap between the bands valance band conduction. has found that the energy gap of the semiconductor in some polymers ranging from (1.5-3 ev) and thus wider than the gap in the energy inorganic materials that range where the energy gap between 0.1-2.2 ev in and fit so with photon energy in the visible range of the solar radiation[23].

4-6-2 ITO

ITO (Indium Tin Oxide) is a transparent conductive material. It is a mixture of indium oxide (In_2O_3) and tin oxide (SnO_2). ITO is used as one of the electrodes in the solar cell. ITO can absorb light at the same wavelength as MEH-PPV. This is important because only the light absorbed by MEHPPV may result excitations.

4-6-3 Rhodamine B

Constitution 2-[6-(Diethylamino)-3-(diethylimino)-3H-xanthen-9-yl] benzoic acid
 Rhodamine 610 - $\text{C}_{28}\text{H}_{31}\text{N}_2\text{O}_3\text{Cl}$ · MW: 479.02

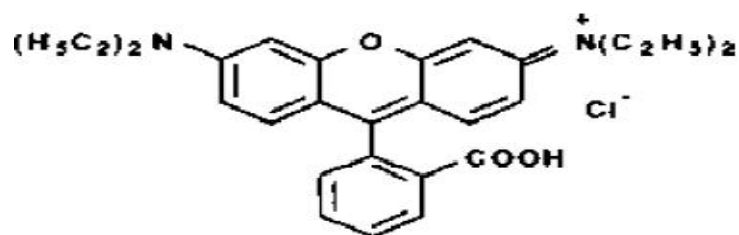


Fig (4.3) Rhodamine B

Characteristics Lambdachrome® number: 6100 CAS registry number: 81-88-9
 Appearance: green, crystalline solid Absorption maximum (in ethanol): 552 nm
 Molar absorptivity: $10.7 \times 10^4 \text{ L mol}^{-1} \text{ cm}^{-1}$ Fluorescence maximum (in ethanol): 580 nm for research and development purposes only.

4-6-4 Coumarin 500

Constitution

$\text{C}_{12}\text{H}_{10}\text{NO}_2\text{F}_3$ · MW: 257.21

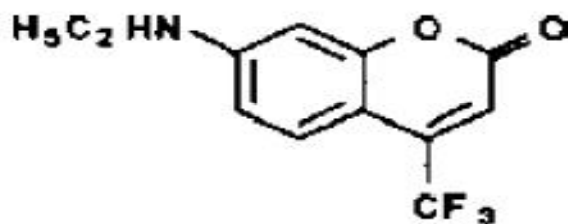


Fig (4-4) Coumarin 500

Characteristics

Lambda chrome® number: 5010 CAS registry number: - Appearance: yellow, crystalline solid Absorption maximum (in ethanol): 395 nm Molar absorptivity:

$1.85 \times 10^4 \text{ L mol}^{-1} \text{ cm}^{-1}$ Fluorescence maximum: - For research and development purposes only

4-6-5 Blue 8GX

Constitution 5-Amino-9-diethyliminobenzo[a]phenoxazonium

Perchlorate $\text{C}_{20}\text{H}_{20}\text{N}_3\text{O}_5\text{Cl}$ · MW: 417.85

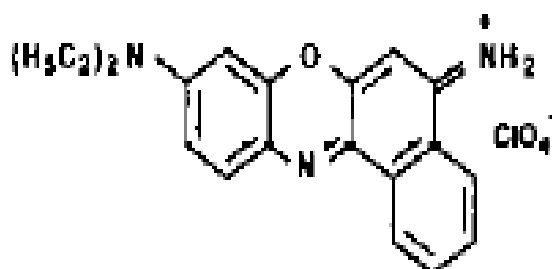


Fig (4.5) Blue

8GX

Characteristics λ_{max} number: 6900 CAS registry number: 53340-16-2

Appearance: green, crystalline solid Absorption maximum (ethanol): 633 nm Molar absorptive: $7.75 \times 10^4 \text{ L mol}^{-1} \text{ cm}^{-1}$ Fluorescence maximum (in bas. ethanol): 672 nm for research and development purposes only.

4-6-6 DDTTCI

Constitution 3,3'-Diethyl-4,4',5,5'-dibenzothiatriccyanine

Iodide Hexadibenzocyanine $\text{C}_{45}\text{H}_{33}\text{N}_2\text{S}_2\text{I}$ · MW: 644.43

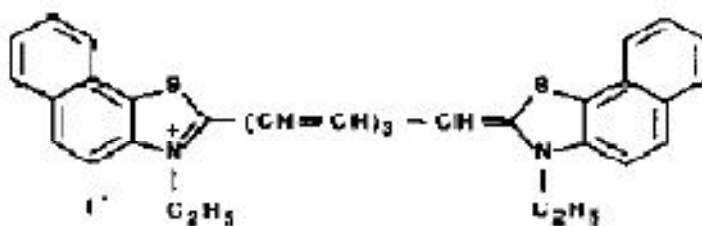


Fig (4.6) DDTTCI

Characteristics
 Lambda
 chrom@ number: 9280
 CAS registry number: -
 Appearance: bronze colored, crystalline solid
 Absorption maximum (in ethanol): 798 nm
 Molar absorptivity: $19.6 \times 10^4 \text{ L mol}^{-1} \text{ cm}^{-1}$
 Fluorescence maximum: -

For research and development purposes only

4-7 The principle of polymer solar cell Desired HOMO/LUMO energy level

The Highest Occupied Molecular Orbital (HOMO) and Lowest Unoccupied Molecular Orbital (LUMO) of the polymer should be carefully tuned for several considerations. First of all, the HOMO energy level of a material, which describes the accessibility of the material molecule to be oxidized, reflects the air stability of the material. The oxidation threshold of air is $-5.2 \text{ eV} \sim -5.3 \text{ eV}$ against vacuum level. Therefore, the HOMO level cannot be more positive than this value to provide the air stability to the polymer. Secondly, the maximum open circuit voltage (V_{oc}) is correlated to the difference between the LUMO energy level of Rhodamine 6G and the polymer's HOMO energy level based on experimental evidence [24]. Therefore, in order to achieve high V_{oc} in the device, HOMO level should be reasonably low.

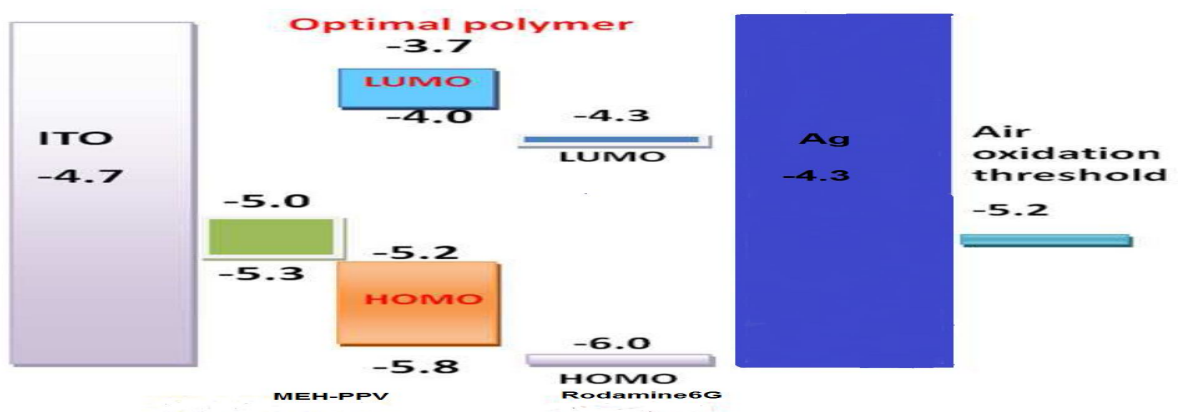


Fig4-7: Optimal HOMO/LUMO energy level of optical polymer used in BHJ solar cell with RohdaminB as acceptor [25].

To ensure efficient electron transfer from the polymer donor to the MEH-PPV acceptor in the BHJ blend, the LUMO energy level of the polymer material must be positioned above the LUMO energy level of the acceptor by at least 0.2-0.3 eV. Based on these factors, as shown in [Fig3-3] , the ideal polymer HOMO level should range from -5.2 eV to -5.8 eV against vacuum level due to the compromise of stability, band gap and open circuit voltage.

The ideal polymer LUMO level should range from -3.7 eV to -4.0 eV against vacuum level to assist electron injection from polymer to acceptor.

4-8 The principle of polymer solar cells

Various architectures for organic solar cells have been investigated in recent years. In general, for a successful organic photovoltaic cell four important processes have to be optimized to obtain a high conversion efficiency of solar energy into electrical energy.

- Absorption of light
- Charge transfer and separation of the opposite charges
- Charge transport
- Charge collection

For an efficient collection of photons, the absorption spectrum of the photoactive organic layer should match the solar emission spectrum and the layer should be sufficiently thick to absorb all incident light. A better overlap with the solar emission spectrum is obtained by lowering the band gap of the organic material, but this will ultimately have some bearing on the open-circuit voltage. Increasing the layer thickness is advantageous for light absorption, but burdens the charge transport.

Polymer solar cells are typically comprised of a photon absorbing active layer sandwiched between two electrodes and placed on a substrate of glass or clear plastic foil[26]. One of the electrodes is transparent in order to allow photons to penetrate into the absorbing layer. Indium tin oxide (ITO) is commonly used as transparent electrode and metals like aluminum, calcium or silver as the other electrode. The absorbed photons excite electrons in the active layer and thereby promoting them from the highest occupied molecular orbital (HOMO) to the lowest unoccupied molecular orbital (LUMO) within the polymer. The excitation of an electron leaves behind an empty electron space in the HOMO level called “a hole”[27]. The hole and the excited electron are not totally independent but associated to one another in a form called an excitation [28].

In most organic molecules excitation is followed shortly by relaxation, typically in the form of recombination when the excited electron falls back into the hole. This releases the absorbed energy as either radioactive or non-radioactive energy which cannot be utilized for electricity. In polymer solar cells recombination still occurs but not right away. Instead the excitation is separated into a free hole and a free electron which are then transported to different electrodes due to differences in the electrodes' ionization energy. The electron is then forced to travel from one electrode through an external circuit to the other electrode in order to recombine with the hole. The absorbed energy can then be utilized in the external circuit [29]. The separation of the electron from the hole in polymer solar cells is achieved by utilizing an electron accepting material along with the electron donating polymer [30]. The electron donor and acceptor are mixed to form a heterogeneous active layer. This type of device is known as a bulk hetero-junction solar cell. The charge separation occurs when an excitation has diffused to the donor/acceptor interface [31]. Here a difference in potential of the two phases pulls the electron into the electron accepting phase leaving behind the hole in the electron donating phase.

The electron and the hole are then free to move through their respective phases to the electrodes [32] (figure 4-2).Upon excitation the electron is transferred into the electron accepting phase due to an offset in the LUMO levels of the donor and acceptor materials. Charges are then transported to their respective electrodes.

In order for a material to act as an electron acceptor it has been found empirically that the potential of the LUMO level has to be at least 0.3 eV lower than the potential of the LUMO level of the electron donor [33].

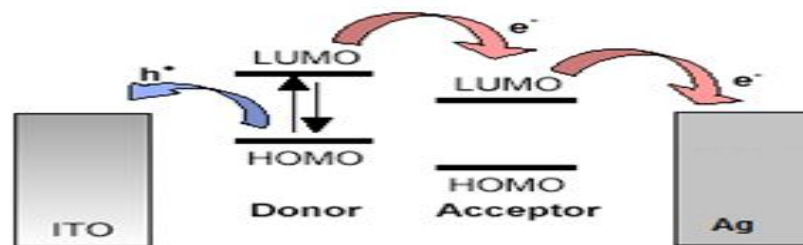


Fig4-8: Charge separation within the active layer

4.9The Methodology

For the purpose of the present study polymeric devices were made following the generally accepted methods. The fabrication process started by preparing the polymer and the dye of interest then spin coated on indium tin oxide glass. Silver electrode was used to complete the formation of organic polymer solar cell. The formed devices were characterized by Ultra violet-visible spectroscopy.

(4-9)Summary and critique

All attempts made in the exhibited papers are concerned with the effect of polymer thickness on efficiency. Some studied ZnO and CuO, and CuO and their optical and electrical properties. But none of them compare the effect of energy gap of both chemical dye on their efficiency.

4-10 Sample preparation

The polymer solar cell was made on ITO glass. The ITO glasses were firstly cleaned by ethanol and distilled water. 10mg of poly (2-methoxy-5-(2'-ethyl-hexyloxy)-1,4-phenylenevinillin) (MEH-PPV) was dissolved into 0.5ml of chloroform and 3mg of dyes dissolved into 0.5 of high pure chloroform was deposited on polymer. Been insert electrical circuit containing the (voltmeter and Ammeter and a light source "Lamp with the intensity radiological" and a solar cell). Cell was offered to light and fulfilled taking the results of the current and voltage .

4-11 Spin coater

Usually a polymer thin film is made by the spin coating method. It is versatile and simple .The number of round depended of the voltage, the number of round proportional increases with the voltage, then the thickness decreases with an increase in the number of round.



Fig4-9: Spin coating device

4-12-Device UV- visible spectrometer

Measures absorbance, emission and permeability. The range from 190-1100nm range for registration -3.99-3.99. Named UV mini 1240 spectrophotometer made in a Japanese company called Shimadzu measures two types of fluids and can measure the solids in the form of slides. The device components are: light source – a cell sample – uniform wavelength – Scout – Screen. The working principle of the device

Each of the articles has a characteristic absorption of a specific wavelength. Any material have a certain extent of absorption to unchangeable but the material properties change works on the principle Berlambert based on assumptions:

*Absorbance is directly proportional to the concentration.

*Absorbance is directly proportional to the length of the optical path within the sample.



Fig 4-10: UV device

4-13-Device X- Ray Diffraction meter device

Made in Japan by Rigaku Company under name Oitina VI



Fig 4-11:X- Ray Diffraction meter device

4-14-Device scanning Electron Microscope device

This device made in Cheek from TESCAN O₂company .Modal 00584



Fig 4-12:scanning Electron Microscope device

Chapter Five

The Effect of Dye type on the performance of solar cell

5-1 Introdoction

In this work 7 polymer solar cells doped with some chemical and natural dyes were prepared at Alneelain University Lap. Their absorption morphology and performance were studied

5.2 Results

In this chapter we present the results and curves obtained by the Ultra-Violet device and the IV characteristic curve. And X-ray diffraction and at last scanning electronic microscopy (FESEM) image

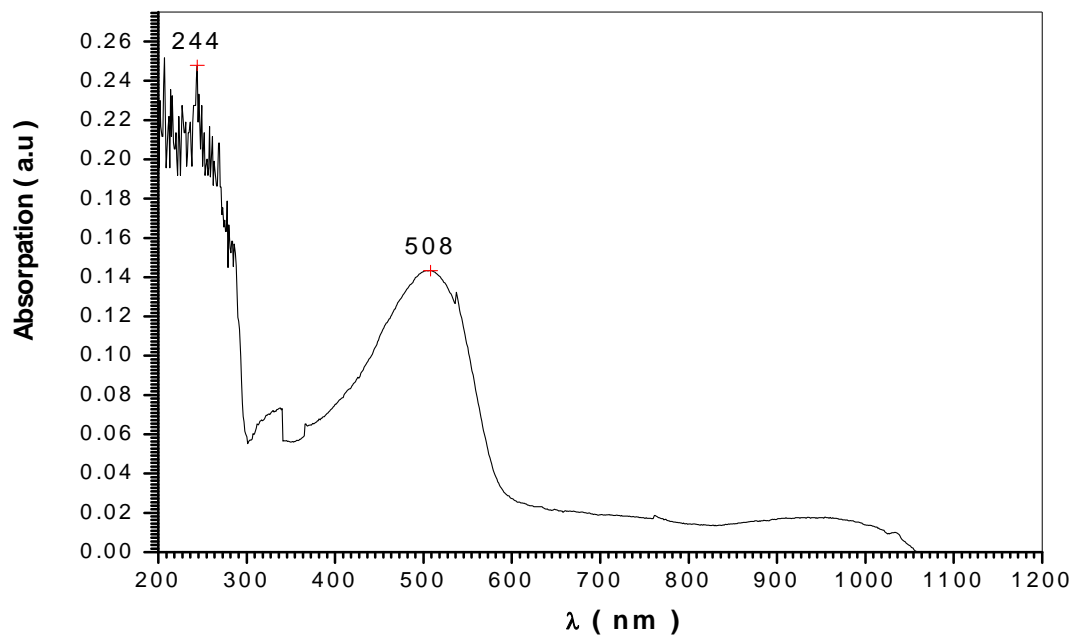


Fig (5-1)spectra of Coumarin500 Absorption in room temperature

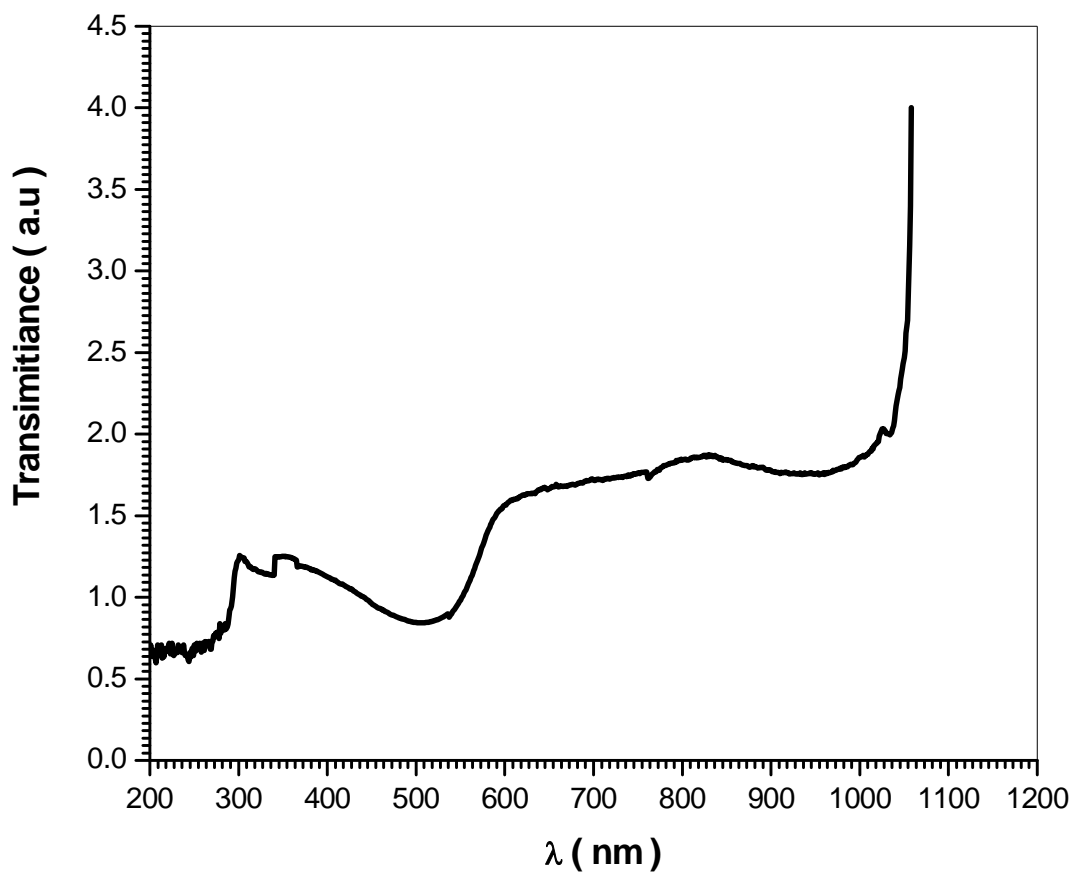


Fig (5-2) shows the relation between transparent and wavelength of Coumarin 500, we had been found rapid decrease in low energies and sudden increase in high wavelengths intransparent value.

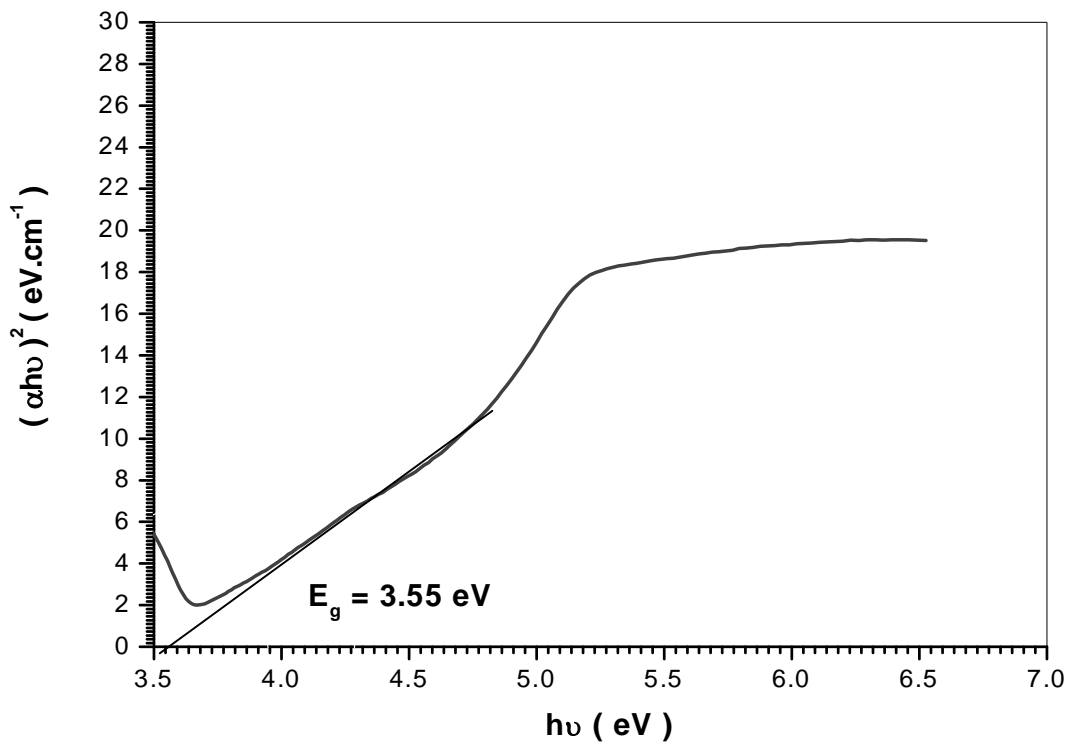


Fig (5-3) the optical energy gap (E_g) value of Coumarin 500. The optical energy gap (E_g) has been calculated by the relation $(\alpha h\nu)^2 = C(h\nu - E_g)$ where (C) is constant. By plotting $(\alpha h\nu)^2$ vs photon energy ($h\nu$) as shown in fig .

Table5-1the current and voltage of Coumarin 500 solar cell

(v)v	(I)MA
1.942	31.316
1.962	31.316
1.982	31.316
1.992	31.316
2.002	31.316
2.012	31.316
2.092	31.316
2.052	29.316
2.062	25.316

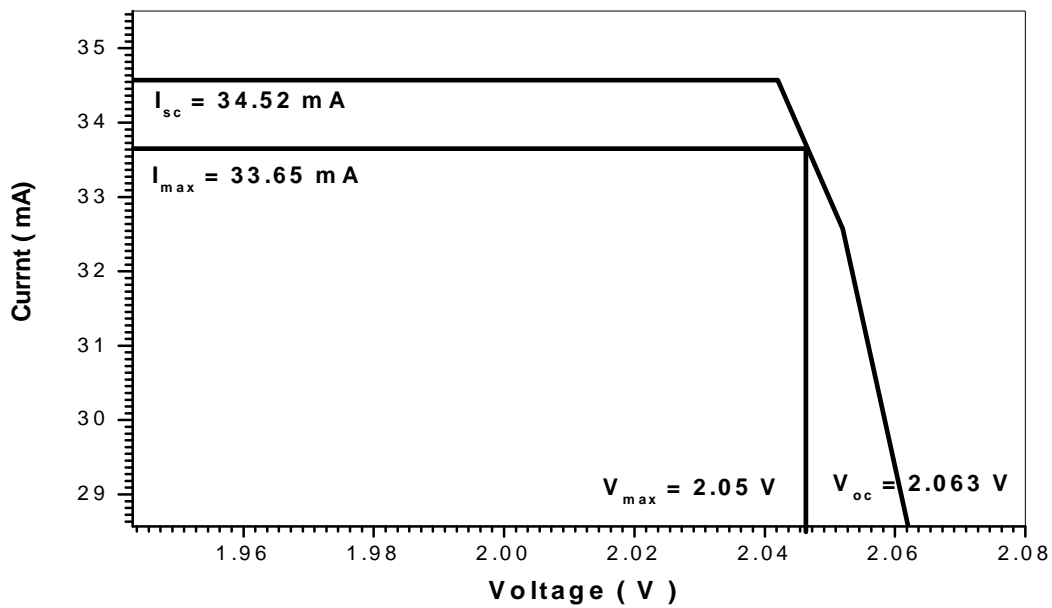


Fig (5-4)several factors for characterization of Coumarin 500solar cell

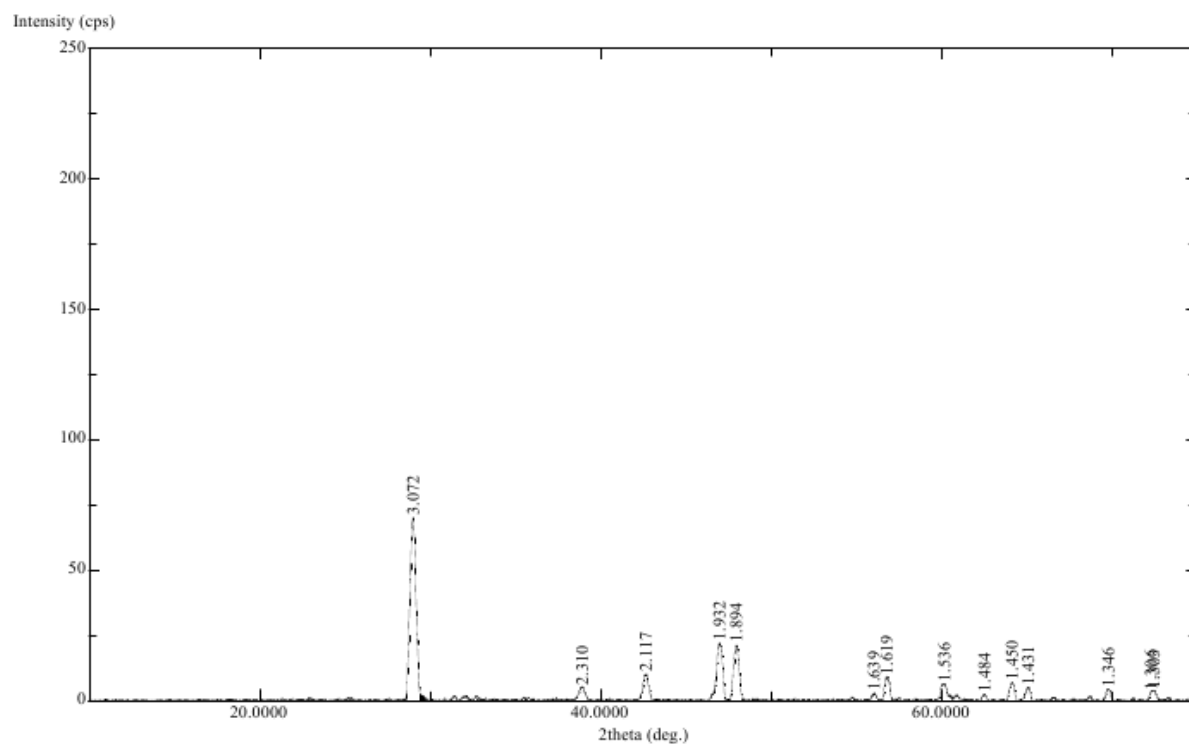


Fig (5-5) X-ray diffraction for Coumarin 500 measurements demonstrated that the Coumarin500 is a polycrystalline structure



Fig (5-6)Field emission scanning electronic microscopy (FESEM) images of Coumarin500 with different magnification .

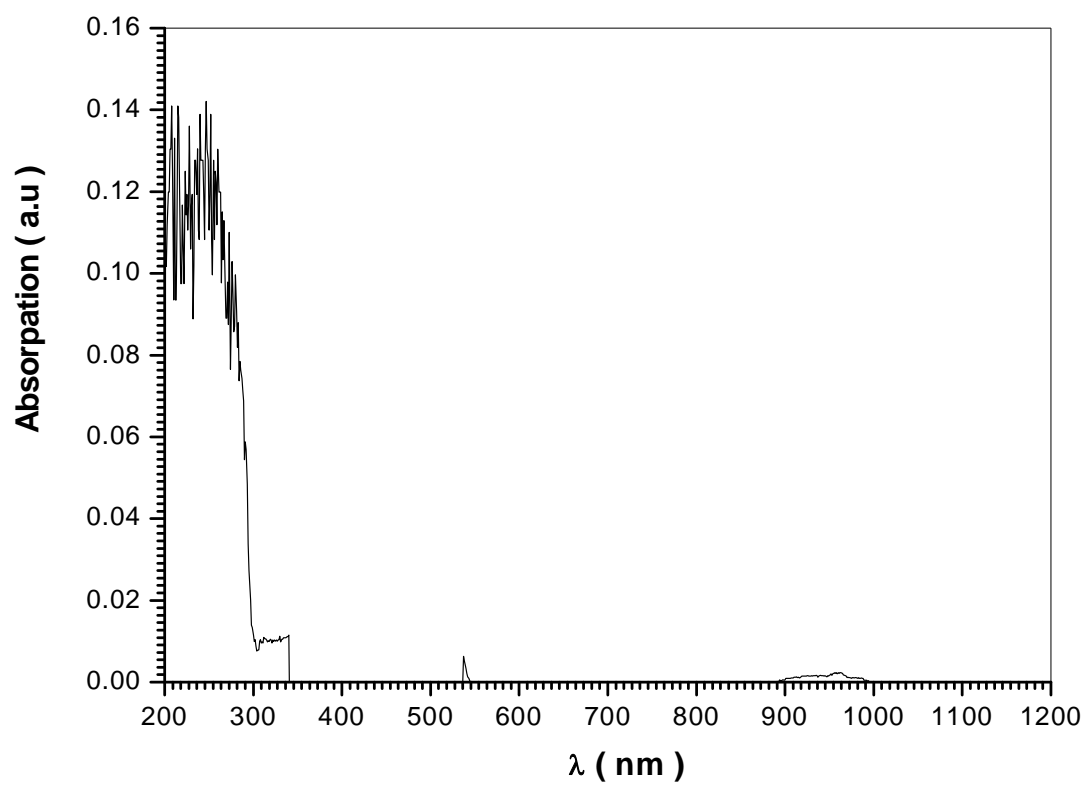


Fig (5-7)spectra ofLawsoniaAbsorption in room temperature

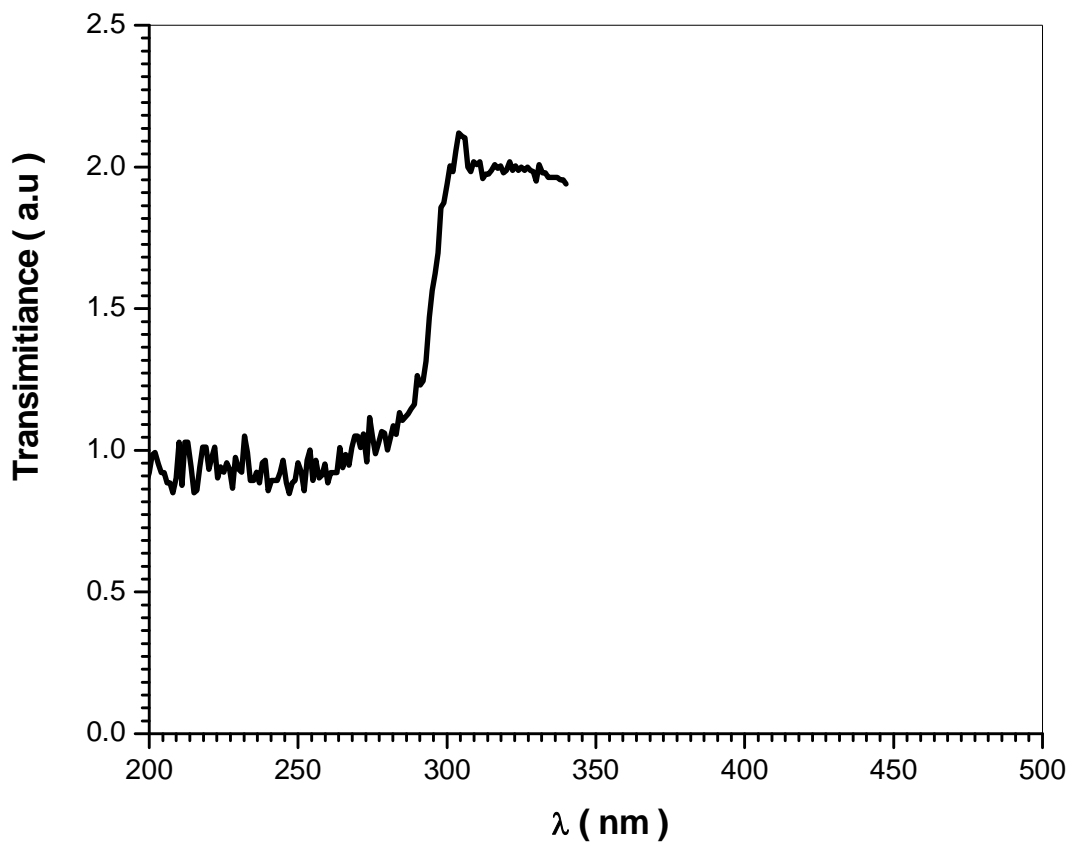


Fig (5-8) shows the relation between transparent and wavelength of Lawsonia, we had been found rapid decrease in low energies and sudden increase in 300 nm transparent value.

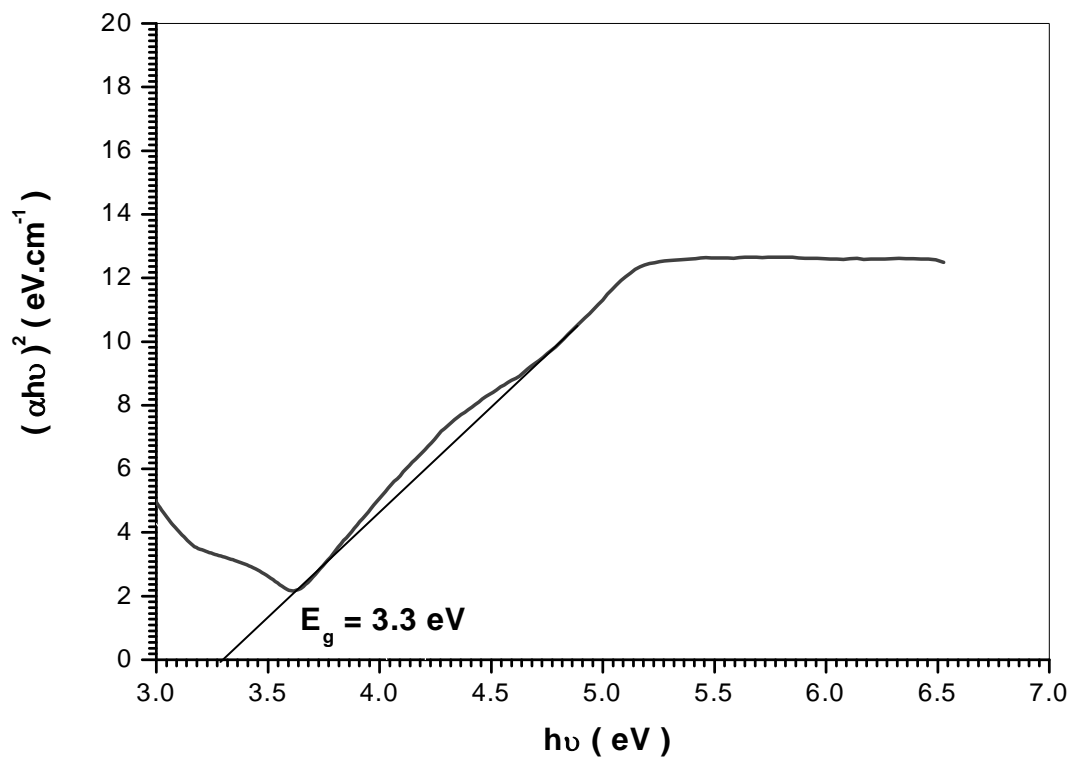


Fig (5-9) the optical energy gap (E_g) value of Lawsonia. The optical energy gap (E_g) has been calculated by the relation $(\alpha h\nu)^2 = C(h\nu - E_g)$ where (C) is constant. By plotting $(\alpha h\nu)^2$ vs photon energy ($h\nu$) as shown in fig .

Table5-2 the current and voltage of Lawsoniasolar cell

(v)v	(l)MA
1.058	35.75
1.078	35.75
1.098	35.75
1.108	35.75
1.118	35.75
1.128	35.75
1.158	35.75
1.168	33.75
1.178	29.75

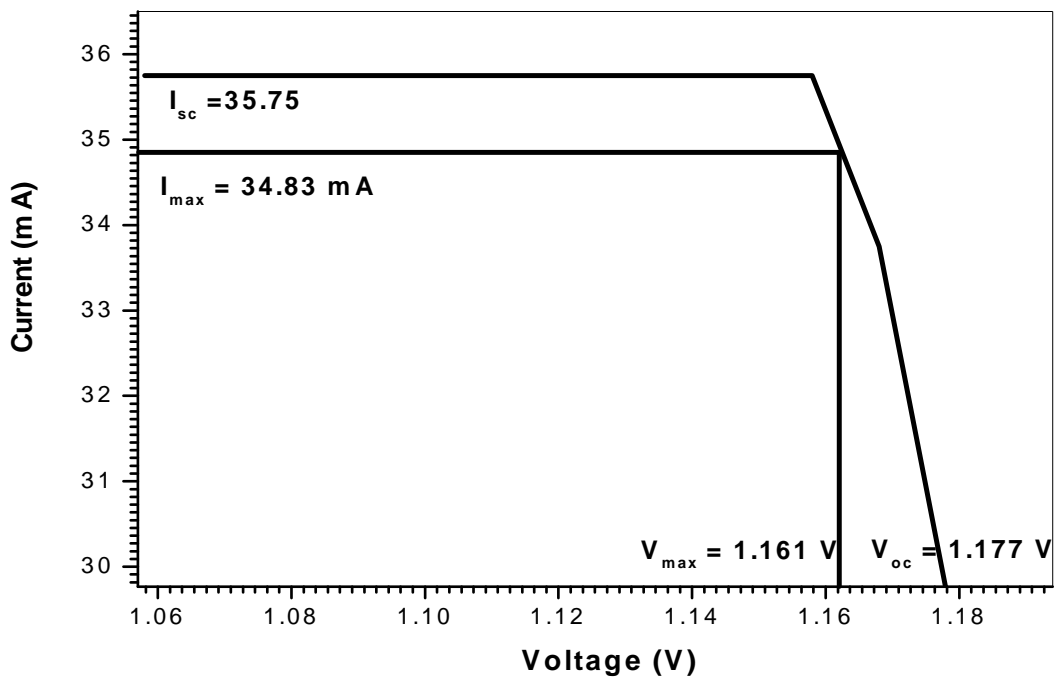


Fig (5-10)several factors for characterization of Lawsonia solar cell

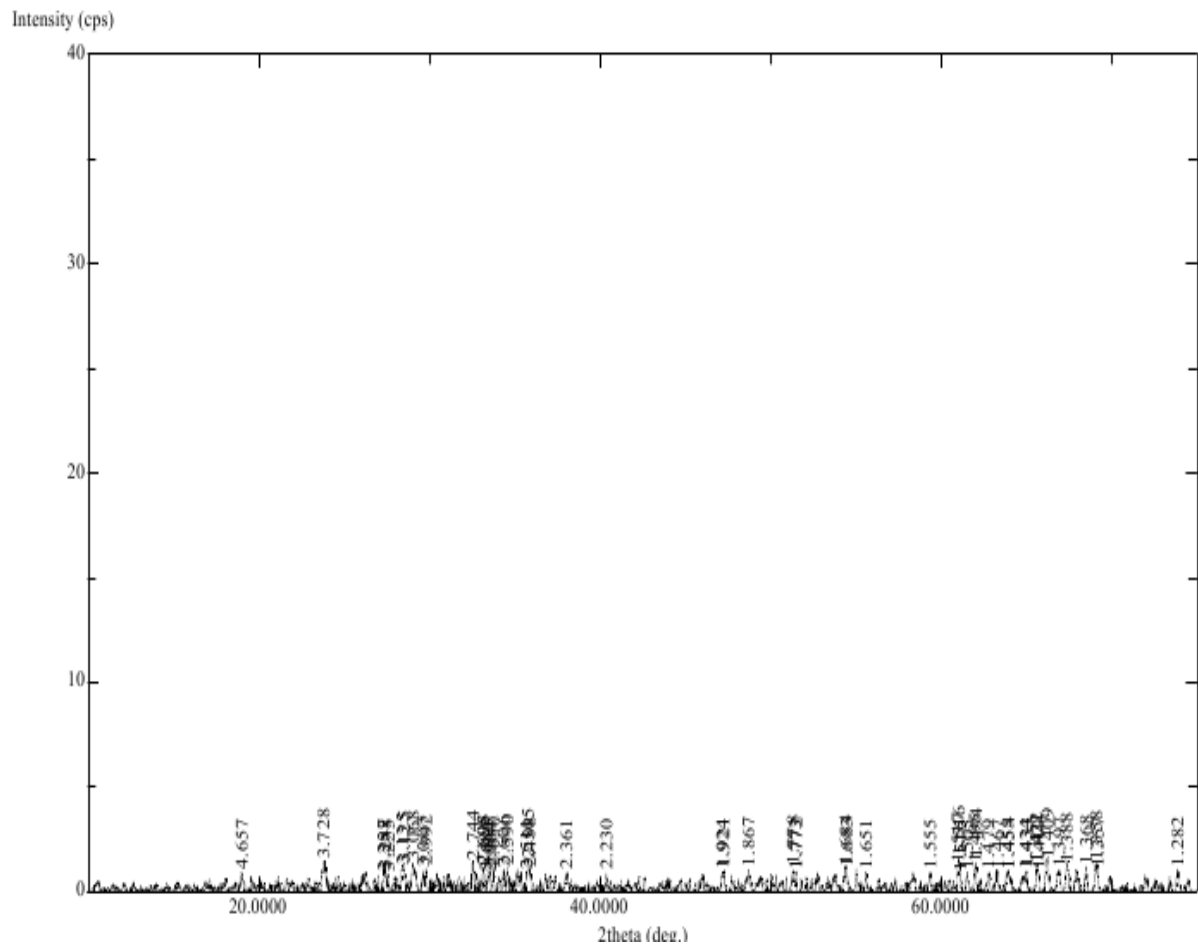


Fig (5-11) X-ray diffraction for Lawsonia measurements demonstrated that the Lawsonia is a polycrystalline structure

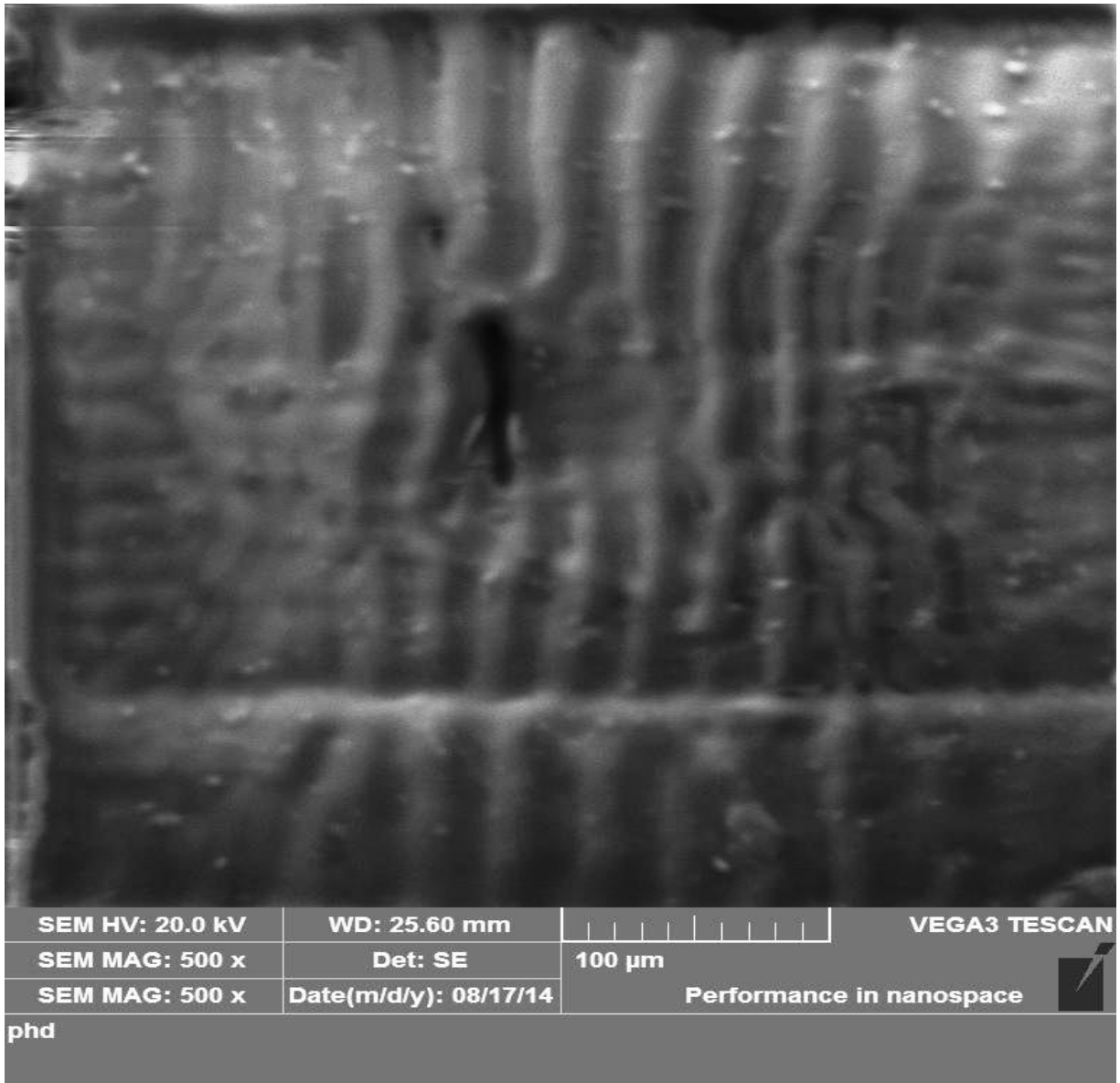


Fig (5-12)Field emission scanning electronic microscopy (FESEM) images of Lawsonia with different magnification

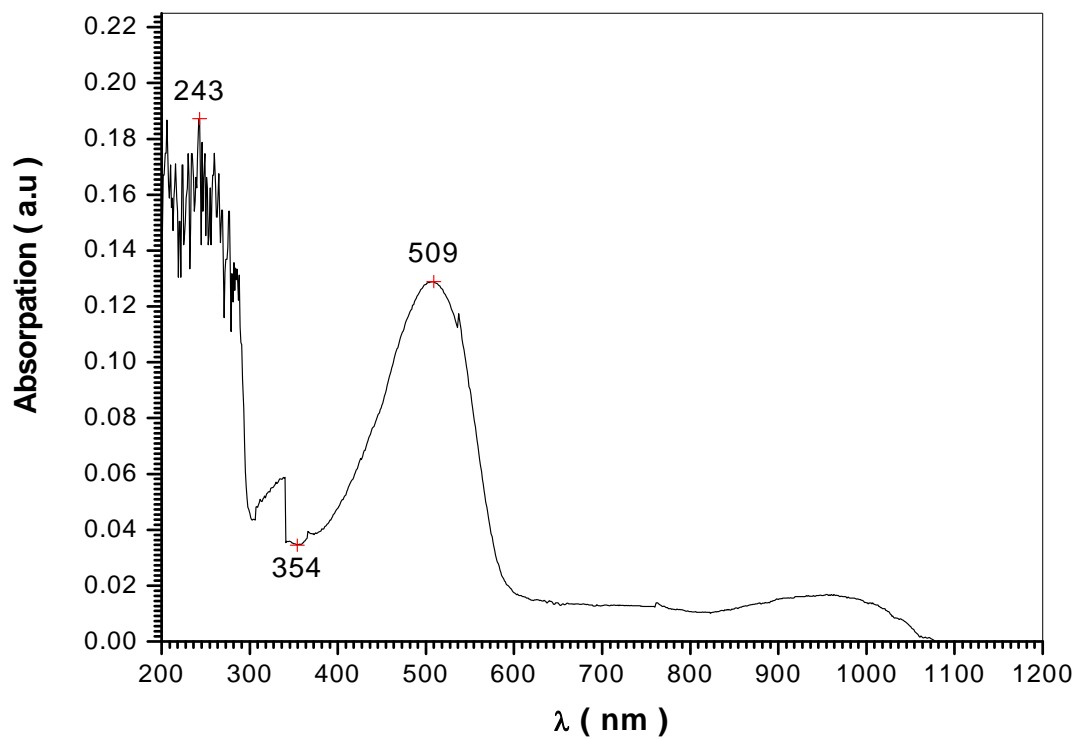


Fig (5-13)spectra ofRhodamin B Absorption in room temperature

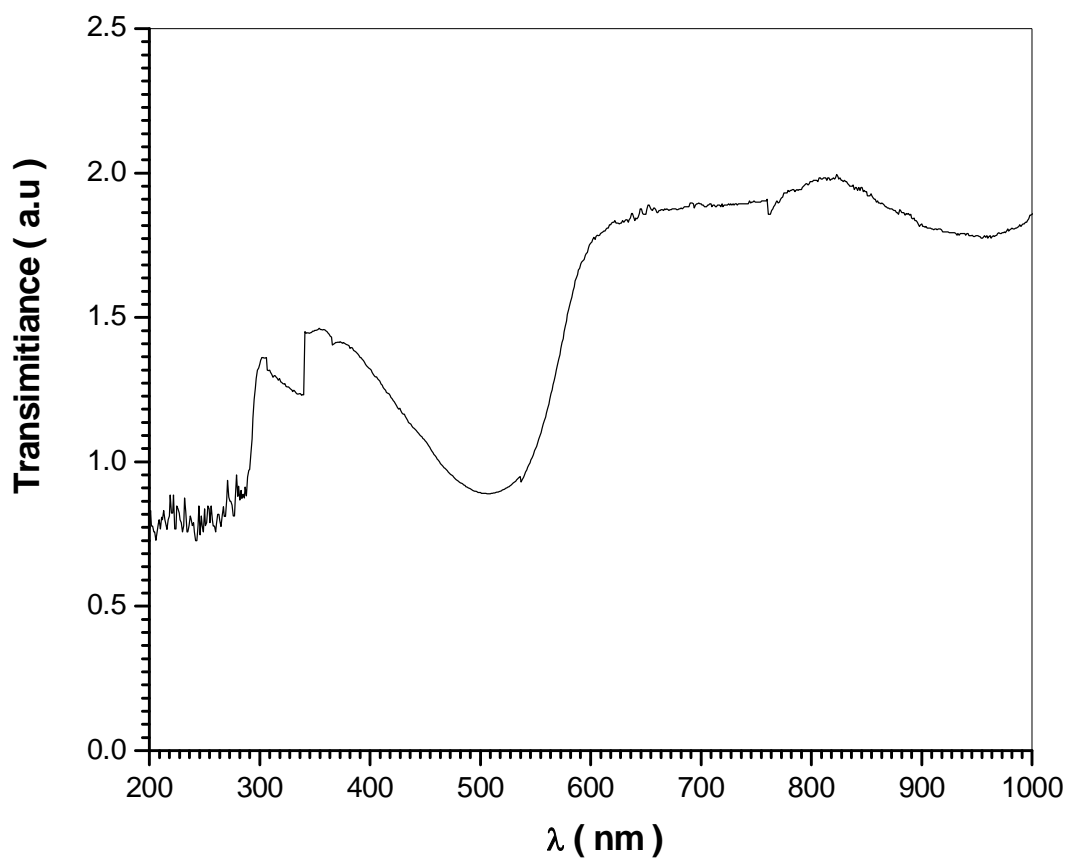


Fig (5-14) shows the relation between transparent and wavelength of Rohdamin B we had been found rapid decrease in low energies and sudden increase in 500 nm intransparent value.

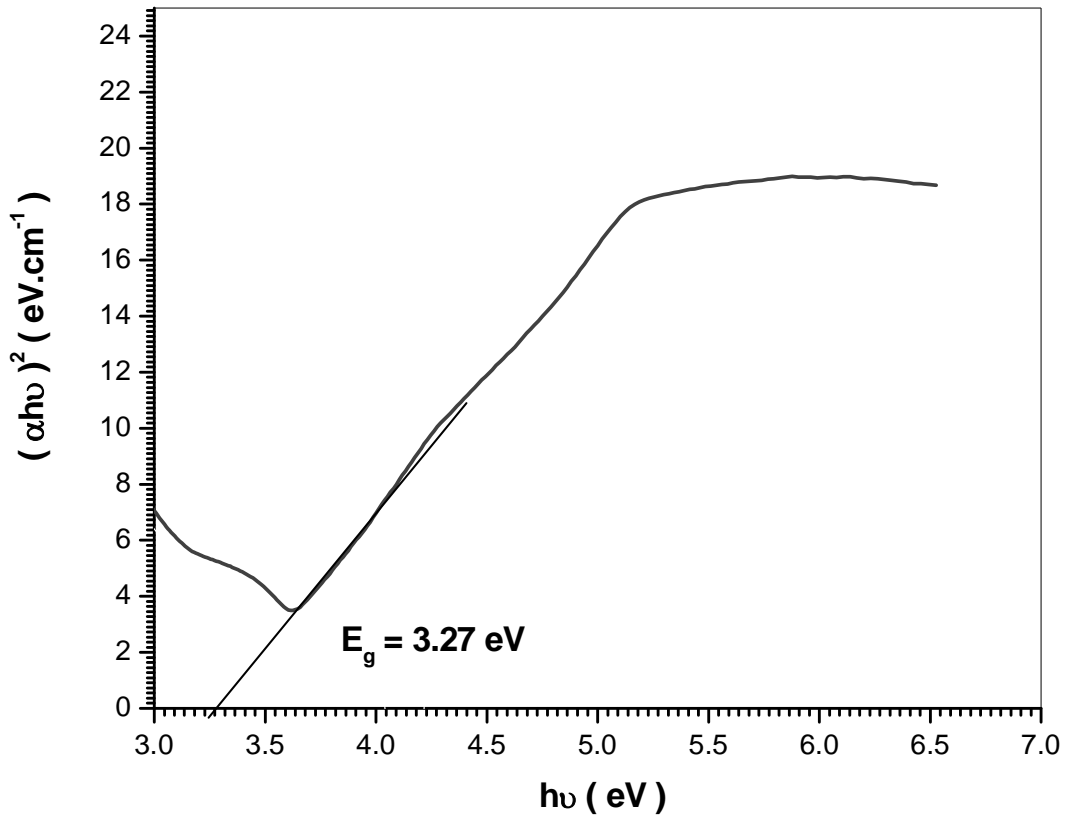


Fig (5-15) the optical energy gap (E_g) value of Rohdamin B The optical energy gap (E_g) has been calculated by the relation $(\alpha h\nu)^2 = C(h\nu - E_g)$ where (C) is constant. By plotting $(\alpha h\nu)^2$ vs photon energy ($h\nu$) as shown in fig .

Table 5-3 the current and voltage of RohdaminB solar cell

(v)v	(l)MA
1.942	34.57
1.962	34.57
1.982	34.57
1.992	34.57
2.002	34.57
2.012	34.57
2.0142	34.57
2.0152	32.57
2.0162	28.57

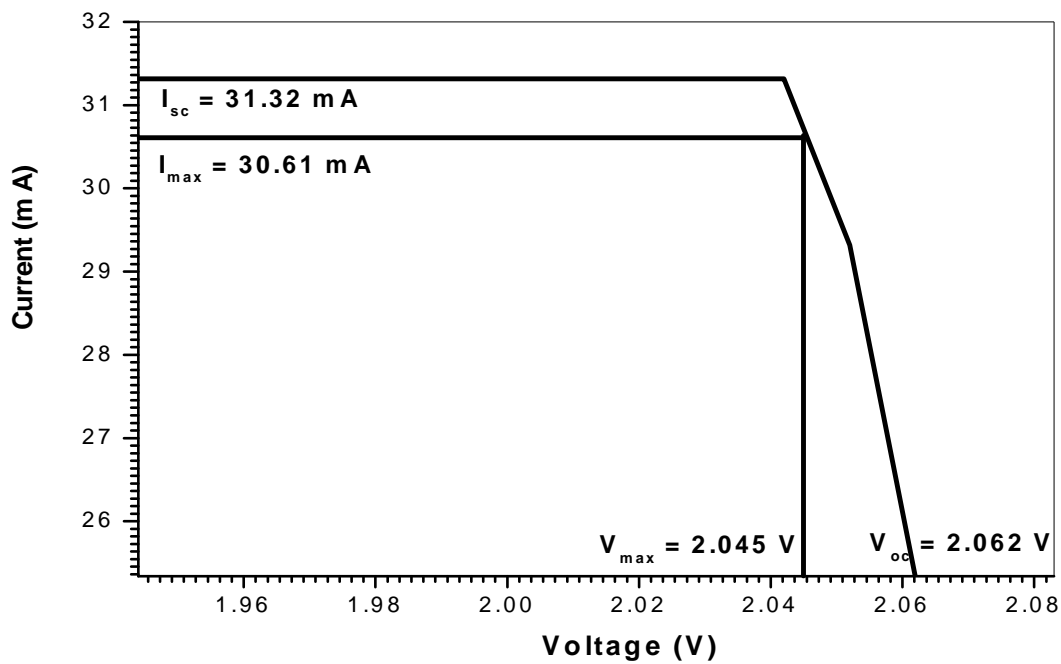


Fig (5-16)several factors for characterization of Rohdamin B solar cell

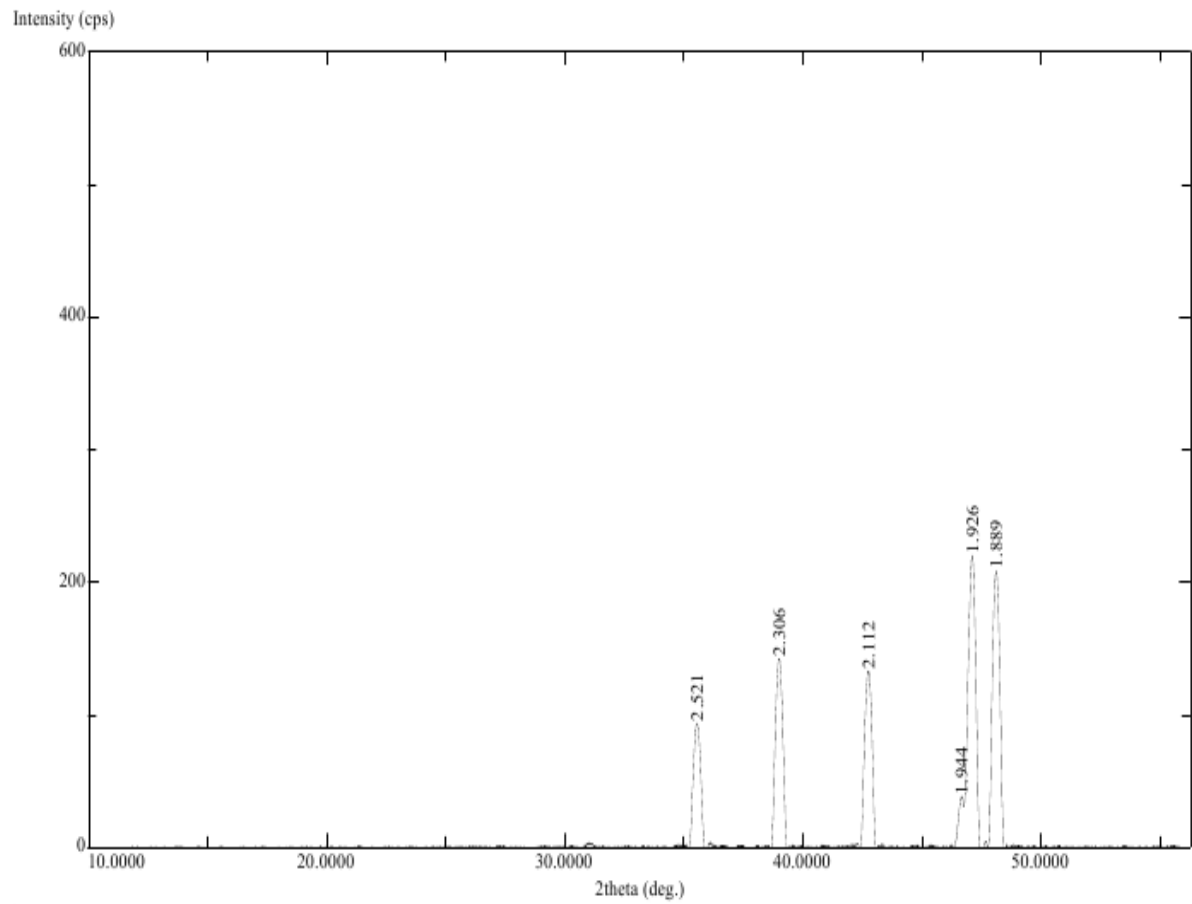


Fig (5-17) X-ray diffraction for Rohdamin B measurements demonstrated that the RohdaminB is a polycrystalline structure

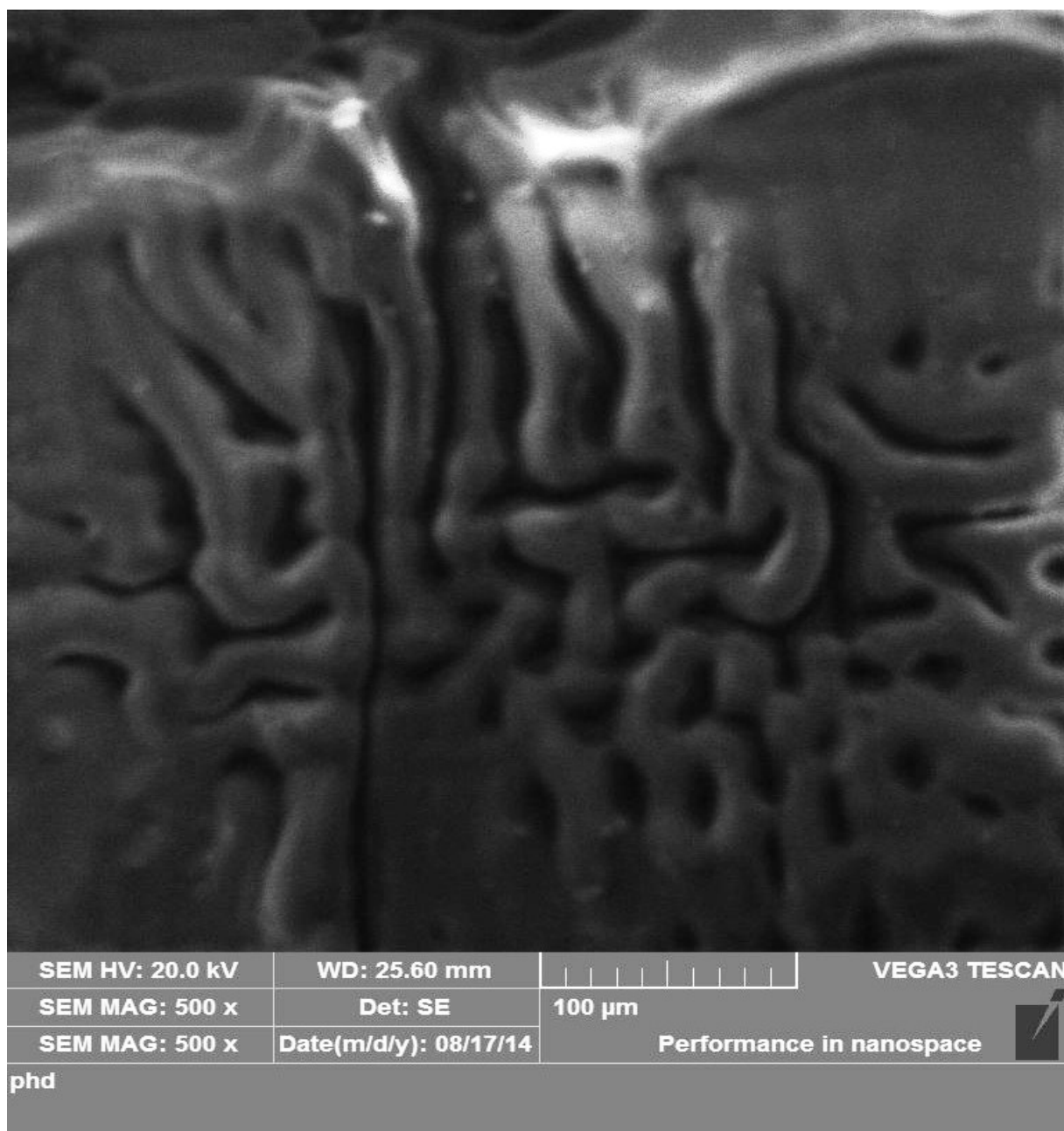


Fig (5-18)Field emission scanning electronic microscopy (FESEM) images of Rohdamin B with different magnification

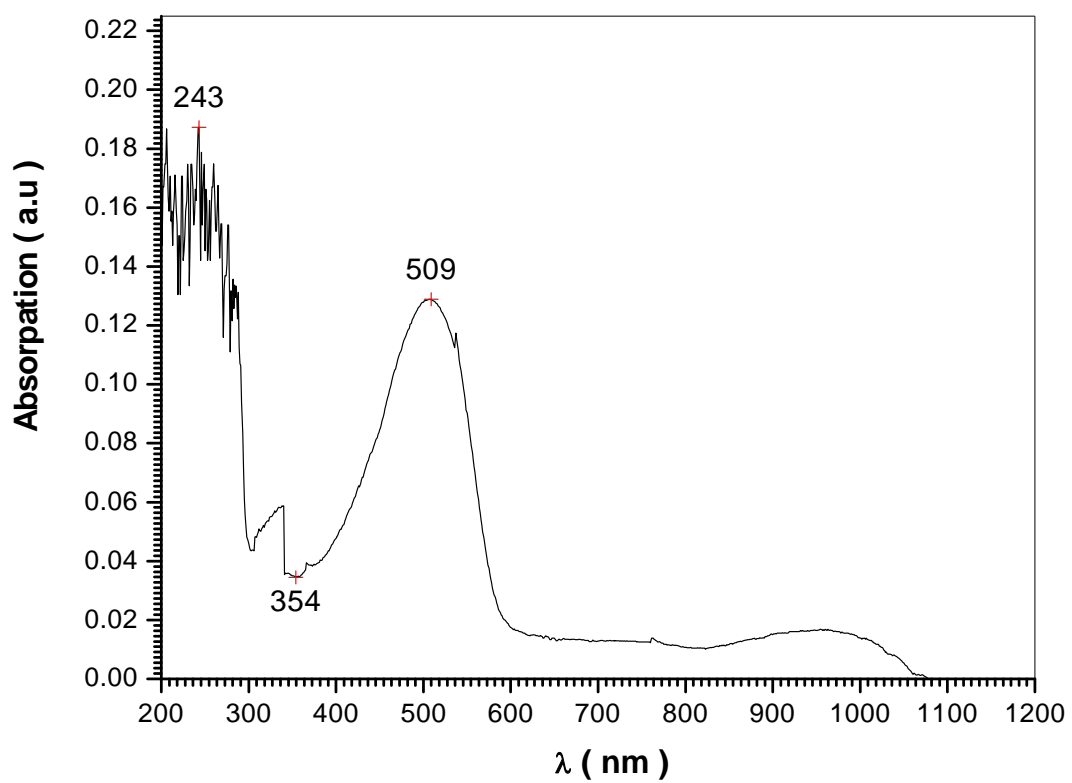


Fig (5-19)spectra ofBlue 8GXAbsorption in room temperature

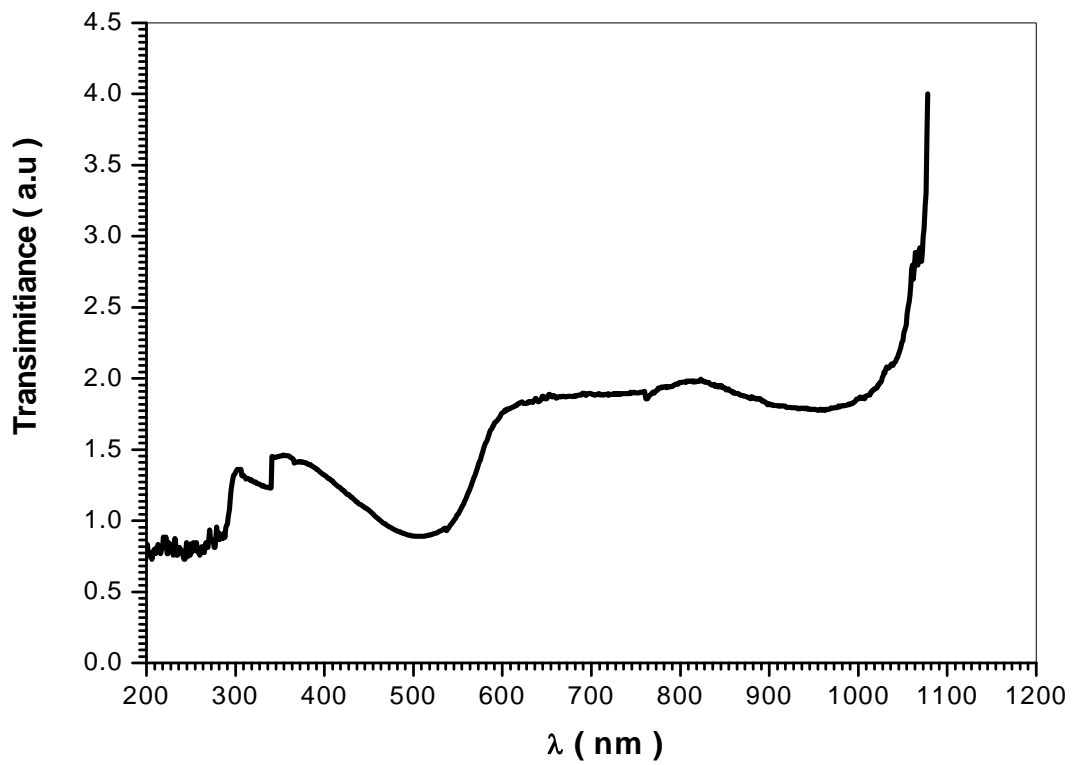


Fig (5-20) shows the relation between transparent and wavelength of Blue 8GX we had been found rapid decrease in low energies and sudden increase in 500 nm intransparent value.

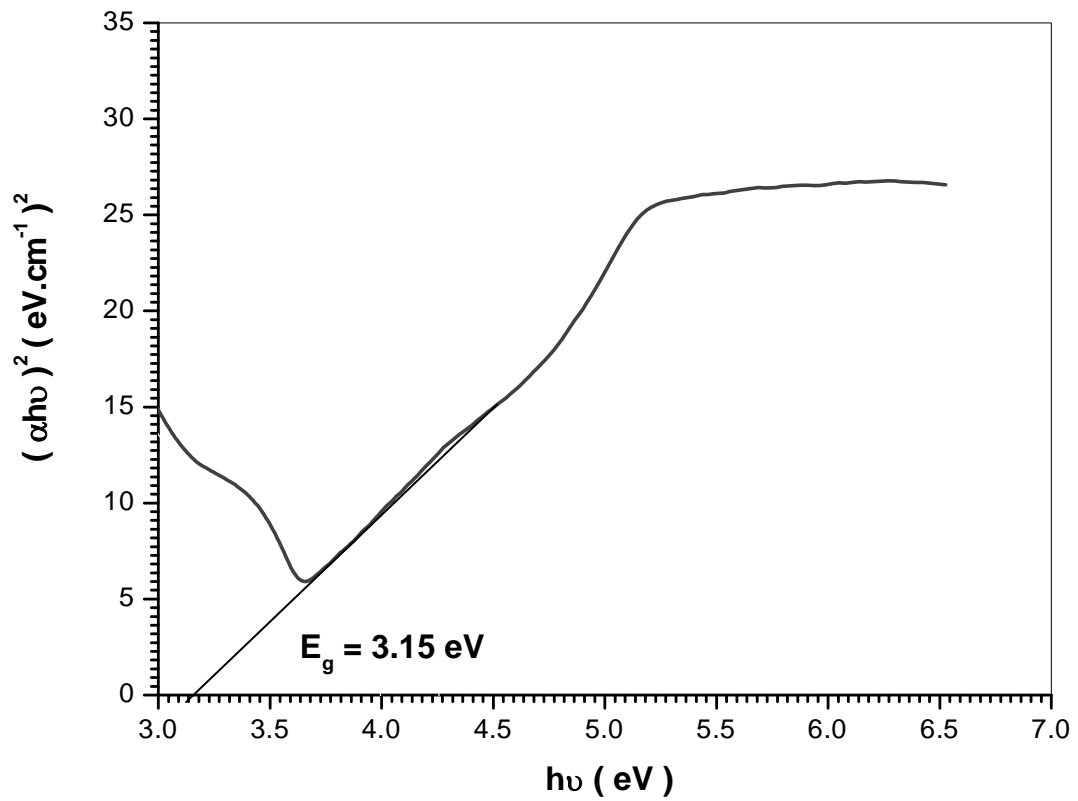


Fig (5-21) the optical energy gap (E_g) value of Blue 8GX. The optical energy gap (E_g) has been calculated by the relation $(\alpha h\nu)^2 = C(h\nu - E_g)$ where (C) is constant. By plotting $(\alpha h\nu)^2$ vs photon energy ($h\nu$) as shown in fig .

Table5-4 the current and voltage ofBlue 8GX solar cell

(v)v	(I)MA
1.942	32.57
1.962	32.57
1.992	32.57
2.002	32.57
2.012	32.57
2.042	32.57
2.052	30.57
2.062	26.57

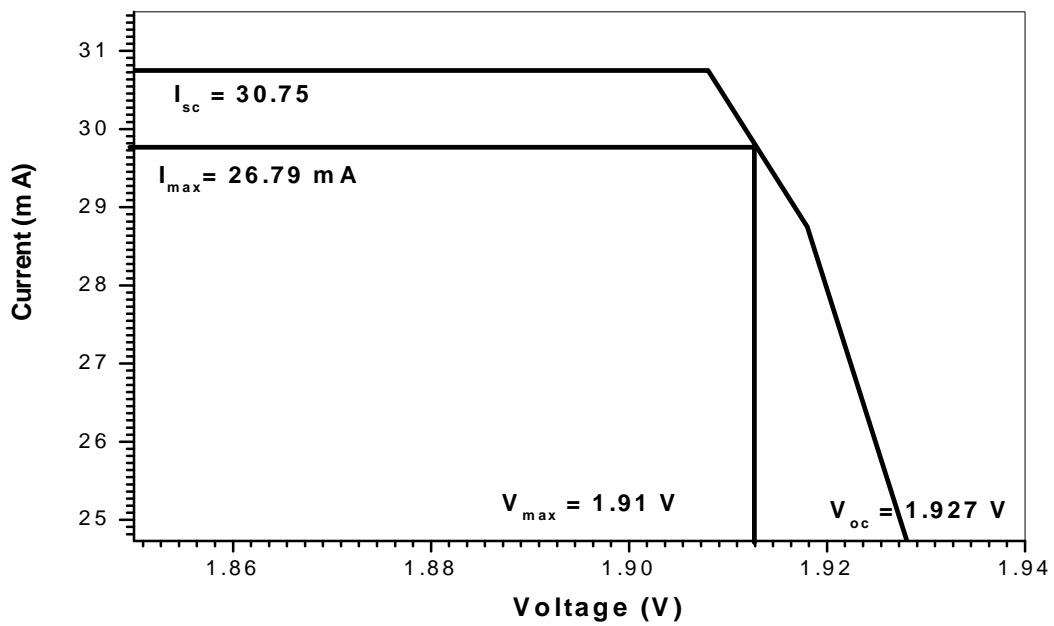


Fig (5-22)several factors for characterization of Blue 8GX solar cell

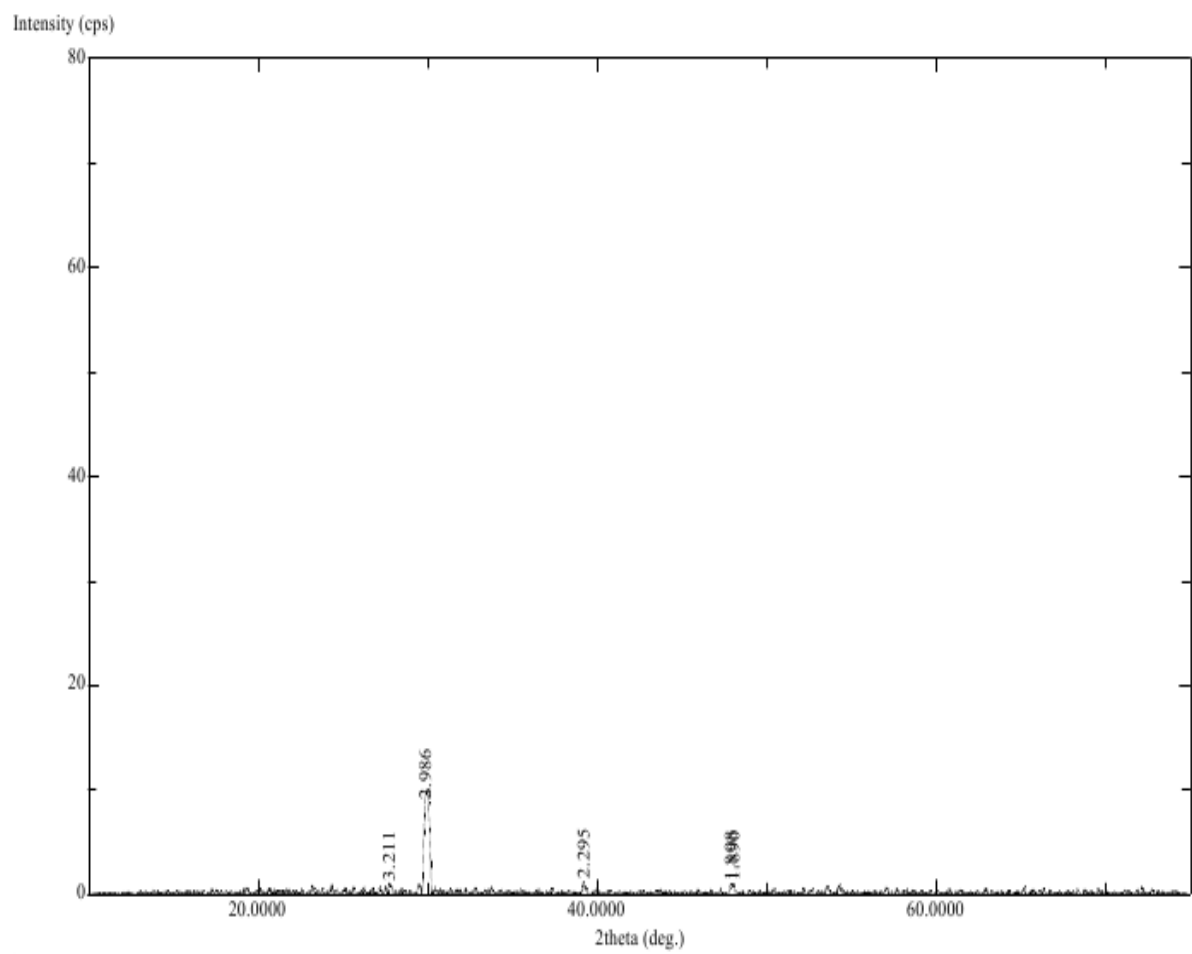


Fig (5-23) X-ray diffraction for Blue 8GX measurements demonstrated that the Blue 8GX is a polycrystalline structure

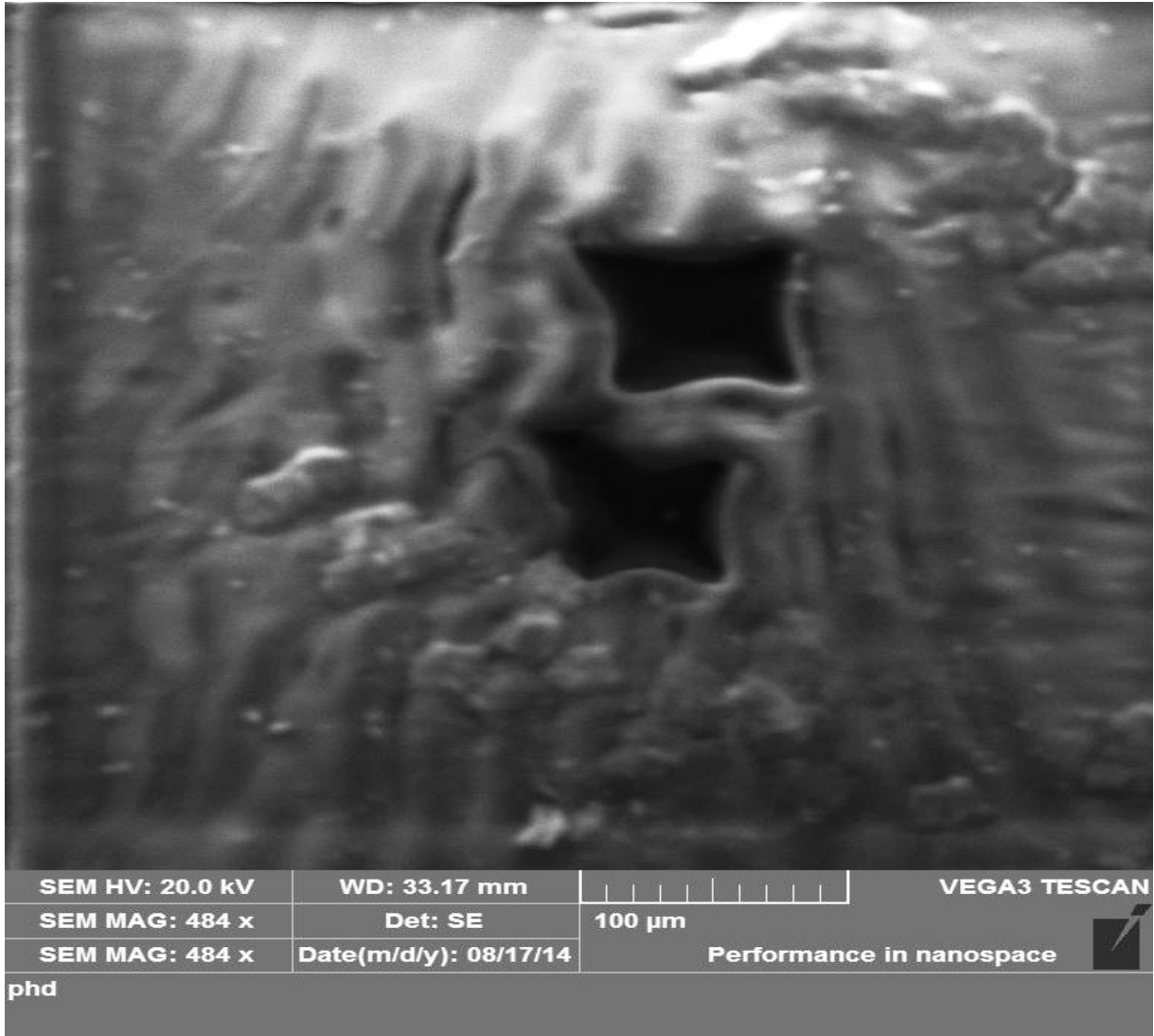


Fig (5-24)Field emission scanning electronic microscopy (FESEM) images of Blue 8GX with different magnification

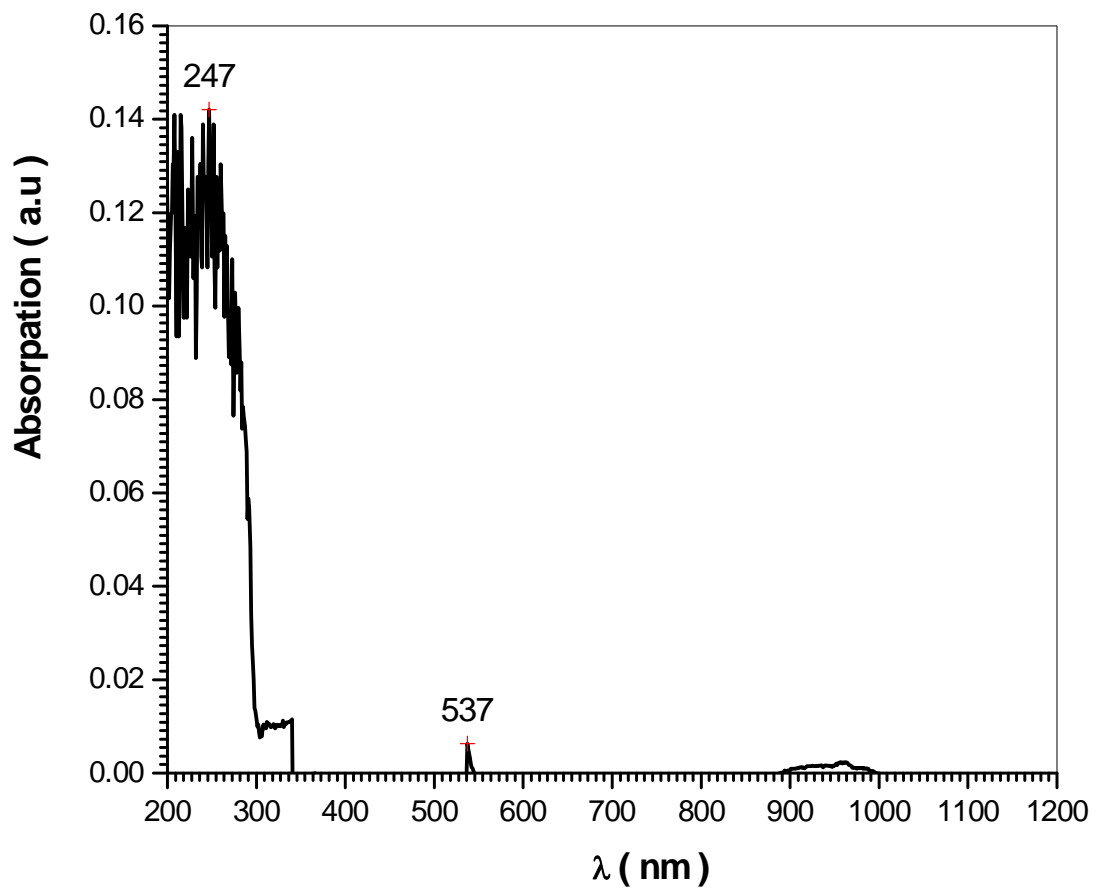


Fig (5-25)spectra ofRoselleAbsorption in room temperature

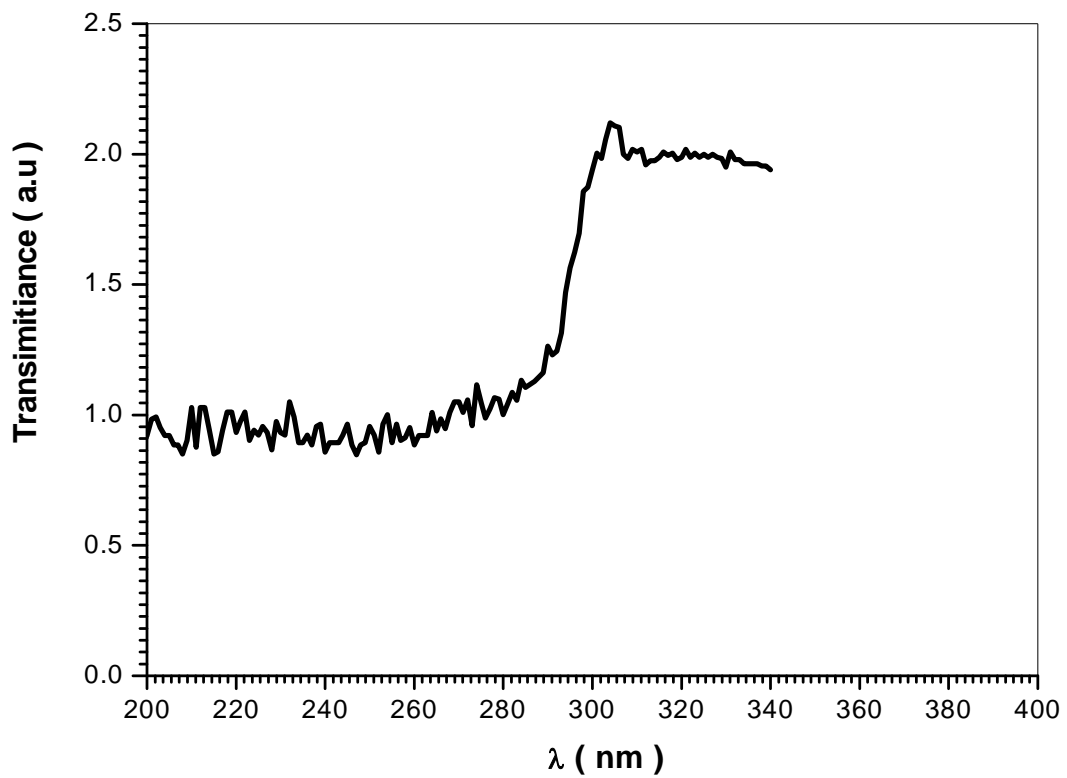


Fig (5-26) shows the relation between transparent and wavelength of Roselle we had been found rapid decrease in low energies and sudden increase in 280 nm in transparent value

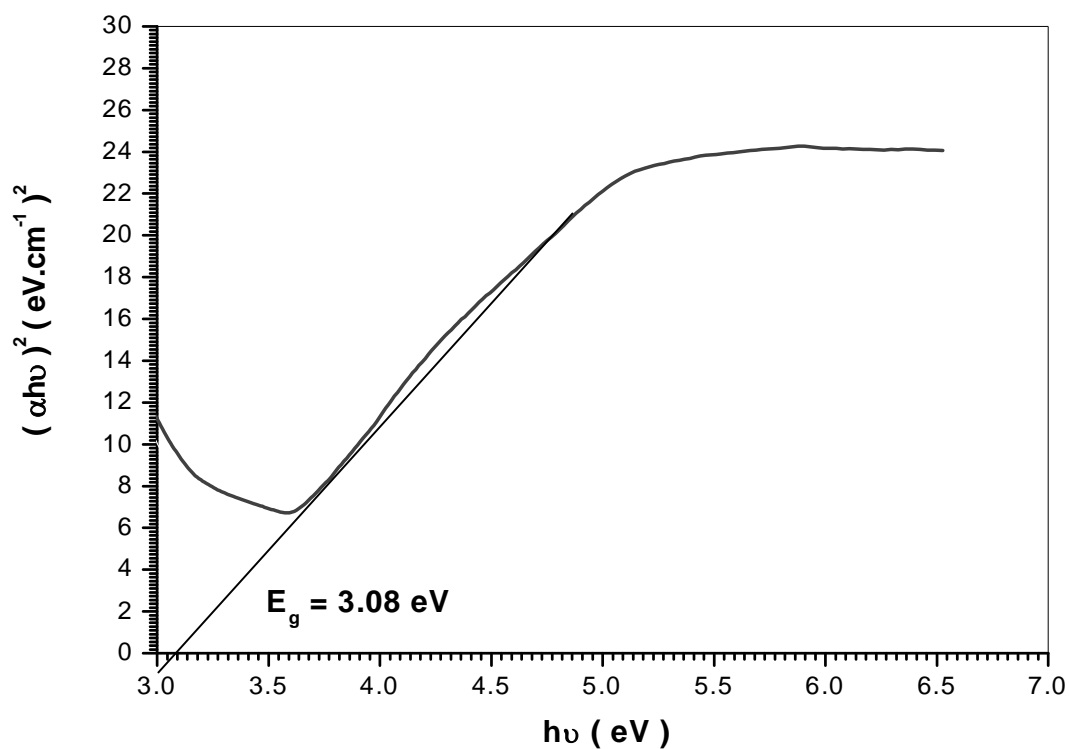


Fig (5-27) the optical energy gap (E_g) value of Roselle. The optical energy gap (E_g) has been calculated by the relation $(\alpha h\nu)^2 = C(h\nu - E_g)$ where (C) is constant. By plotting $(\alpha h\nu)^2$ vs photon energy ($h\nu$) as shown in fig

Table5-4 the current and voltage ofRoselle solar cell

(v)v	(I)MA
1.808	30.75
1.828	30.75
1.848	30.75
1.858	30.75
1.868	30.75
1.878	30.75
1.908	30.75
1.918	28.75
1.928	24.75

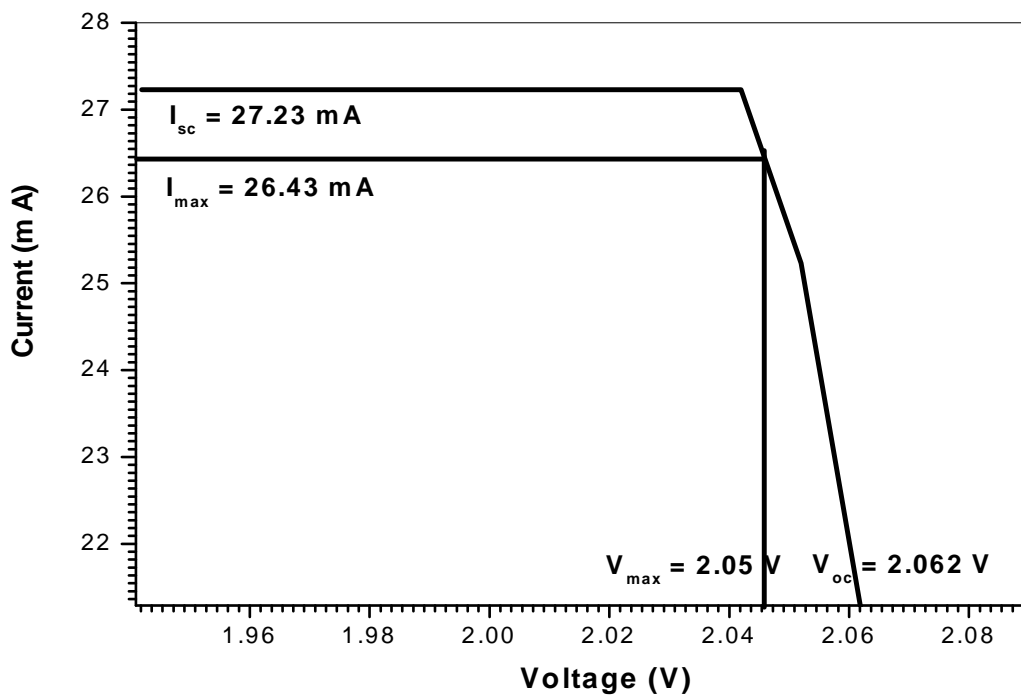


Fig (5-28)several factors for characterization of Roselle solar cell

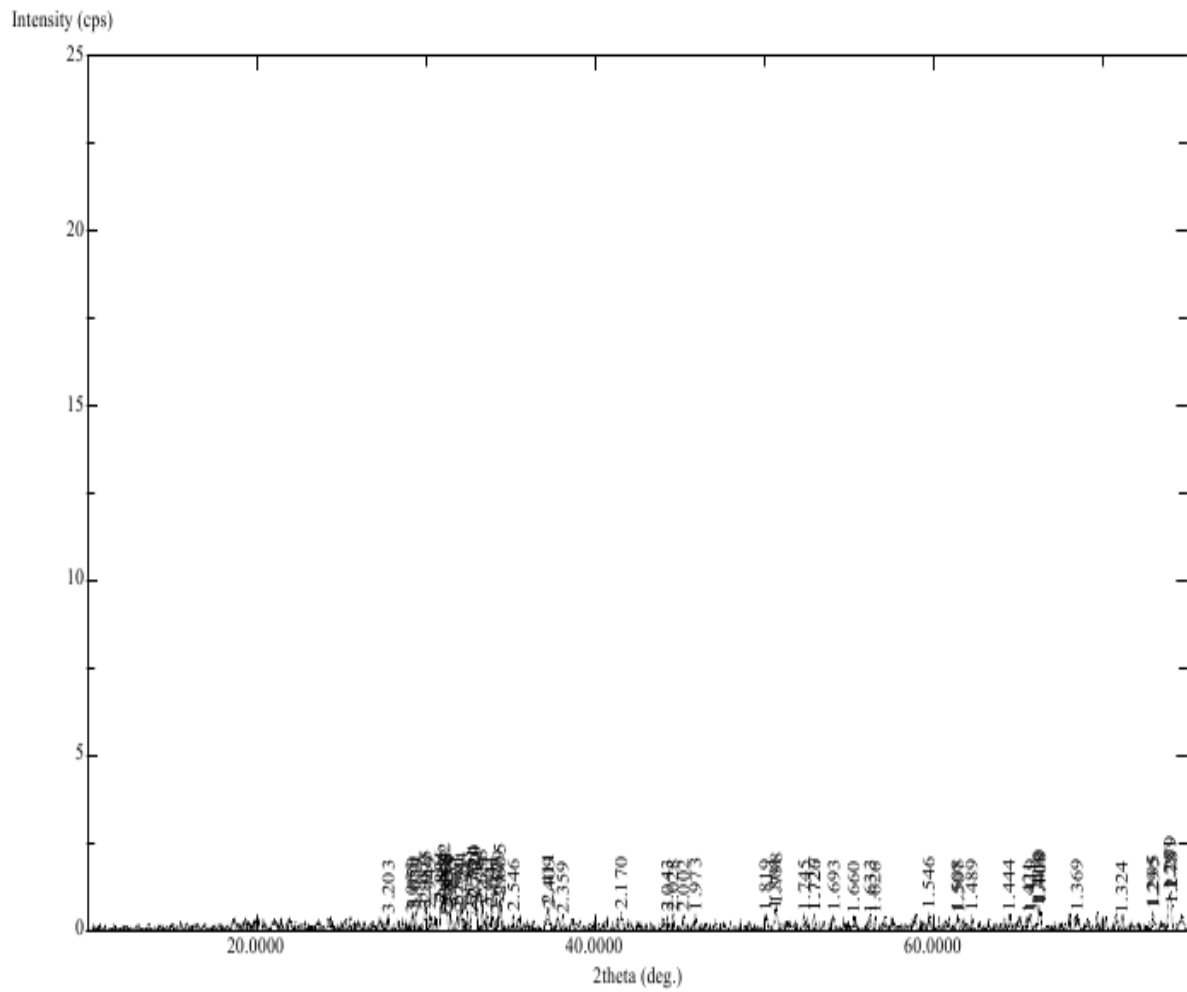


Fig (5-29) X-ray diffraction for Roselle measurements demonstrated that the Roselle is a polycrystalline structure

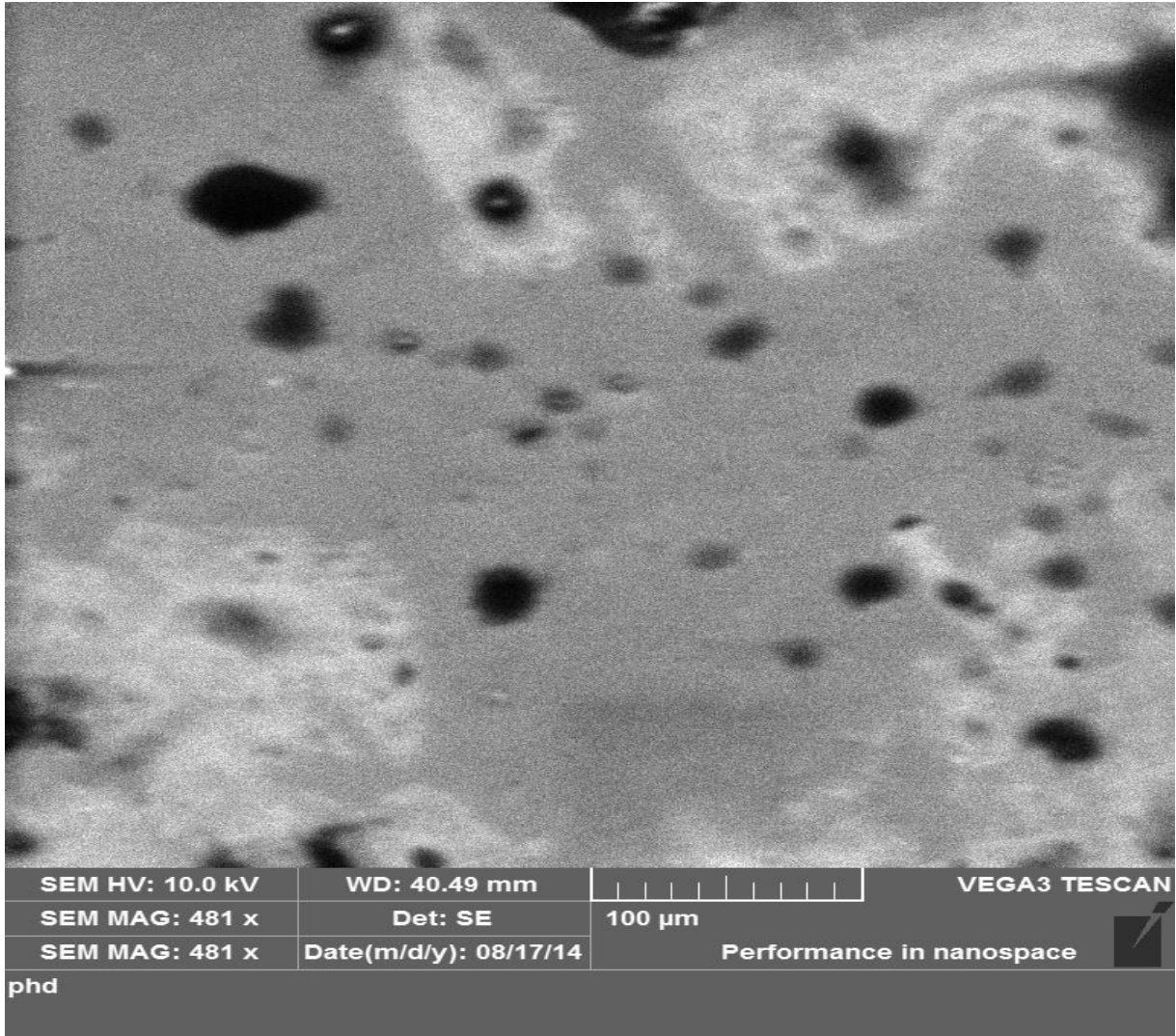


Fig (5-30)Field emission scanning electronic microscopy (FESEM) images of Roselle with different magnification

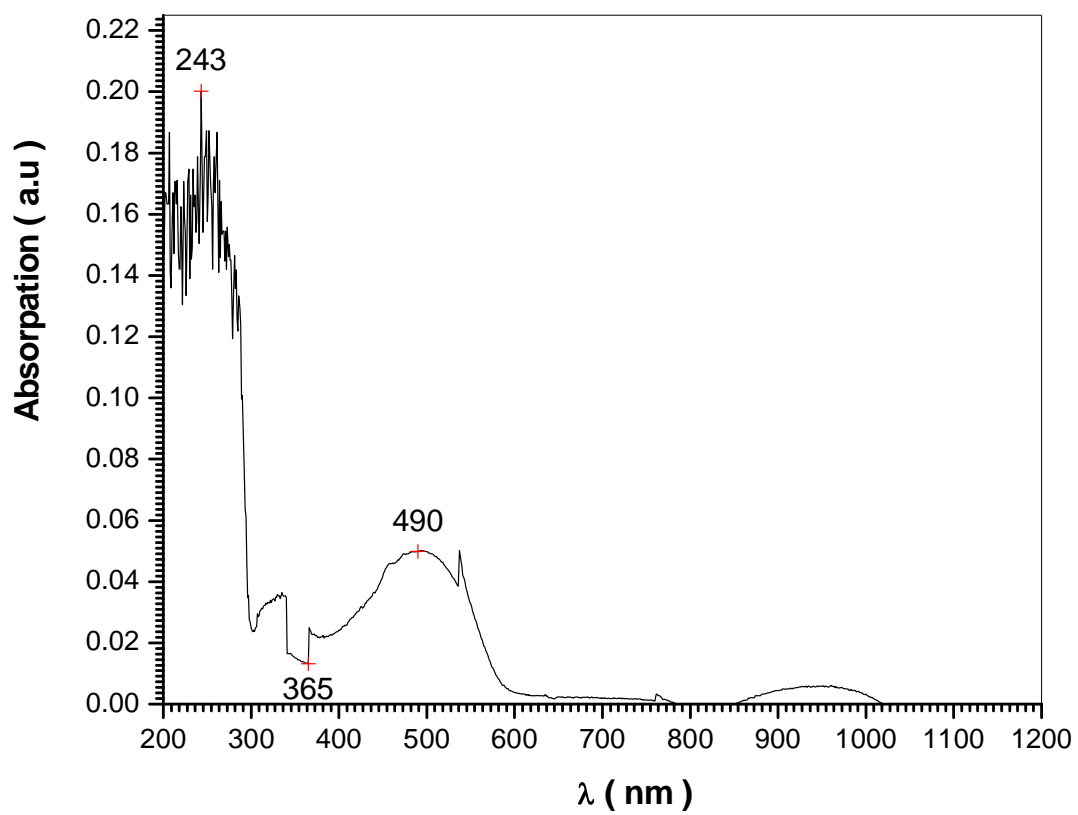


Fig (5-31)spectra of DDTTC Absorption in room temperature

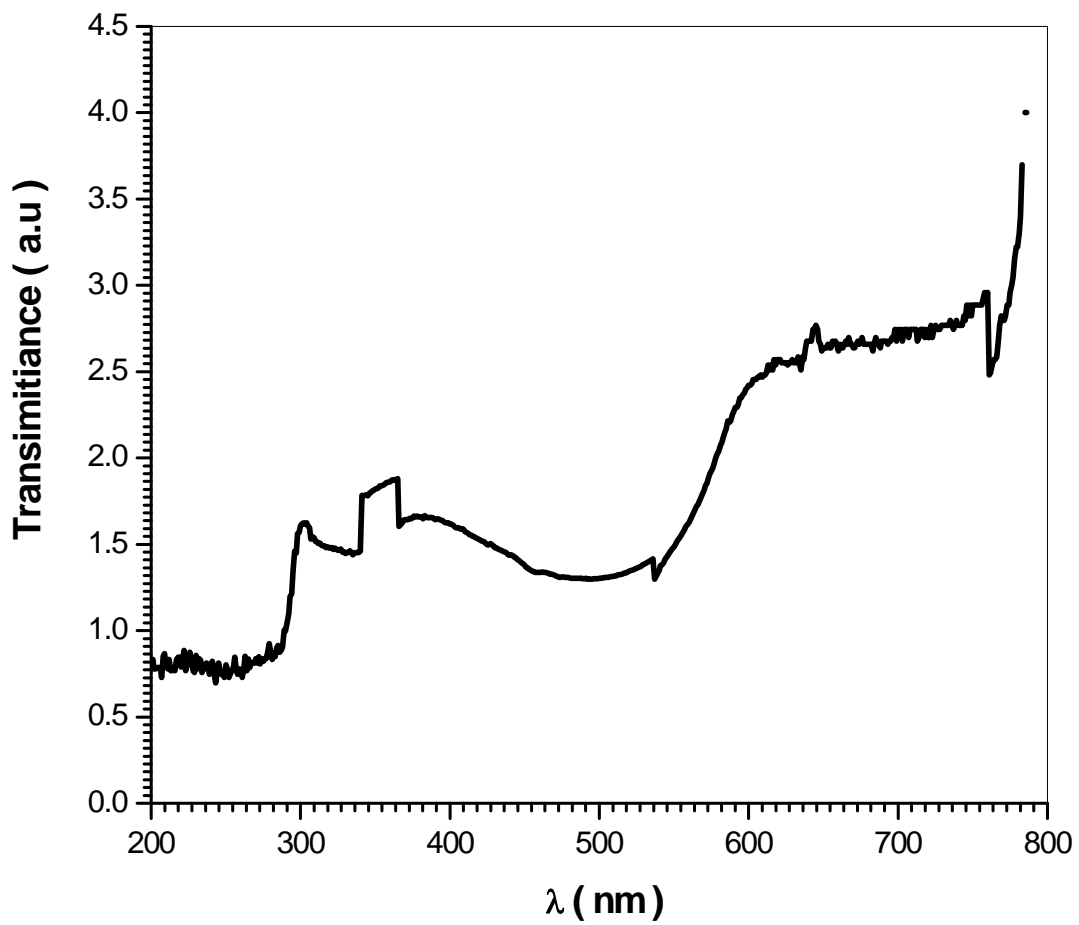


Fig (5-32) shows the relation between transparent and wavelength of DDTTC we had been found rapid decrease in low energies and sudden increase in 300nm intransparent value

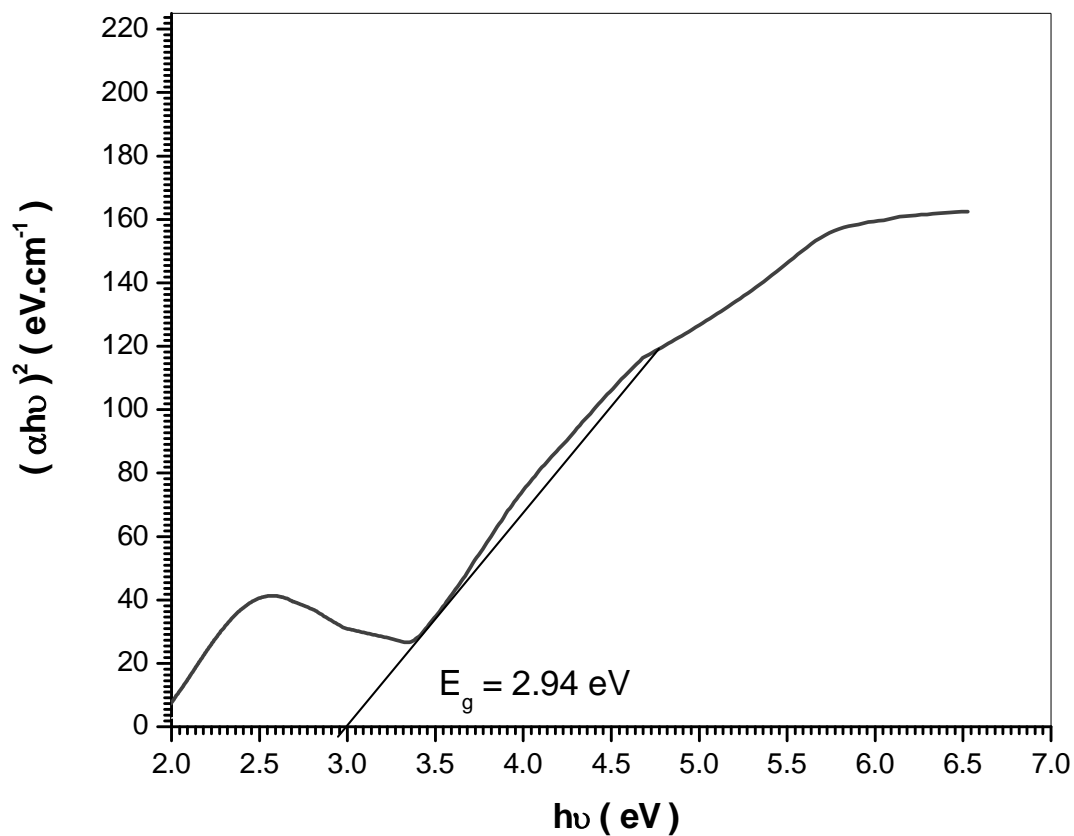


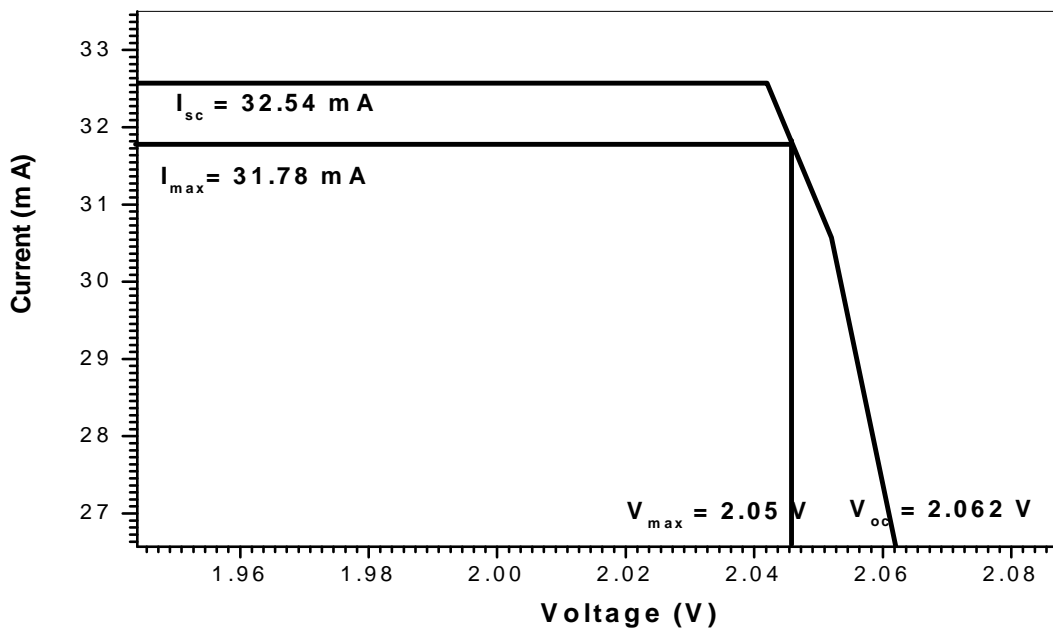
Fig (5-33) the optical energy gap (E_g) value of DDTTC. The optical energy gap (E_g) has been calculated by the relation $(\alpha h\nu)^2 = C(h\nu - E_g)$ where (C) is constant. By plotting $(\alpha h\nu)^2$ vs photon energy ($h\nu$) as shown in fig

Table5-5 the current and voltage of DDTTC solar cell

Fig

(5-

(v)v	(I)MA
1.942	27.23
1.962	27.23
1.982	27.23
1.992	27.23
2.002	27.23
2.012	27.23
2.042	27.23
2.052	25.23
2.062	21.21



34)several factors for characterization of DDTTC solar cell

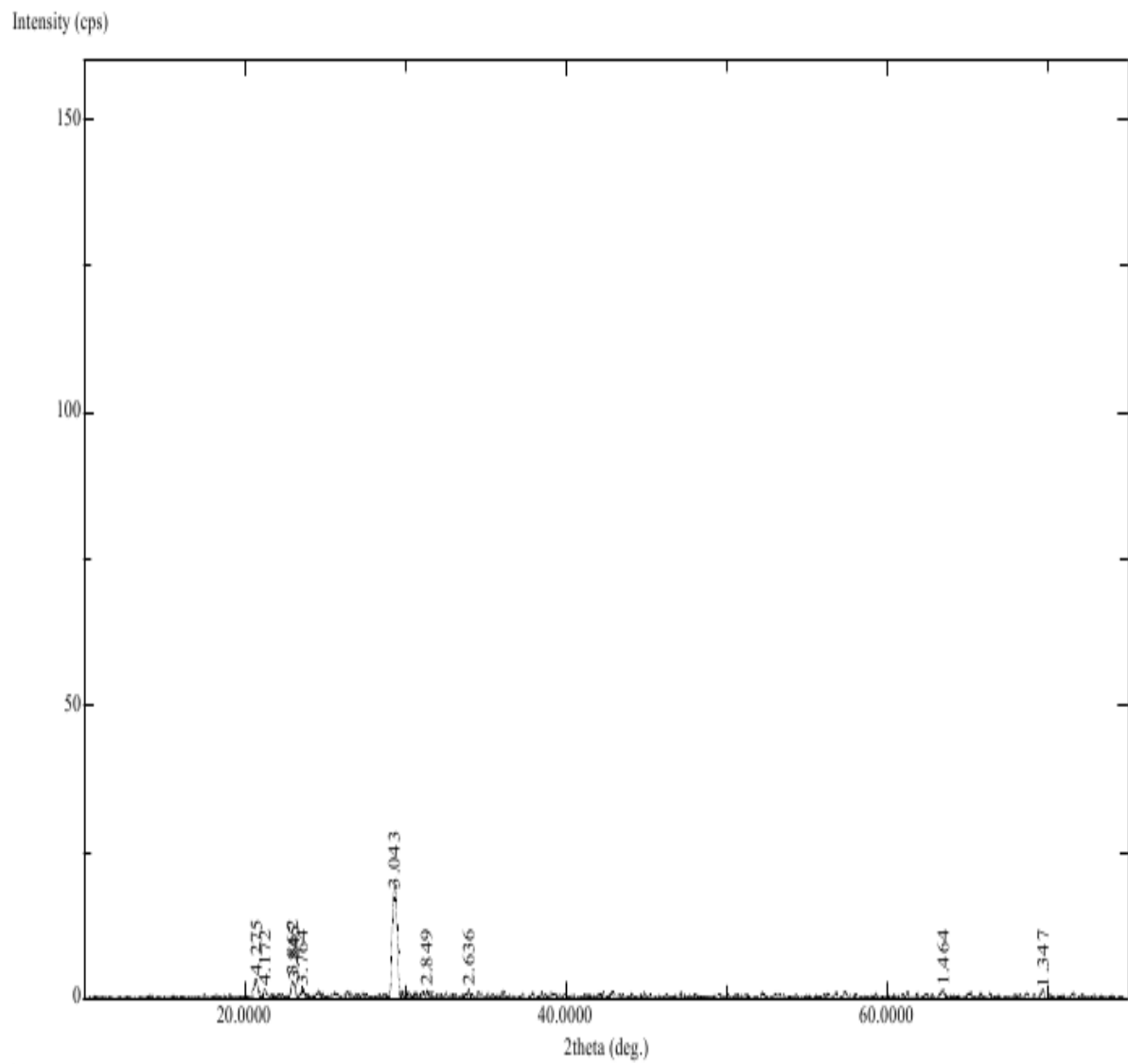


Fig (5-35) X-ray diffraction for DDTTC measurements demonstrated that the DDTTC is a polycrystalline structure

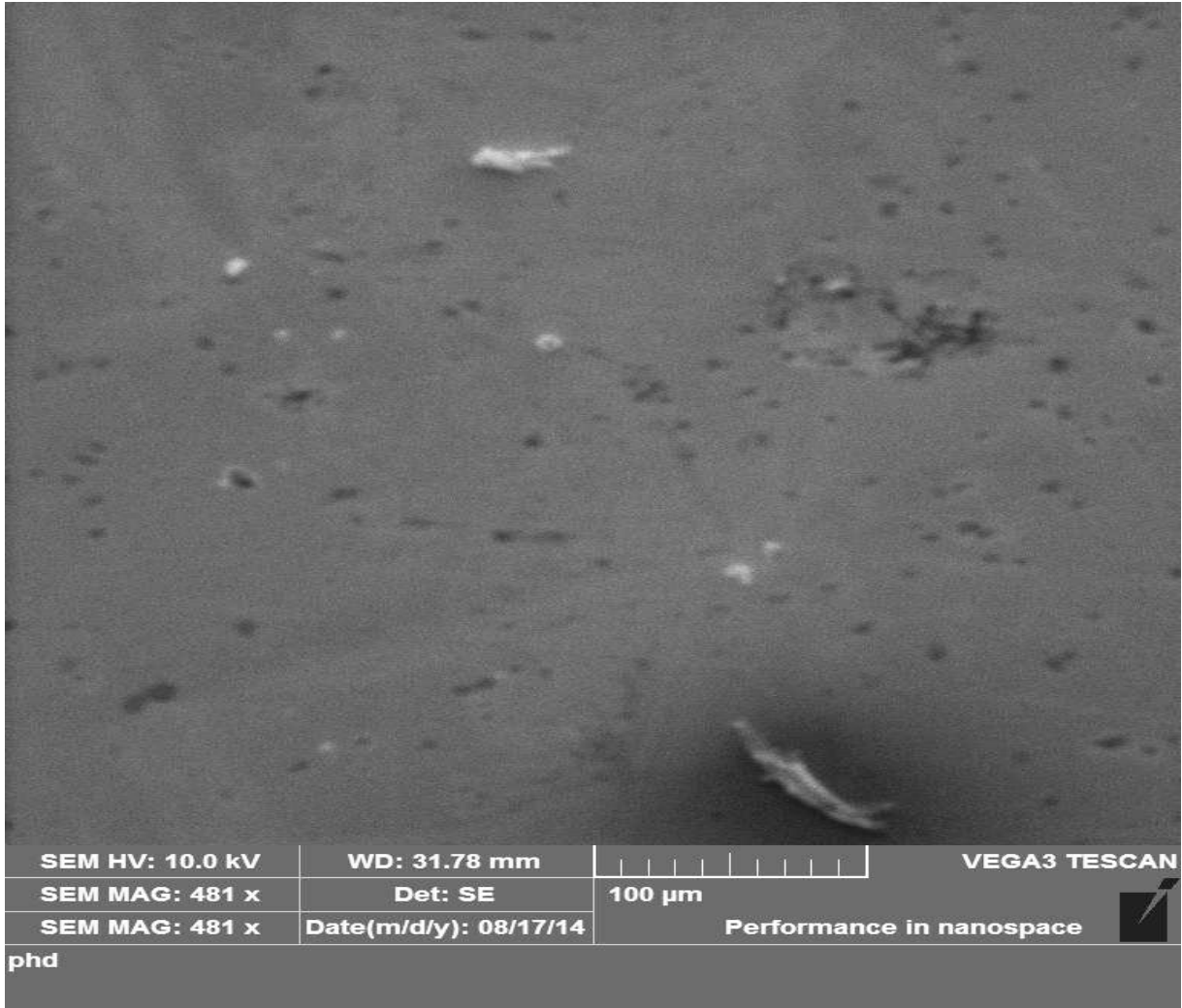


Fig (5-36)Field emission scanning electronic microscopy (FESEM) images of DDTTC with different magnification

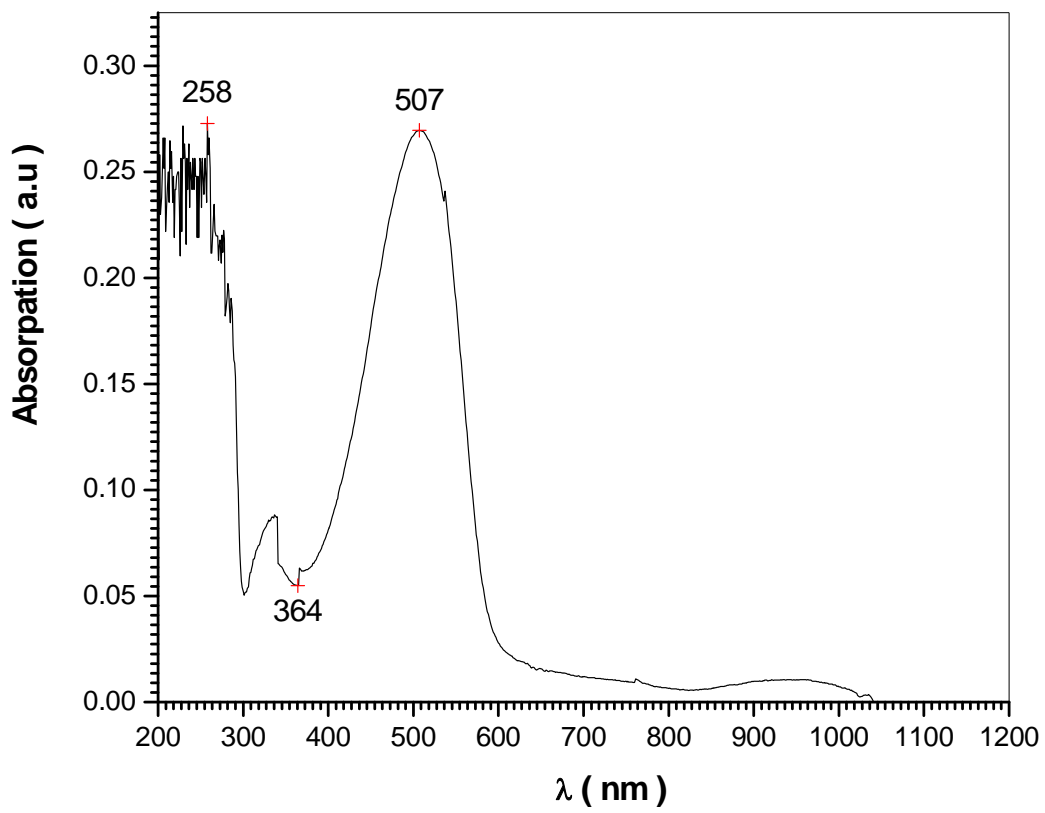


Fig (5-37)spectra of Ero-Chrom black T Absorption in room temperature

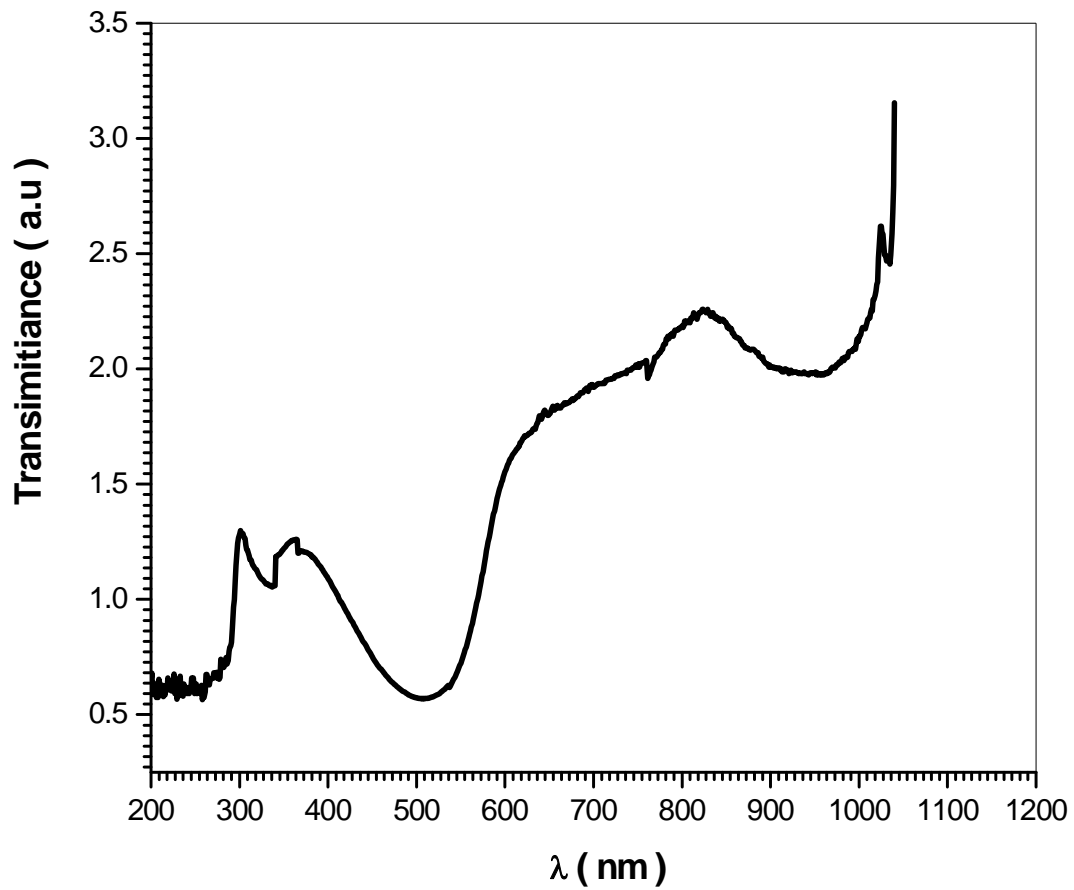


Fig (5-38) shows the relation between transparent and wavelength of Ero-Chrom black T we had been found rapid decrease in low energies and sudden increase in 520 nm intransparent value

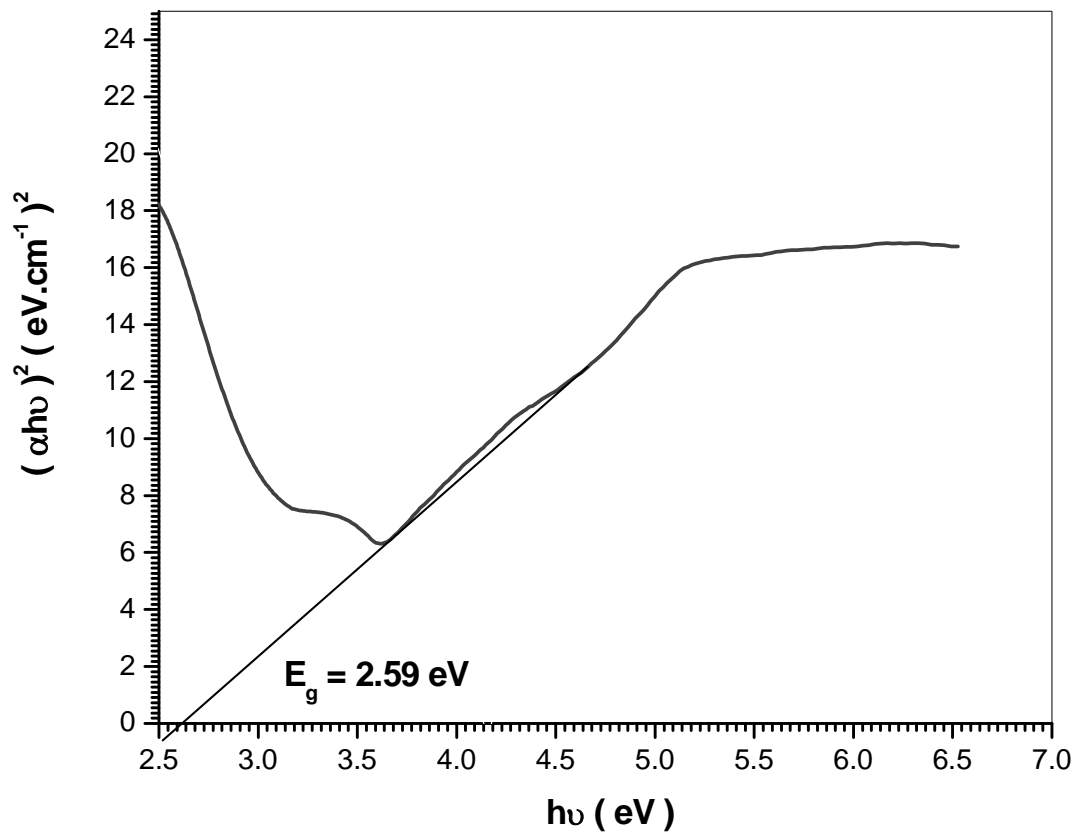


Fig (5-39) the optical energy gap (E_g) value of Ero-Chrom black T. The optical energy gap (E_g) has been calculated by the relation $(\alpha h\nu)^2 = C(h\nu - E_g)$ where (C) is constant. By plotting $(\alpha h\nu)^2$ vs photon energy ($h\nu$) as shown in fig

Table5-6 the current and voltage of Ero-Chrom black T solar cell

(v)v	(I)MA
1.09	39
1.11	39
1.13	39
1.14	39
1.15	39
1.16	39
1.19	39
1.21	39
1.21	37

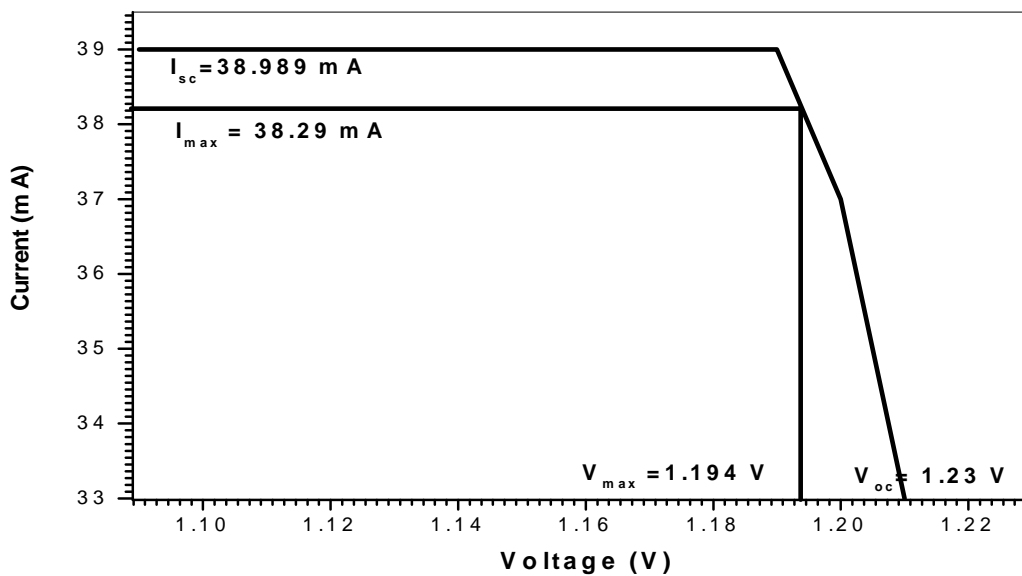


Fig (5-40)several factors for characterization of Ero-Chrom black T solar cell

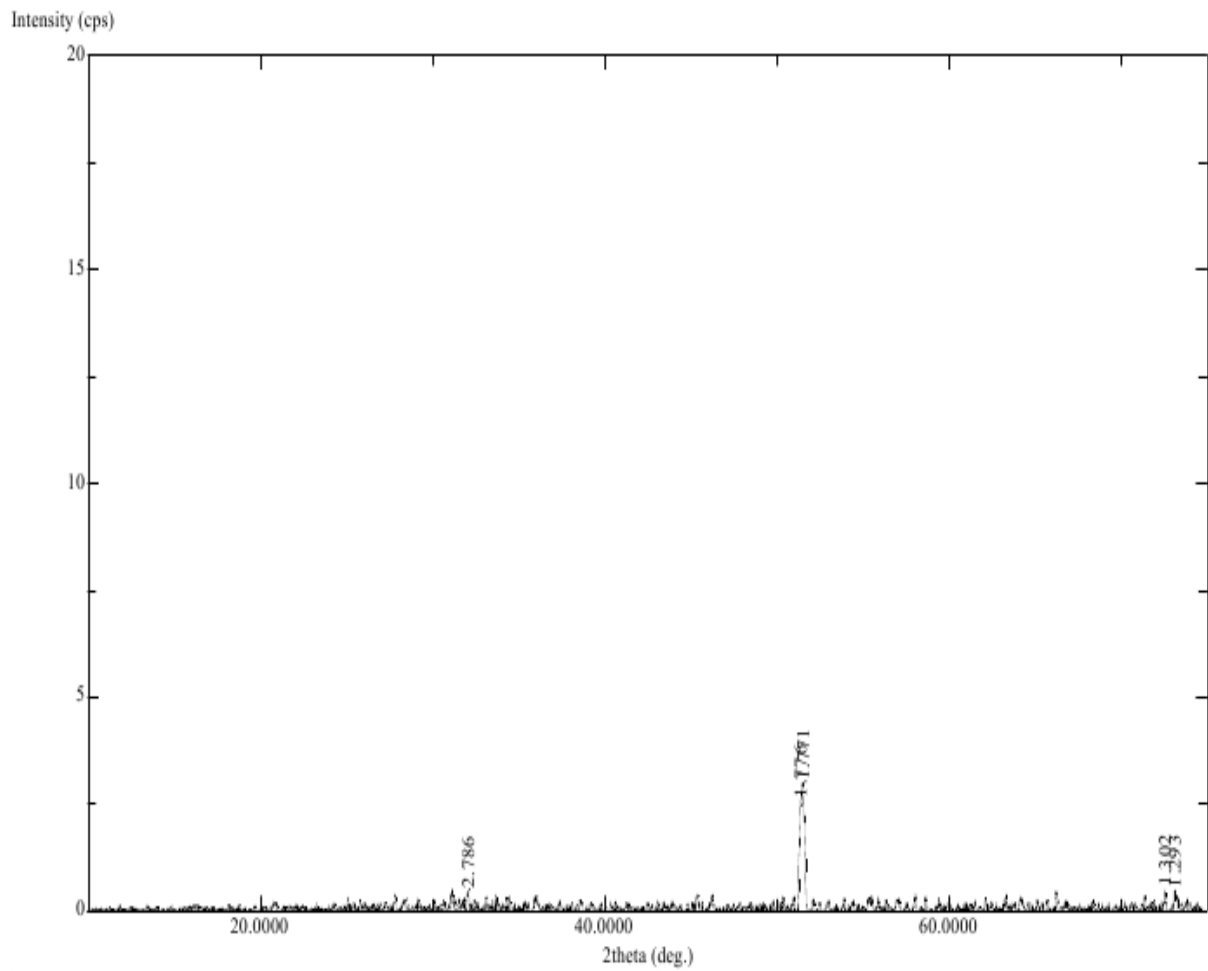


Fig (5-41) X-ray diffraction for Ero-Chrom black T measurements demonstrated that the Ero-Chrom black T is a polycrystalline structure

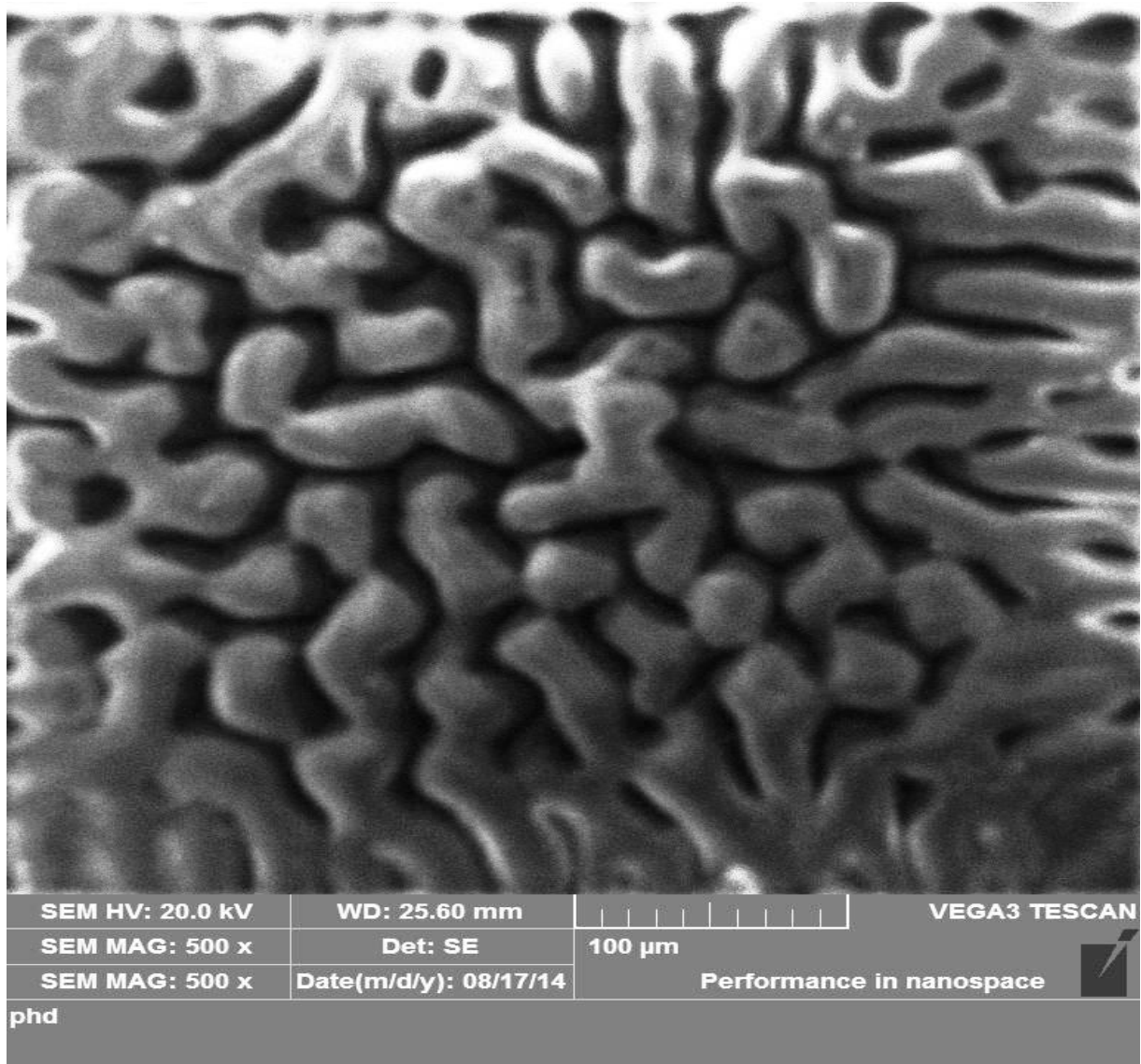


Fig (5-42)Field emission scanning electronic microscopy (FESEM) images of Ero-Chrom black T with different magnification

5-3 Discussions

- ❖ Fig 5-1 shows the absorption Spectra of Coumarin 500 the maximum absorption is at the wavelength 508 nm. The range of absorption for Coumarin 500 is in ultra-violet and visible range (200-1000nm). Previous studies show the absorption search in the range (244-508) nm, resulting The widening of range may be related to the Structure of Coumarin. In Fig 5-3, the optical energy gap (Eg) value of Coumarin 500 was found. The optical energy gap (Eg) has been calculated by the relation $(\alpha h\nu)^2 = C(h\nu - E_g)$ where (C) is constant. By plotting $(\alpha h\nu)^2$ vs photon energy (hν) as shown in fig (5.3) the energy gap is found to be 3.55 eV. The electrical properties for coumarin were determined from Fig 5-4. These include (I_{sc}) the Short-circuit current which is found to be 34.52 mA. If the external circuit is simply a wire and has no appreciable resistance, the current that flows is the short-circuit current (I_{sc}) and is directly related to the number of photons of light being absorbed by the cell. Short-circuit current density (J_{sc}) is short-circuit current per active area $J_{sc} = I_{sc} \div \text{active area} = 13.28 \text{ mA cm}^{-2}$. Open-circuit voltage (V_{oc}) is given by V_{oc} = 2.063 V. The fill factor (FF) is obtained by dividing the product of current and voltage measured at the power point (maximum output power P_{max}) by the product of short-circuit current and the open-circuit voltage. The power point is the maximum product of the cell voltage and the photocurrent obtained on the I-V curve. $FF = P_{max} \div I_{sc} \times V_{oc} = 0.96865$. Power conversion efficiency The power conversion efficiency (η) of the dye-sensitized solar cell is determined by the photocurrent density measured at short-circuit, V_{oc}, the FF of the cell, and the open-circuit current. Thus $\eta = V_{oc} \times I_{sc} \times FF \div P_{in} = 0.070$. Fig (5.5) shows the XRD patterns of Coumarin 500. The spectra in this study shows peaks at the position of 14.52°, 19.475°, 21.335°, 23.495° and 23.995°. This finding suggests that the thin

film is polycrystalline and has a hexagonal wurtzite structure of Coumarin 500 phase. In order to attain the detailed structure information, the grain size G along the c-axis was calculated according to the Scherrer's equation $G = \frac{0.9\lambda}{\beta \cos\theta}$. fig (5.6) depicts the field emission scanning electronic microscopy (FESEM) images of the surface morphologies of Coumarin 500. According to morphology., Large rods with a diameter of 100 μm are observed on the surface of the Coumarin 500. Additionally, the diameter and density of rods increases with an increasing Coumarin500 concentration However, the morphology transforms from a sheet structure to aggregative rods. The different morphology structures between samples prepared by different dye sources (correlate well with the differences in their XRD patterns. The SEM images indicate that the films are polycrystalline, which corresponds to the XRD analysis results and also implies the difficulty in controlling the morphology of the film when copper nitrate is used

- ❖ Fig 5-7 shows the absorption Spectra of Lawsonia and the maximum absorption is at The range of absorption for Lawsonia ultra-violet of visible radiation (200-350nm) this agrees what was found in (250 nm). Fig 5.9 shows the optical energy gap (E_g) value of Lawsonia. in fig (5.9) it be com 3.3eV . Fig 5.10: shows v-I characteriesics of Lawsonia solar cell. is the short-circuit current (I_{sc}) and is directly related to the number of photons of light being absorbed by the cell. Short-circuit (J_{sc}) is short-circuit current is are $I_{SC} = 35.75\text{m A}$ $J_{sc} = I_{sc} \div \text{active aera} = 13.75\text{mAcm}^{-2}$, Open – circuit voltage $(V_{oc})V_{oc}=1.177$. $FF = P_{max} \div I_{sc} \times V_{oc}$ the Full factor is=0.96102. The efficiency is given by $\eta = V_{oc} \times I_{sc} \times FF \div P_{in}=0.040$. Fig (5.11) shows the XRD patterns of Lawsonia ,The spectra have peaks at the position of 17.8° , 19.5° , 21° , 23° and 23.5° . This finding

suggests that the thin film is polycrystalline and has a hexagonal wurtzite structure of Lawsoniaphase. In order to attain the detailed structure information, the grain size G along the c-axis was calculated according to the Scherrer's equation $G = \frac{0.9\lambda}{\beta \cos\theta}$. Fig (5.12) depicts the field emission scanning electronic microscopy (FESEM) images of the surface morphologies of Lawsonia observed. According to morphology. Large rods with a diameter of 100 μm are observed on the surface of the Lawsonia. Additionally, the diameter and density of rods increases with an increasing Lawsonia concentration. However, the morphology transforms from a sheet structure to aggregative rods. The different morphology structures between samples prepared by different dye sources (correlate well with the differences in their XRD patterns). The SEM images indicate that the films are both polycrystalline, which comforswith XRD analysis results and also implies the difficulty in controlling the morphology of the film when copper nitrate is used

- ❖ Fig 5-13 shows the absorption spectra of Rohdamin B with maximum absorption at 508 nm. The range of absorption for RohdaminB is in ultra-violet and visible ranges (200-1000nm). Previous research was used in the absorption search up between 243-509 nm, resulting in this difference due to different state of matter .Fig5- 15 the optical energy gap (E_g) value of Rohdamin B. The optical energy gap (E_g) has been calculated as shown in fig (5.15) to be 3.27eV . Fig 5-16 show I-V characteics of Rohdamin B solar cell. Short-circuit current (I_{sc}) is given by , $I_{SC} = 31.32\text{m A}$ $J_{SC} = I_{SC} \div \text{active aera} = 12.05\text{mAcm}^{-2}$ Open – circuit voltage (V_{oc}) is $V_{oc}=2.062\text{ V}$ Fill factor (FF) 0.96927 The power conversion efficiency (η_{sc} . $\eta = V_{oc} \times I_{sc} \times FF \div P_{in}=0.063$. Fig (5.17) shows the XRD patterns of RohdaminB .The

spectra have peaks at the position of 36.5° , 36.9° , 53.4° and 53.4° . This finding suggests that the thin film is polycrystalline and has a hexagonal wurtzite structure of Rohdamin B phase. In order to attain the detailed structure information, the grain size G along the c -axis was calculated according to the Scherrer's equation $G = \frac{0.9\lambda}{\beta \cos\theta} Fg$ (5.18) depicts the field emission scanning electronic microscopy (FESEM) images of the surface morphologies of Rohdamin B observed. According to morphology. Large rods with a diameter of $100 \mu\text{m}$ are observed on the surface of the Rohdamin B. Additionally, the diameter and density of rods increases with an increasing Rohdamin B concentration. However, the morphology transforms from a sheet structure to aggregative rods. The different morphology structures between samples prepared by different dye sources (conforms with their XRD patterns). The SEM images indicate that the films are both polycrystalline, which conforms with XRD analysis. It also implies the difficulty in controlling the morphology of the film when copper nitrate is used

- ❖ Fig 5-19 shows the absorption spectra of Blue8GX with maximum absorption at 508 nm . The range of absorption for Blue8GX is in the ultra-violet to visible region ($200\text{-}1100\text{ nm}$). Previous research shows the absorption in the range ($243\text{-}508$) nm this difference is due to different state of matter. Fig 5-21 shows the optical energy gap (E_g) value of Blue8GX. The optical energy gap (E_g) has been calculated where 3.15 eV . Fig (5-22) of Blue8GX solar cell. The short-circuit current (I_{sc}) is given by $I_{sc} = 30.75\text{ mA}$, Open-circuit voltage is $V_{oc} = 1.927$ Fill factor $FF = 0.86669$ Power The power conversion efficiency (η). $\eta = V_{oc} \times I_{sc} \times FF \div P_{in} = 0.051$ Fig (5.23) shows the XRD patterns of Blue8GX. The spectra have peaks at the position of 13.5° , 15° , 19.5° , 23.5° and 24° . This finding suggests that the thin film is polycrystalline and

has a hexagonal structure of Blue8GX phase. In order to attain the detailed structure information, the grain size G along the c-axis was calculated according to the Scherrer's equation $G = \frac{0.9\lambda}{\beta \cos\theta}$ Fig (5.24) depicts the field emission scanning electronic microscopy (FESEM) images of the surface morphologies of Blue8GX observed. According to morphology. Large rods with a diameter of 100 μm are observed on the surface of the Blue8GX. Additionally, the diameter and density of rods increases with an increasing Blue8GX concentration. However, the morphology transforms from a sheet structure to aggregative rods. The different morphology structures between samples prepared by different dye sources (conforms with XRD patterns. The SEM images indicate that the films are both polycrystalline, which conforms with to the XRD analysis. It also implies the difficulty in controlling the morphology of the film when copper nitrate is used

- ❖ Fig 5-25 shows the absorption spectra of Roselle with maximum absorption at 508 nm. The range of absorption for Blue8GX is in ultra-violet of visible region (200-537nm). Previous research shows in the range 247-537 nm, this difference due to different state of matter. Fig5- 27 the optical energy gap (E_g) value of Roselle. The optical energy gap (E_g) has been calculated to be 3.308eV. Fig (5-28) shows V-I of Roselle solar cell. The Short-circuit current (I_{sc}) is given by $I_{sc} = 27.23 \text{ mA cm}^{-2}$, Open - circuit voltage (V_{oc}) is $V_{oc} = 2.062 \text{ V}$ (FF) = 0.96497. The power conversion efficiency (η) $\eta = V_{oc} \times I_{sc} \times FF \div P_{in} = 0.054$. Fig (5.29) shows the XRD patterns of Roselle. The spectra have peaks at the position of 9.5° , 11.5° , 13.5° , 13.7° and 13.8° . This finding suggests that the thin film is polycrystalline and has a hexagonal structure of Blue8GX phase. In order to attain the detailed structure information, the grain size G along the c-axis was calculated according to the

Scherrer's equation $G = \frac{0.9\lambda}{\beta \cos\theta}$ Fig (5.30 depicts the field emission scanning electronic microscopy (FESEM) images of the surface morphologies of Roselle observed. According to morphology. Large rods with a diameter of 100 μm are observed on the surface of the Roselle. Additionally, the diameter and density of rods increases with an increasing Roselle concentration. However, the morphology transforms from a sheet structure to aggregative rods. The different morphology structures between samples prepared by different dye sources (conforms well with their XRD patterns. The SEM images indicate that the films are both polycrystalline, which conforms with to the XRD analysis. It also implies the difficulty in controlling the morphology of the film when copper nitrate is used

- ❖ Fig 5-31 shows the absorption spectra of DDTTC 243 nm. The range of absorption for DDTTC is in ultra-violet spectrum and absorption of visible region (200-1000nm). Previous research was used in the absorption search up between 243-490 nm, resulting in this difference is due to different state of matter. Fig 5-33 the optical energy gap (E_g) value of DDTTC. The optical energy gap (E_g) has been calculated 2.94eV. Fig (5-34) of DDTTC solar cell. The Short-circuit current (I_{sc}) is given by $I_{sc} = 32.54\text{m A}$, Open – circuit voltage (V_{oc}) is $V_{oc} = 2.062\text{ V}$ Fill factor (FF) = 0.97096. The power conversion efficiency (η). $\eta = V_{oc} \times I_{sc} \times FF \div P_{in} = 0.065$. Fig (5.35) shows the XRD patterns of DDTTC. The spectra have peaks at the position of 10° , 11.5° and 11.8° . This finding suggests that the thin film is polycrystalline and has a hexagonal structure of DDTTC phase. In order to attain the detailed structure information, the grain size G along the c-axis was calculated according to the Scherrer's equation $G = \frac{0.9\lambda}{\beta \cos\theta}$ Fig (5.36) depicts the field emission scanning electronic microscopy (FESEM) images of the surface morphologies

ofDDTTC observed. According to morphology. Large rods with a diameter of 100 μm are observed on the surface of theDDTTC .Additionally, the diameter and density of rods increases with an increasing DDTTC concentration However, the morphology transforms from a sheet structure to aggregative rods. The different morphology structures between samples prepared by different dye sources (conforms with the their XRD patterns. The SEM images indicate that the films are both polycrystalline, which conforms with to the XRD analysis It and also implies the difficulty in controlling the morphology of the film when copper nitrate is used

- ❖ Fig 5-37 shows the absorptionspectra ofEro-Chrom black T s with maximum absorption 507 nm. The range of absorption for Ero-Chrom black T is in ultra-violet spectrum and absorption of visible region (200-1000nm). Previous research shows absorption in the range(258-507) nm, resulting in this difference is due to different state of matter .Fig5- 39 the optical energy gap (Eg) value ofEro-Chrom black T . The optical energy gap (Eg) has been calculated to be where 2.59eV . Fig(5- 40): ofEro-Chrom black T solar cell The Short-circuit current (I_{sc}) is given by $I_{SC} = 38.989\text{m}$, Open – circuit voltage (V_{oc})is $V_{oc}=1.23\text{V}$ Fill factor (FF) =0.96925The power conversion efficiency (η) $\eta = V_{oc} \times I_{sc} \times FF \div P_{in}=0.046$. Fg (5.41) shows the XRD patterns ofEro-Chrom black T . The spectra have peaks at the position of $16^\circ, 26.5^\circ$, and 36.5° . This finding suggests that the thin film is polycrystalline and has a hexagonal structure of Ero-Chrom black T phase. In order to attain the detailed structure information, the grain size G along the c-axis was calculated according to the Scherrer's equation $G = \frac{0.9\lambda}{\beta \cos\theta}$ Fig (5.42) depicts the field emission scanning electronic microscopy (FESEM) images of the surface morphologies of Ero-Chrom black Tobserved. According to

morphology. Large rods with a diameter of 100 μm are observed on the surface of the Roselle. Additionally, the diameter and density of rods increases with an increasing Roselle concentration. However, the morphology transforms from a sheet structure to aggregative rods. The different morphology structures between samples prepared by different dye sources (conforms with their XRD patterns). The SEM images indicate that the films are both polycrystalline, which conforms with XRD analysis. It also implies the difficulty in controlling the morphology of the film when copper nitrate is used.

Table 5-7 Electrical properties of dyes solar cells

Dye	Area	I_{sc}	J_{sc}	I_{max}	V_{max}	V_{oc}
chrom	2.6	38.989	14.96	38.29	1.194	1.23
Rohdamin	2.6	31.32	12.05	30.61	2.045	2.062
Coumarin	2.6	34.52	13.28	33.65	2.05	2.063
Blue8GX	2.6	30.75	11.82	26.79	1.917	1.927
Hibscus	2.6	27.23	10.47	26.43	2.05	2.062
DDTTC	2.6	32.54	12.52	31.78	2.05	2.062
Lawsonia	2.6	35.75	13.75	34.83	1.161	1.177

Table 5-8 the fill factor, energy gap and efficiency of dyes solar cells

Dye	FF	E_g	η
chrom	0.96925	2.59	0.046
Rohdamin	0.96927	3.27	0.063
Coumarin	0.96865	3.55	0.070
Blue8GX	0.86669	3.15	0.051
Roeslle	0.96497	3.08	0.054
DDTTC	0.97096	2.94	0.065
Lawsonia	0.961021	3.3	0.040

5.4 Conclusion

The application of conducting polymers to optoelectronic devices such as solar cell, light emitting diodes, and electrochemical sensors are of practical significance, because the polymer mixture can be easily prepared and modified by rich chemical procedures to meet optical and electronic requirements.

Organic solar cell based on a Thin Film single organic active layer of (2-methoxy-5-(2-ethylhexyloxy)-p-phenylene) (MEH-PPV) sandwiched between Ag and Indium Tin Oxide (ITO) electrodes with dyes like (Coumarin 500 - Lawson - RohdaminB- Blue8GX - Roselle - DDTTC and EroChrom black T Sows interesting Characteristics . It Shows that the efficiency depends energy gap and energy Level Location.

5.5 Recommendation

We recommend further work in this area to enhance the dye structure and produce and adjust concentration in certain quality to produce good film by finding a common solvent to the dye and the fullerene so that the solvent can be easily evaporated and yield a good film. The (thickness) of the cell must be decreased then wing thin layer of glass can be increased by increasing polymer thickness The cell efficiency. The temperature effect on the cells properties could be further investigated as well. Other doping materials can be used to increase the dye photoconductivity.

Reference

- [1] A khogal , solar energy and the ability of using, sudan coin press, kartoum , 2007
- [2][paulD . Maycock , Edward N . stire ,photouoltaic sun Light to electricity in one step , HarpalBrar, USA.1990](#)
- [3] Wolf , M and prince , M.B New development in silicon photovoltaic devices and their application to electronics
- [4]Wolf, M. (1976) Historical development of solar cells in solar cells. IEEE Press, New York, 274.
- [5]KarlW. Boer Advances in solar energy – Volume 1 publisher :American solar energy society – Univversity of Delaware Newark 1982
- [6] C. J. Brabec, G. Zerza, G. Cerullo, S. De Silvestri, S. Luzzati, J. C. Hummelen. (2001). *Tracing photoinduced electron transfer process in conjugated polymer/fullerene bulk heterojunctions in real time*. Journal of Chemical Physics Letters 340: 232-236.
- [7] N. S. Sariciftci (Ed.), (1998), *Primary photo excitations in conjugated polymers:MolecularExciton versus Semiconductor Band Model*. World Scientific Publishers, Singapore
- [8] I. Montanari, A. F. Nogueira, J. Nelson, J. R. Durrant, C. Winder, M. A. Loi, N. S. Sariciftci. (2002). *Experimental determination of the rate law for charge carrier decay in a polythiophene: Fullerene solar cell*. Journal of Applied Physics Letters 92: 9- 81.

- [9] Sole, J. G., Bausa, L. E. and Jaque, D, (2005). *An Introduction to the Optical Spectroscopy of Inorganic Solids*. John Wiley & Sons. England, pp. 11-12.
- [10] Graham, S. C.; Bradley, D. D. C.; Friend, R. H.; Spangler, (1991). *Raman and photoluminescence spectra of PPV oligomers*. Journal article in the OhioLINK Electronic 41: 1277-1280.
- [11] H. Wolf, *Silicon semiconductor data*, pergamon press, New York (1969)
- [12] D. E. Carlson and S. Wanger, *renewable energy* Island press, Washington, (1993)
- [13] Kirpich A. G. O, Brien & N. Shepard, *solar energy technology hand book*
- [14] E. J. Carlson & J. C. LiEN, *An Al_p-silicon MOS photovoltaic cell* J. Applied physics, 46, 3982, (1975)
- [15] H. K. Charles Jr & A. P. Ariotejo, *Review of amorphous and polycrystalline thin film silicon solar cell performance parameters*, Solar energy, 24, 328 – 339 (1980)
- [16] W. A. Anderson, A. E. Delahoy & R. A. Milano J. Appl. phys, 45, 3913, (1974)
- [17] J. Herion, E. A. Niekisch, G. Schari, *Investigation of metal oxide/cuprous oxide heterojunction solar cells*. Sol. Energy Mater. Sol. cells 2008.
- [18] A. Mittiga, E. Salsa, F. Sarto, M. Tucci, and R. Vasanthi, *Heterojunction solar cell with 2% efficiency based on a Cu₂O substrate*, App. Phys. 2006.
- [19] Shockley, W. and Queisser, H. J. (1961) *Detailed balance limit of efficiency of PN junction solar cells*. *Journal of Applied Physics*, 32, 510-519.

- [20] Maycock, P.D. and Stirewalt, E.N. (1981) Photo voltaic sunlight to electricity in one step. 3rd Edition, Brick House, Andover, 222.
- [21] Graham S . C.;Bradley , D . D . C.; Friend, R. H.; Spangled, (1991) . Raman and photoluminescence spectra of PPV oligomers J ournal article in the OhioLINK Electronic 14 : 1277-1280.
- [22] H. Shirakawa, Angew .Chem,Int> Ed. 2001,40, 2574.
- [23] H. Shirakawa, A ..G. MacDiarmid, A. J. Heeger,Chen . Cmmun, 2003,1.
- [24] Rene' Janssen I'ntroduction to polymer Solar Cell "- (3Y280) Departments of Chemistry and Engin a
- [25] AimiAbass , HonghuiShen, pererBienstman , BJ)rnMaes " Increasing polmer Solar Cell Efficiency with Triangular Silver Gratings"photonics research Grop Ghent University – imec, Department of Information Technology , St. _pietersnieuwstraat 41, 900 Ghent,
- [26] AntonoFaacchetti . (2010). π conjugated polymer for Organic Electrons and photovoltaic Cell Applications . Journal of Chemistry and the Materials Research Center United States Northwestern University 214:202-211.
- [27] Green, M.A. (1981) Solar cell fill factors: General graph and empirical expressions. *Solid State Electronics*, 24, 788-789.
- [28] Mckelvey, J.P. (1966) Solid state and semiconductors physics. Krieger Publishing Company, New York, 512.
- [29] Singh, J. (1994) Semiconductor devices: An inter-duc- tion. McGraw Hill, New York, 669

- [30] C .D. Miiller , A Falcou, N . Reckefuss, M .Rojahn, ,VWiederirn . P .Rudati, H. Frohne, O .Nuyken(2003). OrGANic MetaiiIC Hybrid polemers : Fundamentals and DevieApplicaions Nature . polymer Journal 41 : 511- 520
- [31] C . . J .Brabec .G .Zerza, G .Cerullo, S .De Silvestri, S .Luzzati, J. C. Hummelen. (2001) Tracing photoinduced electron transfer process in conjugated polymer/fullerence bulk herojunctions in real time .journal of Chemical phsics Letters 340: 232- 236.
- [32] F . padinger ,Rittberger, N . s. Sariciftci, (2003). Efjcts of postproduction Treatment on plastic Solar Cells< journal of Advanced Materials 13 : 85-88.
- [33] I. Montananari, A .F .Nogueira, J . Nelson, J .R .Durrant, C . Winder, M .A .Loi, N .S .sariciftci . (2002) . Experimental determination of THE rate law for charge carrier decay in a polythiophene: Fullerene Solar cell . Journal of Applied physics Letters 92:9- 81 .
- [34]Jacob Lund, RasmusRQge ,Ren'epetesen , Tom Laren , (2006). Polymer solar Cells , Aalborg University. Jounal, of Nature 1990, 347,539.
- [35]Liuan Han Dye – Sensitized Solar Cells withNantechnologies" Advanced photovoltaicsCarter NLMS) [2009]
- [36]Santra parlay K . ; Kamat ,prashant V . (2012) . "Mn- Doped Quantum Dot Sensitized Solar Cells: A Strategy to Boost Efficiency Over 5%" . Journal of the American chemical Society 134 (5) : 2508 -11.
- [37]pope, M.; Swenberg , C . E Electronic processes in Organic Crystals and polymers; Oxford UnIversitypress : New YorK,2ed ., 1999.
- [38]Kung –HwaWei .(2013). Development and Characterizatiation of New Donor-Acceptor Conjugated polymers and F ullerence Nanoparticles for High

performance Bulk Heterojunction Solar Cells. Journal of National Chiao Tung University . Department of Materials Science & Eng. 106:34-44.

[39] N. S. Sariciftci (Ed), (1998) Primary photo excitations in conjugated polymers : Molecular Exciton versus Semiconductor Band Model . World Scientific publishers, Singapore .

[40] Moon, Soo-Jin; Itzhaki; Yafit, Yum, Jun – Ho, Zakeeruddin, Shaik M.; Hodes, Gary ; Graetzel, Michael (2010). " Sb₂S₃-Based Mesoscopic Solar Cell using an Organic Hole Conductor" .The Journal of Physical Chemistry Letters 1 (10): 1524. Doi: 10.1021/jz100308q.

[41] H. Kidowaki, T. Oku, T. Akiyama, Fabrication and characterization of CuO/ZnO solar cells, Journal of Physics: Conference Series . 2012

[42] L.C. Olsen, R.C. Bohara, M.W. Urie, Explanation for low-efficiency Cu₂O Schottky-barrier solar cells, App. Phys. 2013

[43] Liu, B. and Aydil, E.S. (2011) Layered mesoporous nano- structures for enhanced light harvesting in dye-sensitized solar cells. *Journal of Renewable and Sustainable Energy*, 3, 043106

[44] Sukhatme, S.P. (2008) Solar energy principles of thermal collection and storage. 3rd Edition, Tata McGraw-Hill, Noida, 341

[45] Gary , H . P and J prakash (2000) Solar energy fundamen – tals and applications . Tata McGraw- Hill , Noida , 434 .

- [46] C. D. Müller, A. Falcou, N. Reckefuss, M. Rojahn, V. Wiederhirn, P. Rudati, H. Frohne, O. Nuyken. (2003). *Organic–Metallic Hybrid Polymers: Fundamentals and Device Applications Nature*. Polymer Journal 41: 511–520
- [47] Chang, R.; Hsu, J. H.; Fann, W. S.; Liang, K. K.; Chiang, C. H.; Hayashi, M.; Yu, J.; Lin, S. H.; Chang, E. C.; Chuang,(2000). *Investigations of Ultrafast Dynamics in Light-emitting Polymers*. Journal of Chinese Chemical Society (1-2): 142–152.
- [48] Jacob Lund, Rasmus Røge, René Petersen, Tom Larsen. (2006). *Polymer solar cells.*, Aalborg University. Journal of Nanoscience and Nanotechnology. 156: 4-75
- [49] Peter Gevorkian. (2007). *Sustainable energy systems engineering: the complete green building design resource*. McGraw-Hill Professional. pp. 498. <http://books.google.com/books?id=i8rc>.
- [50] International Energy Agency.(2007). *Renewables in Global Energy Supply - An IEA Fact Sheet*. IEA Publications. Paris. France
- [51] F. paddinger, R. S. Rittber, N. S. Sariciftci, (2003). Effects of postproduction Treatment on plastic Solar Cells Journal of Advanced Functional Materials 13 : 85-88 .